

STUDY OF EOR-CO₂ MISCIBLE FLOODING PERFORMANCE USING
COMPOSITIONAL RESERVOIR SIMULATION WITH LOCAL GRID
REFINEMENT

A Thesis

by

WEI JIAN YEAP

Submitted to the Office of Graduate and Professional Studies of
Texas A&M University
in partial fulfillment of the requirements for the degree of

MASTER OF SCIENCE

Chair of Committee,	Maria A. Barrufet
Committee Members,	Ding Zhu
	A. Rashid Hasan
	Thomas Blasingame
Head of Department,	A. Daniel Hill

May 2018

Major Subject: Petroleum Engineering

Copyright 2018 Wei Jian Yeap

ABSTRACT

CO₂ injection in oil reservoirs has been widely accepted as an effective technique for enhanced oil recovery (EOR), which has been applied by the oil industry for over 40 years. Concerns over greenhouse gas emissions are leading to the investigation and realization of its potential as a carbon storage method in recent years. To achieve better miscibility and sweep efficiency for CO₂ flooding, production performance needs to be optimized. However, optimization of production performance remains a challenging task in the upstream oil and gas industry due to the physical and/or financial uncertainties.

In this study, a commercial reservoir simulator has been used to analyze optimum development strategies for CO₂ miscible flooding. Since grid-refinement sensitivity is an extremely troublesome problem in many compositionally enhanced solvent simulations, the effect of local grid refinement on conducting CO₂ flooding simulation will be first discussed in this study. Coarse reservoir models without local grid refinement are found to contribute to significant error. The nature of the errors resulting from numerical dispersion and the non-linearity of flash calculations depends on many variables, including petrophysics and fluid types; not using local grid refinement may result in overly optimistic or pessimistic production performances.

The impacts of injection/production variables on oil recovery and CO₂ storage are investigated. Injection variables studied include: injection pore volume, injection initiation timing and produced gas recycling while the production variables include producer bottomhole pressure, target oil rate and gas rate limits. Results show that optimum

injection/ production strategies differ significantly for both light and heavy oil reservoirs. Overall, this study has determined a systematic general injection and production workflow to recover more oil and store more CO₂ underground simultaneously.

ACKNOWLEDGEMENTS

I would like to thank my advisor and chair of committee, Dr Maria Barrufet, for her teachings, guidance and support throughout this thesis. It was a pleasure and an honor to work with her.

My thanks also go to Dr Ding Zhu, Dr Rashid Hasan and Dr Thomas Blasingame, who joined my committee and gave me insightful guidance and help when I needed it.

Dr Zhu, Dr Lee, Dr Pope, Dr Akkutlu and Dr Ayers taught me valuable geology and petroleum engineering knowledge that I have used in this thesis and will use in my future life; my thanks go to them as well.

Thanks also to my colleagues and friends, who made my time at Texas A&M University not only a time of learning, but also an unforgettable human experience.

I finally want to extend my gratitude to Petronas and Harold Vance Department of Petroleum Engineering, for their sponsorship and fellowship throughout my master degree at Texas A&M University.

CONTRIBUTORS AND FUNDING SOURCES

Contributors

This work was supervised by a thesis committee consisting of Professor Maria A. Barrufet of the Department of Petroleum Engineering, Professor Thomas Blasingame of the Department of Petroleum Engineering, Professor Ding Zhu of the Department of Petroleum Engineering and Professor A. Rashid Hasan of the Department of Petroleum Engineering.

All work for the thesis was completed independently by the student.

Funding Sources

Graduate study was supported by a department fellowship from the Department of Petroleum Engineering and study grant from Texas A&M University. This work was also made possible in part by outside funding from Petroliam Nasional Berhad (Petronas).

NOMENCLATURE

B_g	Gas formation volume factor
BHP	Bottomhole pressure, psia
Btu	British thermal unit
C_{drill}	Drilling cost per well, \$
$C_{facilities}$	Facility cost per pattern, \$
C_{tubing}	Tubing cost per well, \$
CAPEX	Capital expenses, \$
CCS	Carbon storage and sequestration
CO ₂	Carbon dioxide
d	Depth, ft
EIA	US Energy of Information Administration
EOR	Enhanced oil recovery
EOS	Equation of state
FGIT	Field gas injection total
GDP	Gross domestic product
IEA	International Energy Agency
$Index_t$	Cost index for tubing
IRS	Internal Revenue Service
k	Permeability, mD
LGR	Local grid refinement

MCM	Multi-contact miscibility
MMP	Minimum miscibility pressure, psia
Mscf	Thousand standard cubic feet
mton	metric ton
NASA	National Aeronautics and Space Administration
NOAA	National Oceanic and Atmospheric Administration
NPV	Net present value
OPEX	Operating expenses, \$
OPEX _{fixed}	Fixed operating expenses, \$
ppm	Parts per million
PV	Pore volume
PVT	Pressure volume and temperature
Q	Annual mass flow rate of CO ₂ , ton
Res bbl	Reservoir barrel
STB	Stock tank barrel
STDEV	Standard deviation
V _{DP}	Dykstra-Parsons coefficient
WTI	West Texas Intermediate

TABLE OF CONTENTS

	Page
ABSTRACT	ii
ACKNOWLEDGEMENTS	iv
CONTRIBUTORS AND FUNDING SOURCES.....	v
NOMENCLATURE.....	vi
TABLE OF CONTENTS	viii
LIST OF FIGURES.....	xi
LIST OF TABLES	xvi
CHAPTER I INTRODUCTION	1
1.1 Objectives.....	1
1.2 Description of Chapters.....	1
CHAPTER II LITERATURE REVIEW	3
2.1 World Energy Demand and Global Warming.....	3
2.2 Carbon Emission Mitigation Strategies.....	6
2.3 Overview of Carbon Capture and Storage	8
2.4 Use of CO ₂ in Enhanced Oil Recovery	10
2.5 Development Strategies of CO ₂ -EOR.....	13
2.6 Grid Sensitivity in Compositional Reservoir Simulator	15
CHAPTER III RESERVOIR MODEL OF CO ₂ -EOR PROJECT	17
3.1 Reservoir Fluid.....	17
3.2 Reservoir Model.....	20
3.2.1 The Pattern	20
3.2.2 The Grid	21
3.2.3 Petrophysics.....	23
3.2.4 Relative Permeabilities	24
3.2.5 Reservoir Initialization	24
CHAPTER IV RESERVOIR RESPONSE TO PRODUCTION/INJECTION CONSTRAINTS	26

4.1 Reference Case – Natural Depletion	26
4.2 Injection Rate	29
4.3 CO ₂ Recycling.....	32
4.4 Injection Initiation Timing	38
4.5 Producer BHP.....	43
4.6 Producer Target Oil Rate.....	46
4.7 Producer Gas Rate Limit.....	50
CHAPTER V LOCAL GRID REFINEMENT APPLICATION	55
5.1 Sensitivity to Injection Rate and Injection Pore Volume	56
5.2 Sensitivity to CO ₂ Recycling.....	62
5.3 Sensitivity to Injection Initiation Time	65
5.4 Sensitivity to Producer BHP	69
5.5 Sensitivity to Producer Target Oil Rate	73
5.6 Sensitivity to Producer Gas Rate Limit.....	77
5.7 Computational Cost.....	81
CHAPTER VI OPTIMUM DEVELOPMENT STRATEGIES	83
6.1 Injection Rate	85
6.2 CO ₂ Recycling.....	89
6.3 Injection Initiation Time.....	91
6.4 Producer BHP.....	95
6.5 Producer Target Oil Rate.....	99
6.6 Producer Gas Rate Limit.....	103
6.7 Completion Location.....	107
CHAPTER VII ECONOMIC ANALYSIS OF CO ₂ -EOR PROJECT.....	113
7.1 General Cost Functions	113
7.1.1 Drilling Costs	113
7.1.2 Completion Costs	115
7.1.3 Surface Facilities Costs	116
7.1.4 Fixed Operating Costs	116
7.1.5 Variable Costs - Production	117
7.1.6 Variable Costs - Injection.....	117
7.2 Cost Functions Specific to CO ₂ -EOR	118
7.2.1 CO ₂ Market Price	118
7.2.2 Recycling Costs.....	120
7.3 Summary of the Economic Model	121
7.4 Sensitivity Study	121
7.4.1 Oil Price.....	122
7.4.2 CO ₂ Price.....	125
7.4.3 Recycling Costs	127

7.4.4 Tax Incentives	130
7.4.5 Local Grid Refinement.....	132
CHAPTER VIII CONCLUSIONS AND RECOMMENDATIONS	134
REFERENCES.....	138
APPENDIX 1 ECLIPSE LIGHT_OIL.PVO FILE	142
APPENDIX 2. ECLIPSE HEAVY_OIL.PVO FILE	150
APPENDIX 3. ECLIPSE *.DATA FILE FOR REFERENCE CASE (NATURAL DEPLETION).....	158
APPENDIX 4. ECLIPSE *.DATA FILE FOR CO ₂ INJECTION CASE	166
APPENDIX 5. ECLIPSE GRID.INC FILE FOR LGR GRID CONFIGURATION	174
APPENDIX 6. ECLIPSE SCHEDULE.INC FILE FOR LGR CASES	177
APPENDIX 7. ECLIPSE SCHEDULE.INC FILE FOR RECYCLING PRODUCED GAS	179
APPENDIX 8. INCREMENTAL NPV DATA USED TO PLOT THE CONTOUR.....	181

LIST OF FIGURES

	Page
Figure 1 – History of global surface temperature since 1880 (Reprinted from Dahlman, 2017).	4
Figure 2 – Global atmospheric carbon dioxide concentrations from Oct. 1 through Nov. 1 as recorded by NASA’s Orbiting Carbon Observatory-2 (Reprinted from First Global Maps from Orbiting Carbon Observatory, 2014).	5
Figure 3 – Global monthly mean carbon dioxide averaged over marine surface sites (data source from NOAA).	6
Figure 4 – CO ₂ from the IEA’s 450 Scenario, relative to the New Policies Scenario with y-axis indicating the amount of CO ₂ measured in Gigatonne (Reprinted from EIA, 2017).	7
Figure 5 – Common storage site for CO ₂ sequestration (Reprinted from Wallace and Kuuskraa, 2014).	9
Figure 6 – Overview of the miscible CO ₂ -EOR process (Reprinted from Wallace and Kuuskraa, 2014).	11
Figure 7 – Projected CO ₂ -EOR operations and CO ₂ sources by 2020 in the United States (Reprinted from Wallace and Kuuskraa, 2014).	12
Figure 8 – Viscous fingering and gravity segregation lead to unfavorable sweep efficiency in CO ₂ -EOR process (Adapted from Wallace and Kuuskraa, 2014).	13
Figure 9 – Phase envelope for the light oil used in the study.....	18
Figure 10 – Phase envelope for the heavy oil used in the study.	19
Figure 11 – The 5-spot pattern and its dimensions used in this simulation study.....	20
Figure 12 – Visualization of the grid configuration.	21
Figure 13 – Local grid refinement setup for the simulation (top view).	22
Figure 14 – Relative permeability curves used in this work.	24
Figure 15 – Production rates and pressure of the light oil reservoir producing under natural depletion.	27

Figure 16 – Production rates and pressure of the heavy oil reservoir producing under natural depletion.	28
Figure 17 – Changes in oil production rate, gas production rate and reservoir pressure due to different injection rates in light oil reservoir.	30
Figure 18 – Changes in oil production rate, gas production rate and reservoir pressure due to different injection rates in heavy oil reservoir.	32
Figure 19 – Molar compositions of the gas produced for 20 years in light oil reservoir.	33
Figure 20 – Molar compositions of the gas produced for 20 years in heavy oil reservoir.	34
Figure 21 – Changes in oil production rate, gas production rate, gas injection rate and reservoir pressure due to CO ₂ recycling in light oil reservoir.	36
Figure 22 – Changes in oil production rate, gas production rate, gas injection rate and reservoir pressure due to CO ₂ recycling in heavy oil reservoir.	38
Figure 23 – Changes in oil production rate, gas production rate and reservoir pressure due to different injection initiation timing in light oil reservoir.	40
Figure 24 – Changes in oil production rate, gas production rate and reservoir pressure due to different injection initiation timing in heavy oil reservoir.	42
Figure 25 – Changes in oil production rate, gas production rate and reservoir pressure due to different producer BHP in light oil reservoir.	44
Figure 26 – Changes in oil production rate, gas production rate and reservoir pressure due to different producer BHP in heavy oil reservoir.	46
Figure 27 – Changes in oil production rate, gas production rate and reservoir pressure due to different producer target oil rate in light oil reservoir.	48
Figure 28 – Changes in oil production rate, gas production rate and reservoir pressure due to different producer target oil rate in heavy oil reservoir.	50
Figure 29 – Changes in oil production rate, gas production rate and reservoir pressure due to different producer gas rate limits in light oil reservoir.	52
Figure 30 – Changes in oil production rate, gas production rate and reservoir pressure due to different producer gas rate limits in heavy oil reservoir.	54

Figure 31 – Summary of error in incremental recovery, gas production and CO ₂ stored by varying injection rate for light oil.	58
Figure 32 – Summary of error in incremental recovery, gas production and CO ₂ stored by varying injection rate for heavy oil.	60
Figure 33 – Comparisons of incremental recovery obtained from cases with and without LGR for each injection rate.	61
Figure 34 – Summary of error in incremental recovery, gas production and CO ₂ stored by changing injection initiation time for light oil.	67
Figure 35 – Summary of error in incremental recovery, gas production and CO ₂ stored by changing injection initiation time for heavy oil.	69
Figure 36 – Summary of error in incremental recovery, gas production and CO ₂ stored by changing producer BHP for light oil.	71
Figure 37 – Summary of error in incremental recovery, gas production and CO ₂ stored by changing producer BHP for heavy oil.	73
Figure 38 – Summary of error in incremental recovery, gas production and CO ₂ stored by changing producer target oil rate for light oil.	75
Figure 39 – Summary of error in incremental recovery, gas production and CO ₂ stored by changing producer target oil rate for heavy oil.	77
Figure 40 – Summary of error in incremental recovery, gas production and CO ₂ stored by changing producer gas production rate limit for light oil.	79
Figure 41 – Summary of error in incremental recovery, gas production and CO ₂ stored by changing producer gas production rate limit for heavy oil.	81
Figure 42 – CO ₂ utilization factor and storage efficiency trend by varying injection rate for light oil.	86
Figure 43 – CO ₂ utilization factor and storage efficiency trend by varying injection rate for heavy oil.	88
Figure 44 – CO ₂ utilization factor and storage efficiency trend by changing injection initiation time for light oil.	93
Figure 45 – CO ₂ utilization factor and storage efficiency trend by changing injection initiation time for heavy oil.	95

Figure 46 – CO ₂ utilization factor and storage efficiency trend by changing producer BHP for light oil.	97
Figure 47 – CO ₂ utilization factor and storage efficiency trend by changing producer BHP for heavy oil.	99
Figure 48 – CO ₂ utilization factor and storage efficiency trend by changing producer target oil rate for light oil.	101
Figure 49 – CO ₂ utilization factor and storage efficiency trend by changing producer target oil rate for heavy oil.	103
Figure 50 – CO ₂ utilization factor and storage efficiency trend by changing producer gas production rate limit for light oil.	105
Figure 51 – CO ₂ utilization factor and storage efficiency trend by changing producer gas production rate limit for heavy oil.	107
Figure 52 – Comparison of CO ₂ concentration at the end of simulation for two different completion designs. (Left – Bottom injector and top producer; right – Bottom injector and bottom producer).....	110
Figure 53 – Crude oil and natural gas prices compared to MIT Composite Drilling Index (Reprinted from Heddle et al., 2003).....	114
Figure 54 – Drilling cost per vertical depth surveyed from 2010 to 2015, with forecast to 2018 (Reprinted from EIA, 2016).....	115
Figure 55 – CO ₂ price published on California Carbon Dashboard website (data from Intercontinental Exchange Inc.).....	119
Figure 56 – Forecast of CO ₂ price depending on different levels of regulations (Reprinted from Luckow et al., 2015).	120
Figure 57 – Overview of oil price from 1984 to 2017 (data source from EIA).	122
Figure 58 – Incremental NPV of the light oil reservoir at different injection pore volumes with varying oil prices.....	123
Figure 59 – Incremental NPV of the heavy oil reservoir at different injection pore volume with varying oil prices.	124
Figure 60 – Incremental NPV of the light oil reservoir at different injection pore volumes with varying CO ₂ prices.	125

Figure 61 – Incremental NPV of the heavy oil reservoir at different injection pore volumes with varying CO ₂ prices.	126
Figure 62 – Incremental NPV resulted from recycling CO ₂ in light oil reservoir.	127
Figure 63 – Incremental NPV resulted from purchasing similar amount of recycled CO ₂ at market price in light oil reservoir.	128
Figure 64 – Incremental NPV resulted from recycling CO ₂ in heavy oil reservoir.	129
Figure 65 – Incremental NPV resulted from purchasing similar amount of recycled CO ₂ at market price in heavy oil reservoir.	129
Figure 66 – Comparisons of the incremental NPV resulted from the cases with and without the Section 45Q tax incentive program in light oil reservoir.	131
Figure 67 – Comparisons of the incremental NPV resulted from the cases with and without the Section 45Q tax incentive program in heavy oil reservoir.	131
Figure 68 – Comparisons of the incremental NPV resulted from the cases with and without LGR in light oil reservoir.	132
Figure 69 – Comparisons of the incremental NPV resulted from the cases with and without LGR in heavy oil reservoir.	133

LIST OF TABLES

	Page
Table 1 – Fluid properties of light reservoir oil used in the simulation study.	17
Table 2 – Fluid properties of heavy reservoir oil used in the simulation study.	17
Table 3 – Summary of petrophysical properties of the reservoir model.	23
Table 4 – Initialization of parameters in the reservoir model.	25
Table 5 – Operating constraints for the reference cases in light and heavy oil reservoirs.	27
Table 6 – Summary of the operating constraints for all injection rate cases.	29
Table 7 – Operating constraints for all CO ₂ recycling cases in light and heavy oil reservoir.	35
Table 8 – Operating constraints for CO ₂ injection initiation timing cases in light oil reservoir.	39
Table 9 – Operating constraints for CO ₂ injection initiation timing cases in heavy oil reservoir.	41
Table 10 – Operating constraints for producer BHP cases in light and heavy oil reservoir.	44
Table 11 – Operating constraints for constraints for producer target oil rate cases in light and heavy oil reservoir.	48
Table 12 – Operating constraints for gas production rate limit cases in light and heavy oil reservoir.	51
Table 13 – Errors resulted from LGR application by varying injection rate for light oil.	57
Table 14 – Errors resulted from LGR application by varying injection rate for heavy oil.	59
Table 15 – Errors resulted from LGR application by recycling produced gas for light oil.	63
Table 16 – Errors resulted from LGR application by recycling produced gas for heavy oil.	63

Table 17 – Oil density, oil saturation and CO ₂ composition comparison between models with LGR and without LGR for light oil.	64
Table 18 – Oil density, oil saturation and CO ₂ composition comparison between models with LGR and without LGR for heavy oil.	64
Table 19 – Errors resulted from LGR application by changing injection initiation time for light oil.	66
Table 20 – Errors resulted from LGR application by changing injection initiation time for heavy oil.	68
Table 21 – Errors resulted from LGR application by changing producer BHP for light oil.	70
Table 22 – Errors resulted from LGR application by changing producer BHP for heavy oil.	72
Table 23 – Errors resulted from LGR application by changing producer target oil rate for light oil.	74
Table 24 – Errors resulted from LGR application by changing producer target oil rate for heavy oil.	76
Table 25 – Errors resulted from LGR application by changing producer gas production rate limit for light oil.	78
Table 26 – Errors resulted from LGR application by changing producer gas production rate limit for heavy oil.	80
Table 27 – Production performance at end of simulation by varying injection rate for light oil.	85
Table 28 – Production performance at end of simulation by varying injection rate for heavy oil.	87
Table 29 – Production performance at end of simulation by recycling produced gas for light oil.	89
Table 30 – Production performance at end of simulation by recycling produced gas for heavy oil.	90
Table 31 – Production performance at end of simulation by changing injection initiation time for light oil.	92

Table 32 – Production performance at end of simulation by changing injection initiation time for heavy oil.	94
Table 33 – Production performance at end of simulation by changing producer BHP for light oil.	96
Table 34 – Production performance at end of simulation by changing producer BHP for heavy oil.	98
Table 35 – Production performance at end of simulation by changing producer target oil rate for light oil.	100
Table 36 – Production performance at end of simulation by changing producer target oil rate for heavy oil.	101
Table 37 – Production performance at end of simulation by changing producer gas production rate limit for light oil.	104
Table 38 – Production performance at end of simulation by changing producer gas production rate limit for heavy oil.	106
Table 39 – Production performance at end of simulation by changing completion location for light oil (completed half of net pay).	108
Table 40 – Production performance at end of simulation by changing completion location for light oil (completed one-third of net pay).	108
Table 41 – Production performance at end of simulation by changing completion location for heavy oil (completed half of net pay).	110
Table 42 – Production performance at end of simulation by changing completion location for heavy oil (completed one-third of net pay).	111
Table 43 – Variable costs for oil and gas production.	117
Table 44 – Gas or CO ₂ injection costs.	118
Table 45 – Summary of the equations and costs used in economic analysis.	121
Table 46 – Development strategies for optimizing CO ₂ utilization factor in both light and heavy oil reservoirs.	136
Table 47 – Development strategies for optimizing CO ₂ storage efficiency in both light and heavy oil reservoirs.	137

CHAPTER I

INTRODUCTION

1.1 Objectives

The main focus of this research is to study the CO₂ enhanced oil recovery in light and heavy oil reservoir using commercial reservoir simulator Eclipse 300. The objectives that have been accomplished in this study include:

1. Investigate the impacts of local grid refinement on reservoir production performance such as incremental recovery, gas production and CO₂ storage
2. Identify the influence of varying injection and production constraints on the light oil and heavy oil reservoir behaviors
3. Determine optimum injection and production strategies to conduct CO₂ miscible flooding by using reservoir performance and economic performance yardsticks

1.2 Description of Chapters

Chapter I discusses the problem and identifies the objectives of the study.

Chapter II provides background of the study. It discusses the current world energy demand and carbon emission. Mitigation strategies in place for carbon emission are also included, especially carbon capture and sequestration through enhanced oil recovery (EOR). The mechanism of carbon sequestration through EOR is discussed. It also gives an overview of published literature about development strategies for CO₂-EOR project

as well as the grid sensitivity and application of local grid refinement in compositional reservoir simulator.

Chapter III discusses the reservoir model used in the CO₂-EOR study. Reservoir fluid model has been included. Besides, reservoir model has been discussed in several aspects such as the pattern, grid, petrophysics, relative permeabilities and reservoir initialization.

Chapter IV discusses the change in the reservoir behaviors towards varying injection and production variables such as injection rate, gas recycling, injection timing, producer BHP, target oil rate and gas rate limit.

Chapter V investigates the impacts of local grid refinement on the incremental recovery, gas production and CO₂ storage. The sensitivity analyses to each injection and production variables have been conducted.

Chapter VI considers the optimum development strategies for CO₂-EOR project by using performance yardsticks such as CO₂ utilization factor and storage efficiency. Each injection and production variable has been studied to determine the optimum practice for CO₂-EOR project.

Chapter VII develops an economic model to evaluate the economics of CO₂-EOR project. Sensitivity analyses towards variables such as oil and CO₂ price, recycling costs, tax incentives have been included in this chapter.

Chapter VIII discusses the conclusions of this study and recommendation for implementation of future work.

CHAPTER II

LITERATURE REVIEW

2.1 World Energy Demand and Global Warming

Quickly growing populations and steady global economic growth lead to rising demand for energy. According to U.S. Energy Information Association (EIA), worldwide energy consumption is forecasted to increase 28% between 2015 and 2040, from 575 quadrillion British thermal unit (Btu) to 736 quadrillion Btu (EIA, 2017). To meet the energy demand, the increase of consumption of fossil fuels becomes inevitable: oil for transportation, while coal and natural gas for power generation.

Rising consumption of fossil fuels is likely to accelerate the global warming effect due to the emission of greenhouse gases. Since 1880, surface temperature has risen at an alarming pace of about 0.13°F (0.07°C) per decade, contributing to a net warming of 1.69°F (0.94°C) through 2016, which is shown in Figure 1 (Dahlman, 2017). According to the official report by National Oceanic and Atmospheric Administration (NOAA), the year of 2016 marks the fifth time in 21st century that a new record high annual temperature has been created.

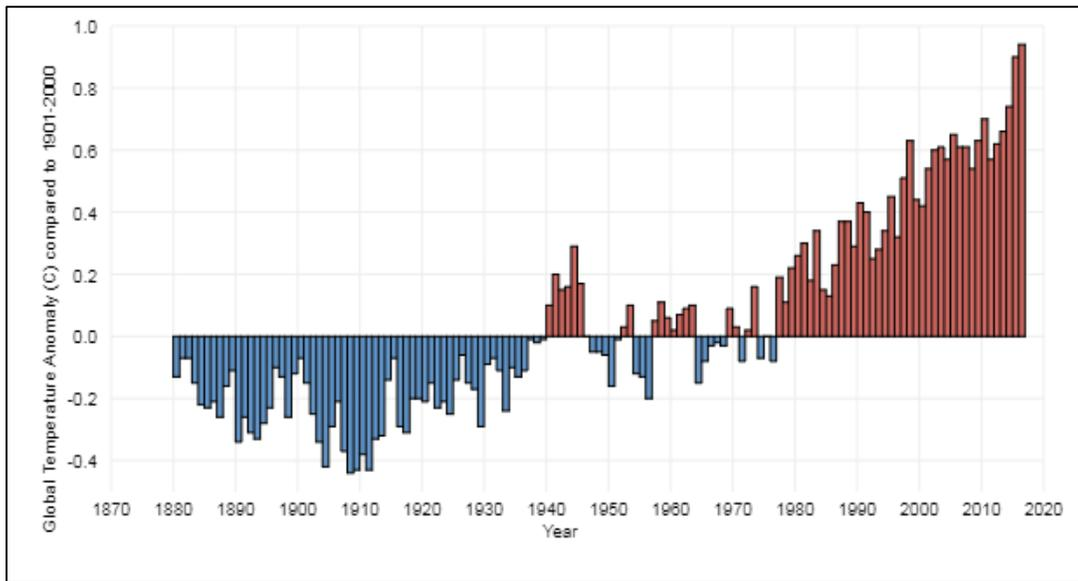


Figure 1 – History of global surface temperature since 1880 (Reprinted from Dahlman, 2017).

The effects of global warming can be extensive and disastrous as studies have suggested that climate change causes human casualties and economic losses. According to the report published by DARA in Climate Vulnerable Forum 2012, global warming includes economic losses of 1.2 trillion each year, which is about 1.6% from the global gross domestic product (GDP). This figure is expected to reach 3.2% of global GDP in 2030 (*Climate Vulnerability Monitor: A Guide to the Cold Calculus of a Hot Planet*, 2012).

Greenhouse effect has been recognized since the 1800s. In 1896, Swedish physicist Svante Arrhenius anticipated that carbon dioxide emitted from coal burning would warm the planet. Most of the climate scientists agree that carbon emissions are the main cause of global warming. Rising concentration of atmospheric CO₂ will trap heat, leading to global warming. A NASA satellite has been mapping the global atmospheric carbon

dioxide concentrations from 1st October to 11th November 2014 and it is shown in Figure 2.

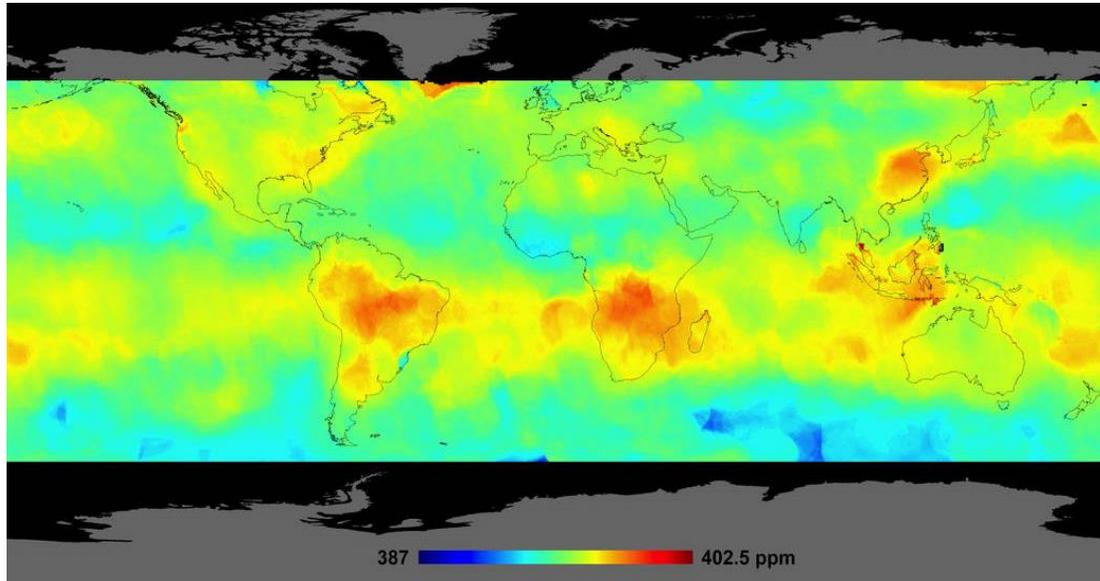


Figure 2 – Global atmospheric carbon dioxide concentrations from Oct. 1 through Nov. 1 as recorded by NASA’s Orbiting Carbon Observatory-2 (Reprinted from First Global Maps from Orbiting Carbon Observatory, 2014).

Swirls of CO₂ released by human activities are certainly noticeable. Recent data published by NOAA has indicated that CO₂ concentrations exceeded the threshold of 400 parts per million in 2016, which is illustrated in Figure 3 (Dahlman, 2017). Since global warming is real and dangerous, greenhouse emissions should be reduced. Mitigation policies should be implemented to control CO₂ emission.

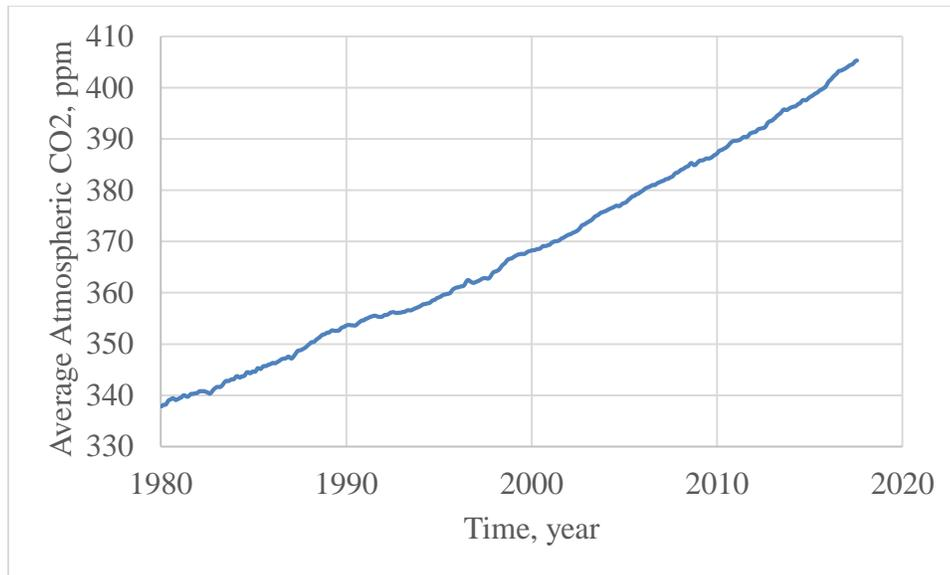


Figure 3 – Global monthly mean carbon dioxide averaged over marine surface sites (data source from NOAA).

2.2 Carbon Emission Mitigation Strategies

There are several policies developed and implemented by IEA to reduce greenhouse gases emission. IEA provided three scenarios: Current Policies, New Policies and the 450 Scenario (EIA, 2017). First, the Current Policies Scenario is a less likely outcome which takes into account only the implementation of mid-2015 policies with the assumptions that those policies remain unchanged. On the other hand, the New Policies Scenario is the most likely scenario which includes the current policies in-place and those that are currently planned. To limit the rise in the long-term average global atmospheric CO₂ concentration at 450 ppm in 2035, IEA introduced the 450 scenario. The 450 Scenario is aimed to limit the rise in the long-term average global temperature to 2°C.

The 450 Scenario is the lowest cost pathway to mitigate the CO₂ concentration level below 450 ppm in 2035. IEA World Energy Outlook report indicated that CO₂

emissions would drop from the “New Policies” to the “450” level by taking several initiatives (Figure 4). Carbon capture and storage (CCS) is anticipated to play an important role in achieving the lowest-cost pathway in mitigating CO₂ emissions, whose share in reduction should increase from 3% in 2020 to 22% in 2035.

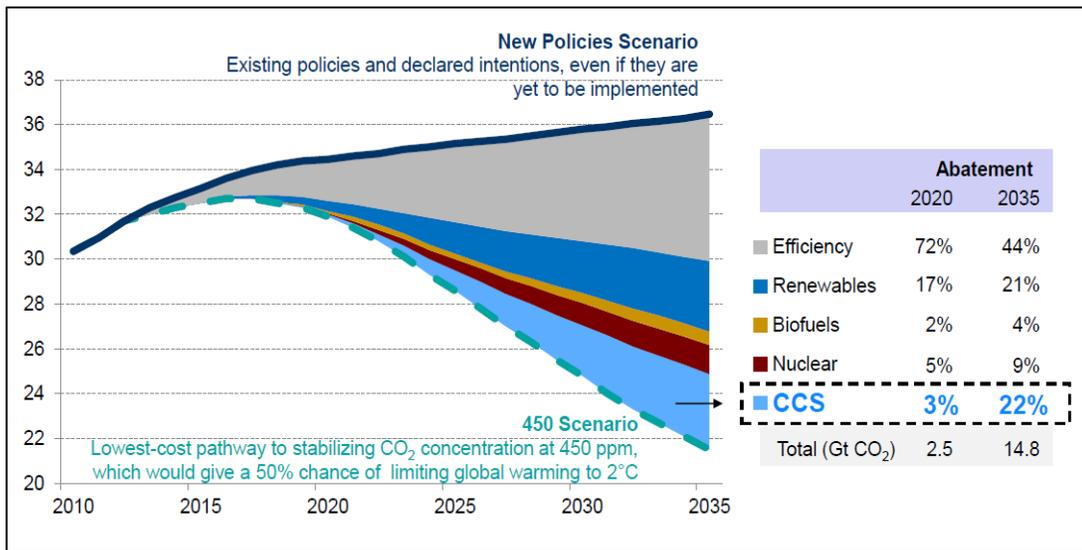


Figure 4 – CO₂ from the IEA’s 450 Scenario, relative to the New Policies Scenario with y-axis indicating the amount of CO₂ measured in Gigatonne (Reprinted from EIA, 2017).

Apart from IEA, the Congress, working with the Department of the Treasury, has enacted tax credit for carbon dioxide sequestration under section 45Q in 2008 (KPMG, 2017; Marshall, 2016). Section 45Q enables a per-ton credit for CO₂ stored in secure geological formation. The program offers an incentive of \$10 per metric ton of CO₂ stored through oil and gas EOR operations and \$20 per metric ton of CO₂ disposed in other geological storage (deep saline formation or salt cavern) without using CO₂ as a tertiary injectant (Marshall, 2016). To account for inflation, the section 45Q credit has been

adjusted to \$11.24 per metric ton of qualified CO₂ through EOR projects and \$22.48 per metric ton of qualified CO₂ for sequestration purposes in 2017 (KPMG, 2017). However, this tax incentive program will expire once 75 million tons of CO₂ are stored. According to the report filed with the IRS, as of May 10, 2017, the total amount of qualified CO₂ claimed under the section 45Q tax credit program is 52,831,877 metric tons (KPMG, 2017). Since the program is going to expire soon as it hits the limit of 75 million tons of qualified CO₂, oil and gas companies and environmental groups are pushing for permanent extension of the federal Section 45Q tax credit for carbon dioxide sequestration. Letter has been sent to the U.S. House Committee on Ways and Means to push for a legislative tax fix (Marshall, 2016).

2.3 Overview of Carbon Capture and Storage

Carbon capture and storage is a technology that allows up to 90% of the carbon dioxide emissions to be captured from the burning of fossil fuels in generating electricity such as hydrocarbon-fueled power plants or industry processes such as factories. The CCS process can be divided into three main parts, namely capture, transportation and storage. First, capture technologies permit the separation of CO₂ from flue gas by the means of three general methods, which include pre-combustion capture, post-combustion capture and oxyfuel combustion. The captured CO₂ is then transported to a storage site for sequestration. Storage sites have to be evaluated to ensure their safety, feasibility and security. There are several common storage sites: depleted oil and gas reservoirs, deep unmineable coal seams or deep saline aquifers, among others (Figure 5).

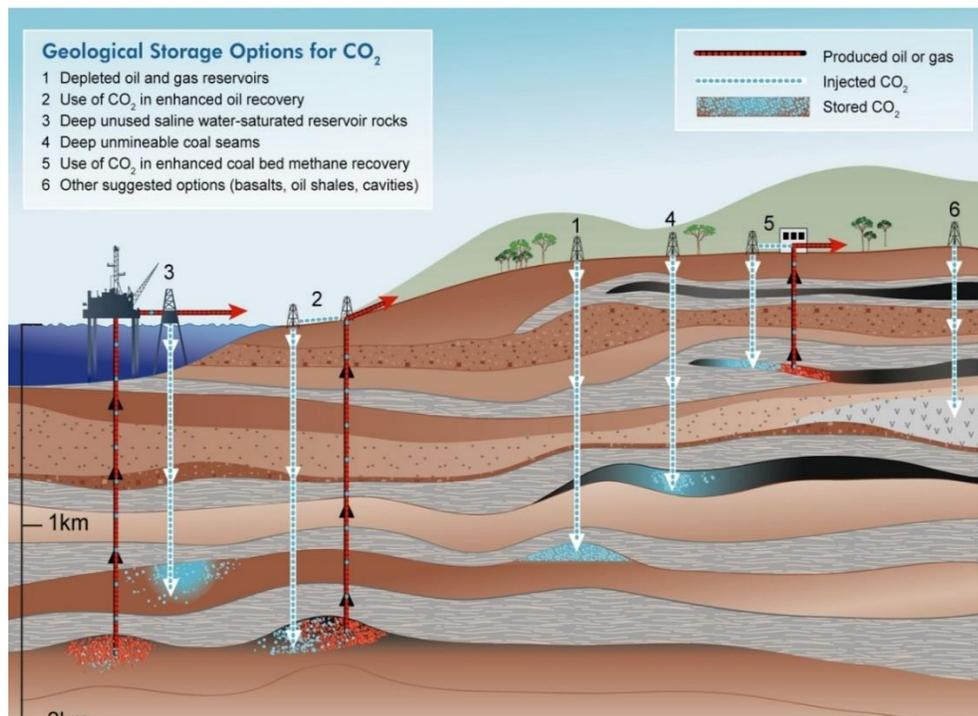


Figure 5 – Common storage site for CO₂ sequestration (Reprinted from Wallace and Kuuskraa, 2014).

There are several issues associated with CCS: CO₂ capture cost, formation storage capacity and uncertainty of the target formation properties. CO₂ capture technologies can be costly. There are four major technologies used for CO₂ capture: absorption, adsorption, cryogenic distillation, and membrane separation. All these technologies aim to capture and concentrate CO₂ efficiently with lower costs.

Besides, limited secured storage site possess challenge to CCS projects. Depleted oil and gas reservoirs are typically well characterized. However, the storage capacity is limited due to the size of the reservoirs. On the other hand, deep saline aquifer offers much greater storage capacity if compared to depleted oil and gas reservoir. Yet, the formations

are usually not well characterized and CO₂ storage densities are low. Researchers have been focusing on alternative storage sites such as deep ocean seafloors. However, since ocean seafloors are not enclosed and secured, there is a risk that injected and stored CO₂ might escape to the atmosphere.

The pace of industrial development of CCS is slow if compared to the target progress outlined by IEA to reach the objectives of the 450 Scenario. This is mainly due to the lack of economic incentive and stringent regulation to develop CCS projects.

2.4 Use of CO₂ in Enhanced Oil Recovery

Oil displacement by CO₂ flooding can be categorized as immiscible or miscible. (Martin and Taber, 1992). In partially miscible displacement (usually referred as immiscible), recovery mechanisms involve reduction in oil viscosity, oil swelling, and dissolved-gas drive. CO₂ miscibility with reservoir oils, however, is not achieved upon first contact in the reservoir. Minimum miscibility pressure (MMP) is long recognized as the key parameter in the displacement by gas injection (Holm and Josendal, 1974). CO₂ MMP is an important parameter for screening and selecting reservoirs for CO₂ injection projects and to simulate reservoir performance as a result of CO₂ injection (Yellig and Metcalfe, 1980). A good oil recovery may occur below MMP because CO₂ is very soluble in crude oil at reservoir pressure, resulting oil swelling and oil viscosity reduction. As miscibility is achieved through vaporizing-gas drive mechanism that CO₂ extract light and intermediate hydrocarbons from the oil, resulting low interfacial tension, the oil- and CO₂-phase flow together more easily. Achieving miscibility, by maintaining the reservoir

pressure above the minimum miscibility pressure (MMP) however, provides higher oil recovery. The process of miscible CO₂-EOR is depicted in Figure 6.

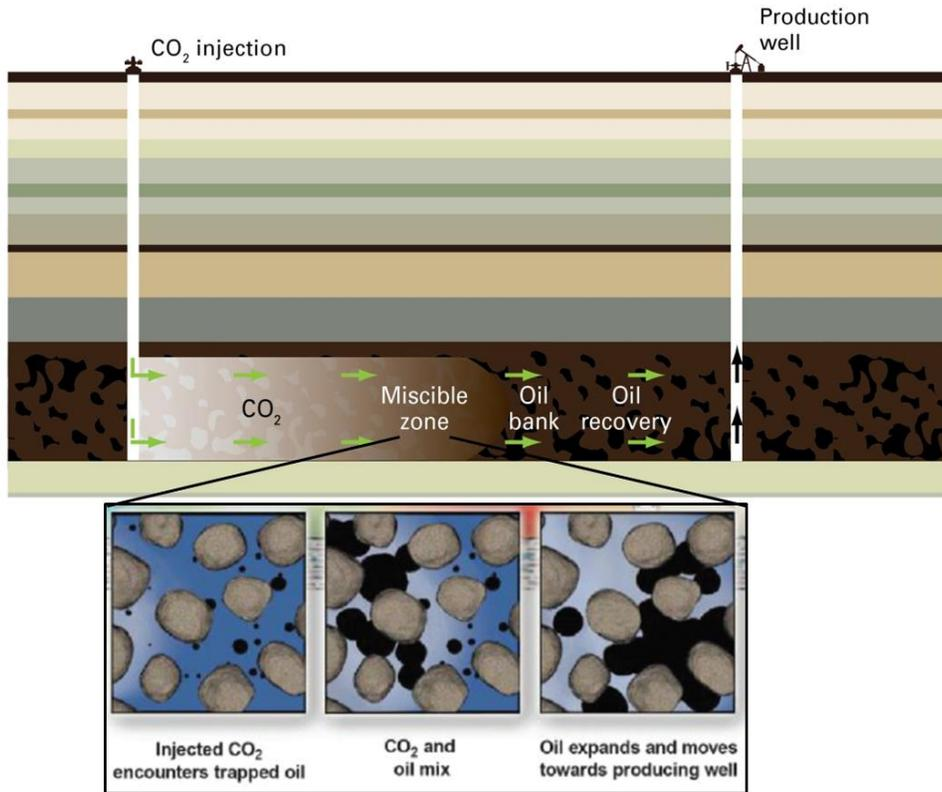


Figure 6 – Overview of the miscible CO₂-EOR process (Reprinted from Wallace and Kuuskraa, 2014).

Continuous injection of CO₂ will result in a breakthrough at the producer. Produced CO₂ is either separated from the natural gas and re-injected, or directly re-injected with the natural gas. At the end of the development project, CO₂ will be trapped by residual trapping or stored as free phase in the pore space. The CO₂ used in most EOR projects today is obtained from natural CO₂ domes due to its lower costs if compared to

carbon capture from power plants. Figure 7 displays the projected sources of CO₂ for EOR operations by 2020 (Wallace and Kuuskraa, 2014).

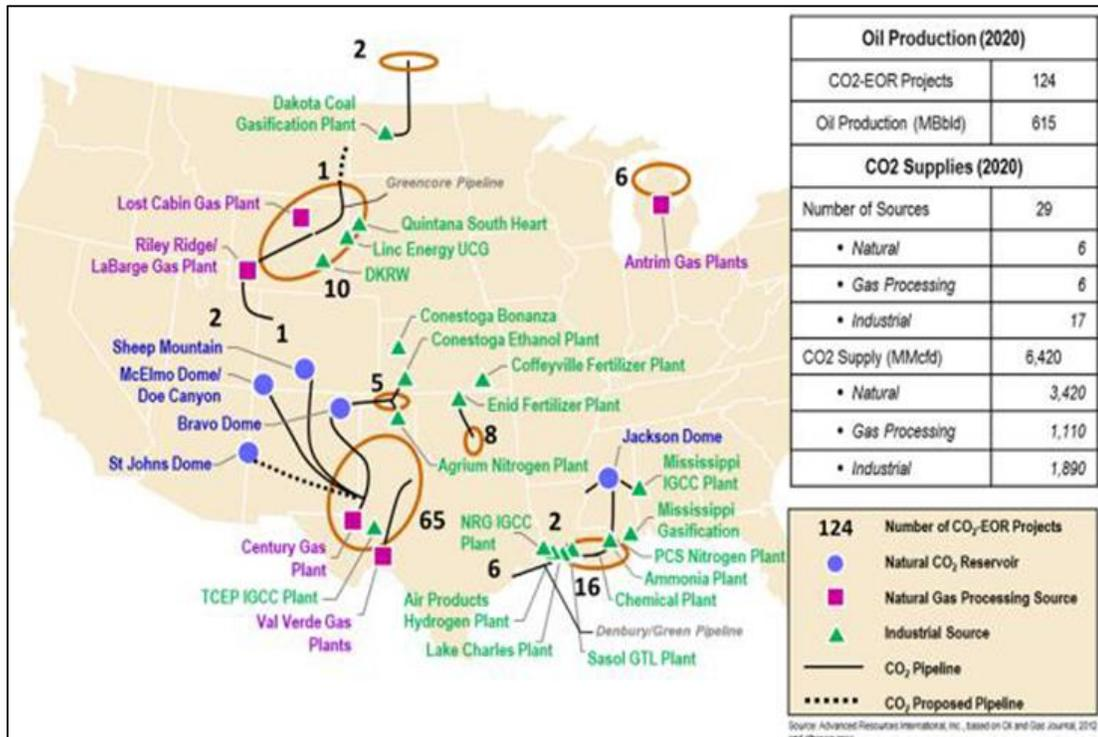


Figure 7 – Projected CO₂-EOR operations and CO₂ sources by 2020 in the United States (Reprinted from Wallace and Kuuskraa, 2014).

Among all the miscible recovery techniques, carbon dioxide enhanced oil recovery (CO₂-EOR) is preferred as it is a plausible option for utilizing anthropogenic CO₂ to increase oil production while storing CO₂ underground. Oftentimes, development strategies to recover more oil and store more CO₂ underground are completely opposite. Thus, more studies have to be done to identify optimum development strategies to recover hydrocarbon while storing considerable amount of CO₂ simultaneously.

2.5 Development Strategies of CO₂-EOR

The performance of CO₂ flooding is significantly influenced by the reservoir heterogeneity, which can reduce the sweep efficiency substantially. Unfavorable sweep efficiency will result in early breakthrough, leaving a significant portion of the reservoir oil unswept. Gravity segregation may occur in miscible EOR processes if the conditions are favorable. Favorable conditions include high vertical permeability, high vertical continuity, high density difference and low oil viscosity. Gravity segregation and override can occur in the reservoir as CO₂ is usually less dense than the reservoir oil. When the vertical communication is high, CO₂ tends to gravity segregate to the top of the reservoir unit and sweep the upper part of the reservoir (Healy et al., 1994). Thus, completion locations of both injector and producer wells have major impacts on the oil recovery in CO₂ flooding. Figure 8 shows the phenomena of viscous fingering and gravity segregation that occur commonly in CO₂ flooding, leading to unfavorable sweep efficiency.

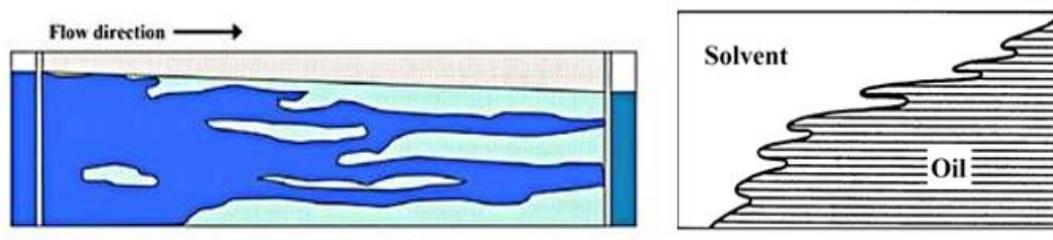


Figure 8 – Viscous fingering and gravity segregation lead to unfavorable sweep efficiency in CO₂-EOR process (Adapted from Wallace and Kuuskraa, 2014).

The performance of CO₂ flooding can be improved by allocating appropriate injected fluids to the injectors and by adjusting the produced fluids from the producers.

This process, which is known as rate control, is experience-demanding and time consuming due to the reservoir complexity and uncertainty. Optimization of the production-injection scheme is usually done by conducting numerous runs of reservoir simulations to determine a reasonable scheme.

Studies on maximizing sweep efficiency by using rate control have been conducted intensively. Sudaryanto and Yortsos (2001) applied optimal control theory to enhance the sweep efficiency for a system with two injectors and one producer at breakthrough in a two-dimensional miscible displacement. Gharbi (2004) coupled a three-dimensional reservoir simulator with an EOR expert system for identifying optimum reservoir management and production strategies in a CO₂ flooding carbonated reservoir. Salem and Moawad (2013) conducted economic studies on miscible CO₂ flooding by varying the injection rate. Chen et al. (2010) conducted optimization on CO₂ flooding production performance by optimizing the net present value (NPV) using a genetic algorithms where the injector well rates and producer flowing bottomhole pressure are selected as controlling variables. However, due to the complications and uncertainty of the field-scale problem, such optimization applications have been mostly limited to small-scale problems. Integration of geological properties, production strategies and economic evaluation causes the field-scale production optimization in a CO₂ flooding reservoir become more complex and difficult. Uncertainty in parameters such as fluid saturation distribution, permeability distribution, oil price and CO₂ price makes the field-scale production optimization even more challenging.

2.6 Grid Sensitivity in Compositional Reservoir Simulator

Oftentimes, obtaining useful estimates for enhanced oil recovery project in a field requires a full-field simulation model. However, grid-refinement sensitivity is an extremely intractable problem in many compositionally enhanced solvent simulations. The forecasted behavior in the reservoir alters as the simulation grid is refined. This behavior can be caused by numerical dispersion or by the inability to accurately resolve the size of solvent tongues or fingers with large grid blocks.

Past research indicated that physical dispersion is crucial in miscible gas displacement. Presently, most commercial compositional simulators used in miscible flooding studies are associated with large truncation errors, inducing what is widely known as numerical dispersion. Nonetheless, the artificial numerical dispersion induced is usually bigger than the real physical dispersion except if very fine grid blocks are set up for the simulations. In order for the numerical dispersion and real physical dispersion to have similar order of magnitude, the grid block size used in compositional simulations would have to be considerably small, especially in reservoir-scale problems. Studies regarding to the effect of numerical dispersion in miscible gas floods have been actively conducted as the resulting errors can cause inaccurate solutions and misleading physical displacement process. Fanchi (1983) concluded that numerical dispersion can induce truncation errors that result in composition and saturation dispersion. Stalkup et al. (1990) investigated the influences of numerical dispersion on the forecasts related to enriched-gas-drive displacements in reservoir-scale problems. Stalkup et al. (1990) conducted his studies based upon a classical three-component condensing gas drive by applying fluid

characterized by twelve components in two types of reservoirs. Results indicated that numerical dispersion induces a remarkably huge increase in recovery with increasing gas enrichment if the gas composition is higher than the multi-contact miscibility critical enrichment. According to Stalkup et al. (1990), it is plausible that the incremental oil recovery (over waterflood recovery) could be over predicted by as high as a factor of two to three. Furthermore, Jerauld (1998) conducted a study of the impact of grid resolution on simulation results and concluded that miscible flood recovery is more sensitive to vertical grid resolution. Thus, appropriate grid resolution is recommended to minimize run times and memory usage while still capturing the fundamental details of the miscible gas process.

However, the use of refined conventional grids is prohibitive in full-field reservoir simulation due to excessive computer memory and computation time. Local grid refinement can be used to overcome this problem. Fixed local grid refinement (LGR) was first introduced by Rosenberg (1982) where an original grid block was separated into four smaller elements. This local grid refinement technique considerably reduces the number of grid blocks and consequently decreases the computation time without the loss of accuracy. By using von Rosenberg's technique, local grid refinement can be extended to be dynamic-LGR, which has been considered by Heinemann et al. (1983). Static local grid refinement is often applied in cases with faults, pinch-outs, fractures and in the neighborhood of wells while dynamic local grid refinement is often applied to track the position of the displacement front. All this local grid refinement is aimed to reduce numerical dispersion.

CHAPTER III

RESERVOIR MODEL OF CO₂-EOR PROJECT

3.1 Reservoir Fluid

This section describes the fluid system and EOS model used in the simulation studies. Two reservoir fluids were used in conducting the simulations. Both fluids have been characterized and calibrated to match the original PVT data. Both fluids are characterized and calibrated by using six pseudo-components. All the EOS component critical properties for the light and heavy oil are given in Table 1 and Table 2 respectively.

Table 1 – Fluid properties of light reservoir oil used in the simulation study.

Pseudo-Components	Composition mol%	M _w lb/lbmole	Crit. P _c psia	Crit. T _c °R	Crit. Volume ft ³ /lb mole	Z _c
CO ₂	0.00237	44.010	909.5	777.1	2.530	0.276
C ₁ N ₂	0.45403	28.014	993.3	400.8	1.233	0.285
C ₂	0.06057	30.070	829.7	559.9	2.050	0.283
C ₃	0.05011	44.097	673.5	670.9	2.999	0.281
C ₄	0.02931	58.124	526.1	733.0	4.088	0.273
C ₅ ⁺	0.40361	100.130	427.2	965.5	5.896	0.243

Table 2 – Fluid properties of heavy reservoir oil used in the simulation study.

Pseudo-Components	Composition mol%	M _w lb/lbmole	Crit. P _c psia	Crit. T _c °R	Crit. Volume ft ³ /lb mole	Z _c
CO ₂	0.00037	44.010	909.5	777.1	2.530	0.276
C ₁ N ₂	0.01425	16.846	975.6	402.8	1.223	0.276
C ₂	0.01641	30.070	829.7	559.9	2.050	0.283
C ₃	0.05176	44.097	673.5	670.9	2.999	0.281
C ₄	0.11629	66.310	505.9	784.7	4.563	0.274
C ₅ ⁺	0.80092	224.084	239.5	1342.4	14.074	0.234

The lighter reservoir fluid has a bubble point of 2054 psi while the heavier reservoir fluid has a bubble point of 174.6 psi at reservoir temperature of 300°F. The phase envelopes for the light oil and heavy oil are shown in Figure 9 and Figure 10 below respectively. At initial reservoir condition, both reservoir fluids are under-saturated.

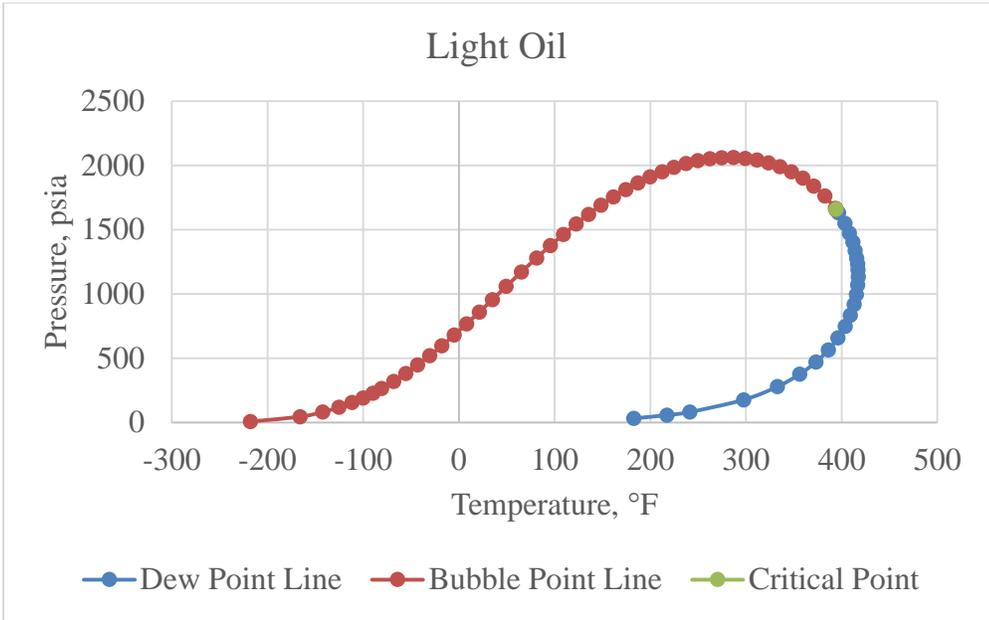


Figure 9 – Phase envelope for the light oil used in the study.

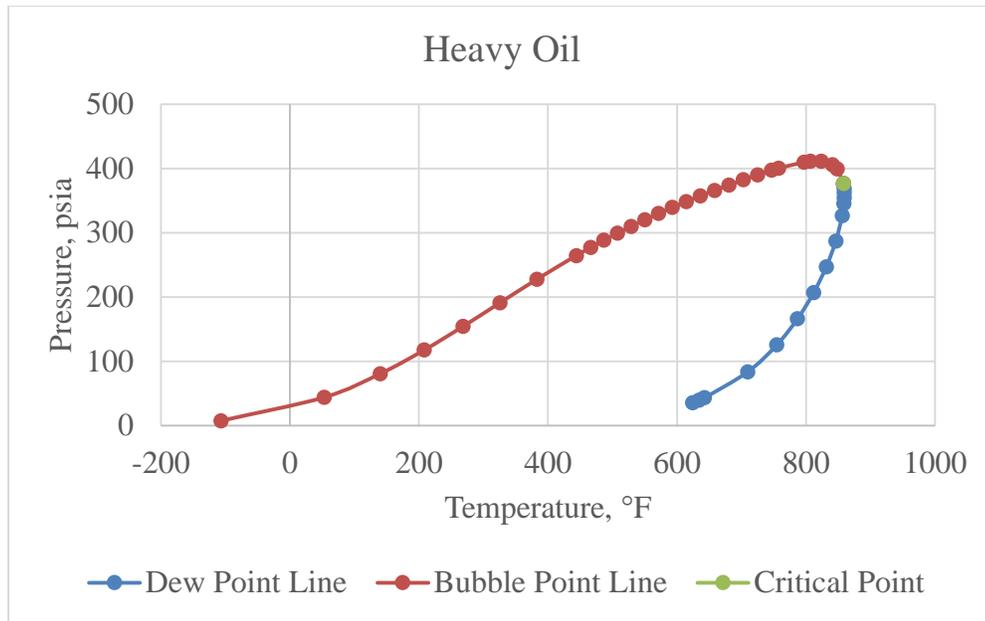


Figure 10 – Phase envelope for the heavy oil used in the study.

The most reliable way to determine the true thermodynamic MMP/MME is by performing a series of slim tube displacement experiments. However, in this study, PVTi has been used to evaluate the thermodynamic MMP by using EOS. The MMP for the light oil is evaluated to be around 2054 psi while the MMP for the heavy oil is 474 psi at reservoir temperature.

3.2 Reservoir Model

For simulation study, Eclipse 300 module (composition model) in Geoquest software will be used. The reservoir model chosen is an 1574-acres spacing, 5-spot well pattern, in a reservoir with no slant.

3.2.1 The Pattern

The pattern chosen in this study is a 5-spot well pattern, which is common for miscible gas EOR projects. There are one injector well, located in the middle of reservoir and four producer wells. The pattern and dimensions used are shown in Figure 11 below.

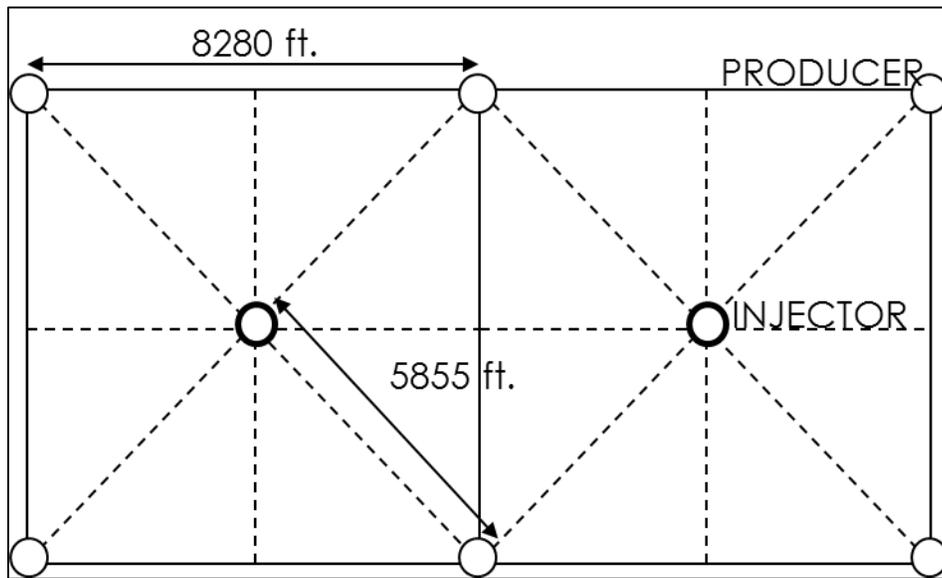


Figure 11 – The 5-spot pattern and its dimensions used in this simulation study.

For the 1574-acre spacing, the distance between a producer and an injector is 5855 feet, and the distance between two consecutive injectors or producers is 8280 ft.

3.2.2 The Grid

Figure 12 illustrates the grid of the model consisting of $17 \times 17 \times 23$ cells in total, i.e. 6647. The cell dimensions are 690 ft \times 690 ft \times 21 ft in the x, y and z directions respectively. The grid configuration used in this study is coarse as the single cell dimension is relatively large.

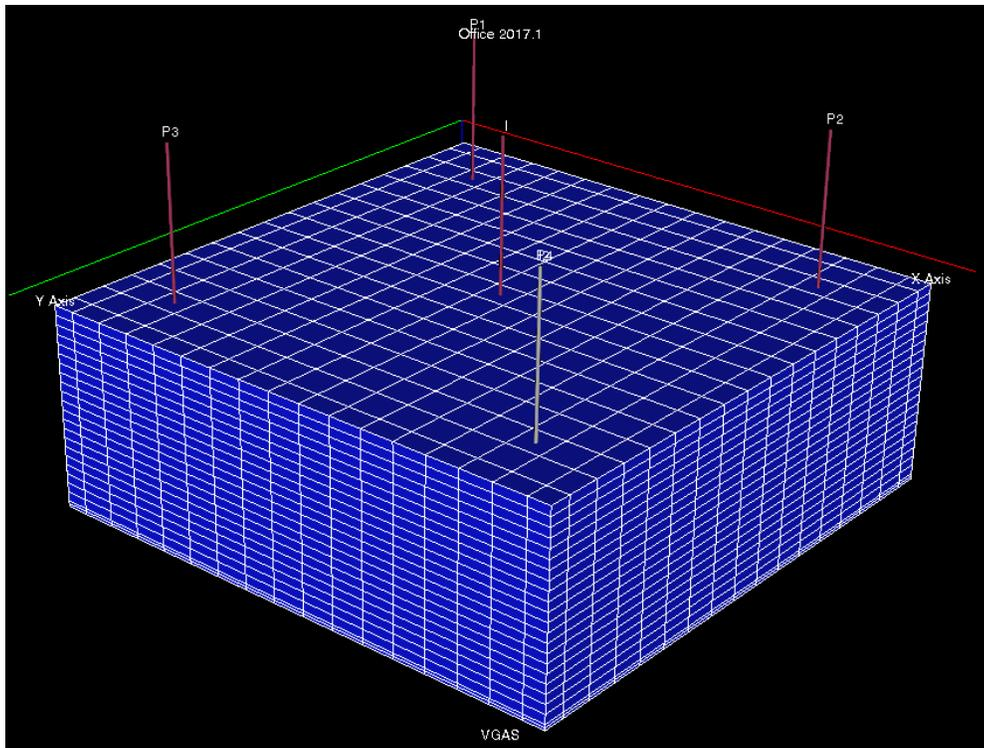


Figure 12 – Visualization of the grid configuration.

To conduct study for local grid refinement, grid around the wells have been refined to capture the fluid behavior more accurately around the well where the velocity gradients are more pronounced. The local grid refinement area around each well is set to 2070 ft × 2070 ft, i.e. 3 cells by 3 cells (Figure 13). Local grid refinement is applied to the z-dimension, by separating every 23 layers into 2 layers each, making a total of 46 layers.

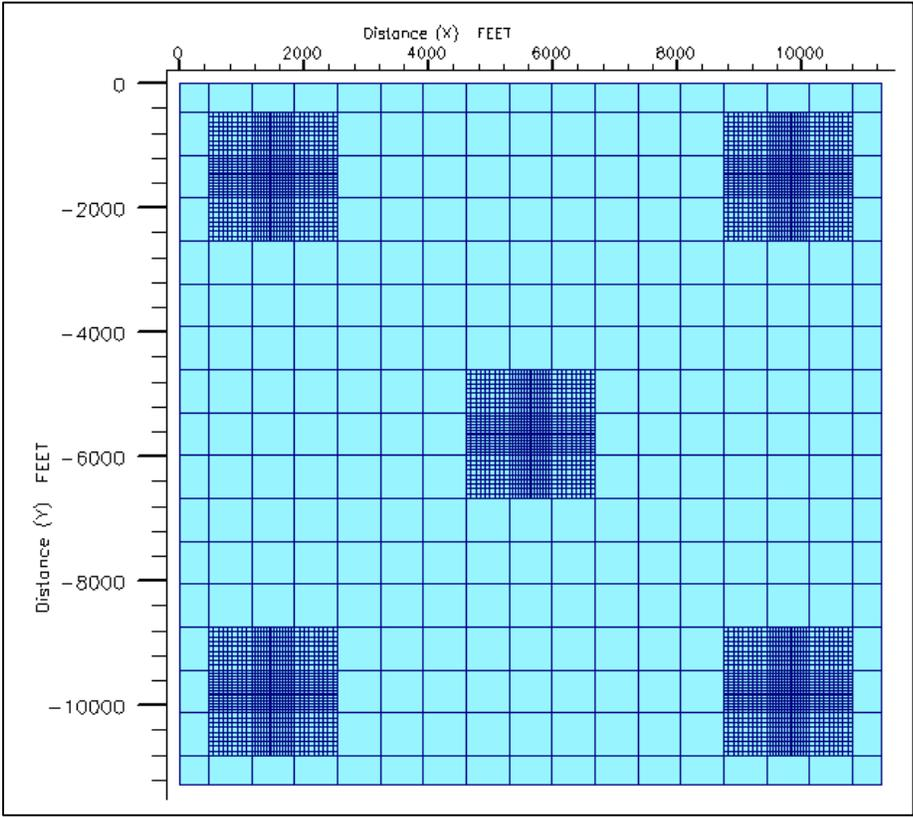


Figure 13 – Local grid refinement setup for the simulation (top view).

3.2.3 Petrophysics

The reservoir model used in this study has similar petrophysical properties as most of the conventional reservoirs in the United States. The porosity of the reservoir varies across each layer. The permeability of the reservoir is considered heterogeneous. The degree of heterogeneity is measured using Dykstra-Parsons coefficient (V_{DP}), which is defined as:

$$V_{DP} = 1 - \exp(-s) \quad \dots\dots\dots (1)$$

Where s in the equation above is the standard deviation of natural log of the horizontal permeability for each layer, as indicated below.

$$s = STDEV(\ln k_i) \quad \dots\dots\dots (2)$$

Dykstra-Parsons coefficient varies from 0 to 1. A fully homogenous reservoir will have a Dykstra-Parsons coefficient of 0. On the other hand, a highly heterogeneous reservoir will have a Dykstra-Parsons coefficient close to 1. Most of the reservoir rocks in the United States have a Dykstra-Parsons coefficient higher than 0.7 (Sahni et al., 2005). The vertical permeability for each layer is set to be one-tenth of the horizontal permeability, making the k_v/k_h ratio to be 0.1. The net reservoir thickness is about 452.85 feet. The porosity, permeability and rock compressibility of the reservoir are summarized in Table 3 below.

Table 3 – Summary of petrophysical properties of the reservoir model.

Petrophysical Properties	
Weighted-average Porosity	13.4%
Weighted-average Permeability	291 mD
V_{DP}	0.788
Rock Compressibility	$4 \times 10^{-6} \text{ psi}^{-1}$

3.2.4 Relative Permeabilities

Generally, the initial relative permeability is defined by using a three-phase relative permeability model. However, the water saturation in the reservoir rock is considered to not exceed its irreducible value, i.e. the water is immobile and only exists in the pore space. Thus, the relative permeability model used in the study only consider two-phase relative permeability model, which include only oil and gas relative permeability curves (shown in Figure 14).

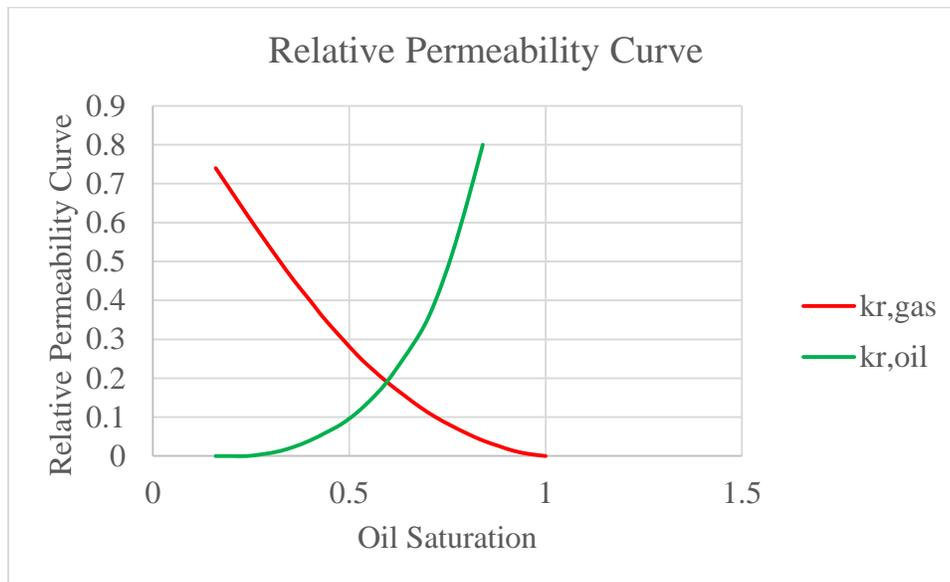


Figure 14 – Relative permeability curves used in this work.

3.2.5 Reservoir Initialization

The model is initialized with the parameters corresponding to the fluid sample. Thus, the reservoir initializations for both fluids (light and heavy oil) are different. For the

light oil, the initial reservoir pressure is fixed at 4128 psi with a reference depth of 9,554 feet, which corresponds to the top of the reservoir. The light oil model has a pore volume of 1393.2 MMresbbl. The original-oil-in-place for the light oil model is 574.1 MMSTB, contributing to about 181.8 MSTB/acre of oil.

For the heavy oil, the initial reservoir pressure is fixed at 5168 psi with a reference depth of 11,964 feet, which corresponds to the top of the reservoir. The heavy oil model has a pore volume of 1393.2 MMresbbl. The original-oil-in-place for the light oil model is 1331 MMSTB, contributing to about 421.4 MSTB/acre of oil. For both cases, there is no water or aquifer at the bottom of the reservoir. The reservoir temperature is set to be 300°F for both cases. All the reservoir initialization parameters are summarized into Table 4 below.

Table 4 – Initialization of parameters in the reservoir model.

Reservoir Parameters	Light Oil	Heavy Oil
Initial Reservoir Pressure (IP), psi	4128	5168
Reference Depth for IP, ft	9554	11964
Pore Volume, MM resbbl	1393.2	1393.2
Original oil in place, MM STB	574.1	1331

CHAPTER IV

RESERVOIR RESPONSE TO PRODUCTION/INJECTION CONSTRAINTS

After fluid and reservoir models have been characterized, simulations are conducted. The simulation starts on 1st January 2017 and ends on 1st January 2037, with a production period of 20 years in total. Cases with production under natural depletion (no CO₂ injection) will be the reference case in this study. All incremental recovery and NPV calculated are based upon the results obtained from the reference cases (light and heavy oils). For the cases with CO₂ injection, the injector bottomhole pressure is maintained at 7500 psi, which is well above the minimum miscibility pressure (MMP). All CO₂ injections are maintained at a constant rate through the production until the simulation ends. Other injection variables include injection rate, recycling of produced gas and injection initiation time. The effects of production constraints on reservoir behaviors have also been studied. These include producer bottomhole pressure, target oil rate and gas rate limit. The influences of these injection and production constraints on oil production rate, gas production rate and reservoir pressure will be discussed later in this chapter.

4.1 Reference Case – Natural Depletion

For the reference case, the reservoir is produced under natural depletion without CO₂ injection. Both light and heavy oil reservoirs will be produced under the same production constraints for 20 years listed in Table 5.

Table 5 – Operating constraints for the reference cases in light and heavy oil reservoirs.

Operating Constraints		
Injector BHP Max	7500	psia
Producer BHP Min	1200	psia
Producer Oil Target Rate (minimum)	20	MSTB/day

Since the bottomhole pressure of the producer is set lower than the average reservoir pressure, the oil will be produced under natural depletion until there no longer is pressure support. The production rates and reservoir pressure for the light oil reservoir are shown in Figure 15.

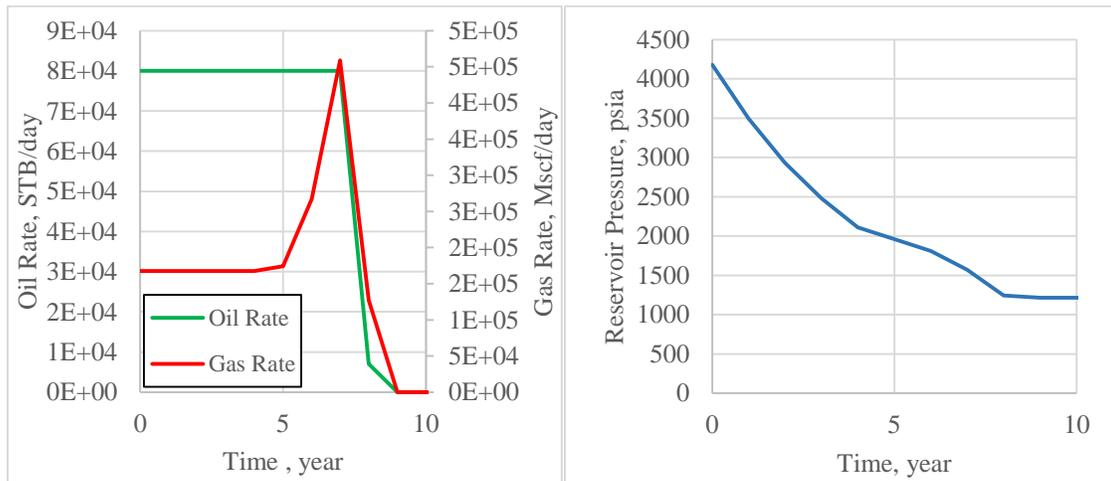


Figure 15 – Production rates and pressure of the light oil reservoir producing under natural depletion.

The initial reservoir pressure is at 4178 psia. Thus, oil production is able to achieve the target oil rate and maintains for about 7 years. Gas production is constant at the beginning and increases to a peak at the 7th year as more oil is produced. Reservoir

pressure starts to drop steadily as more oil and gas are being produced. As the reservoir pressure approaches the minimum producer bottomhole pressure, the production plummets dramatically. Subsequently, the reservoir stops producing oil and gas. The reservoir does not have enough pressure support for further production under natural depletion. Natural depletion can only last for about 8 years in light oil reservoir in this case. Similar observations can be obtained from the heavy oil reservoirs. Figure 16 shows the production rates and reservoir pressure over time for the reference case in heavy oil reservoir.

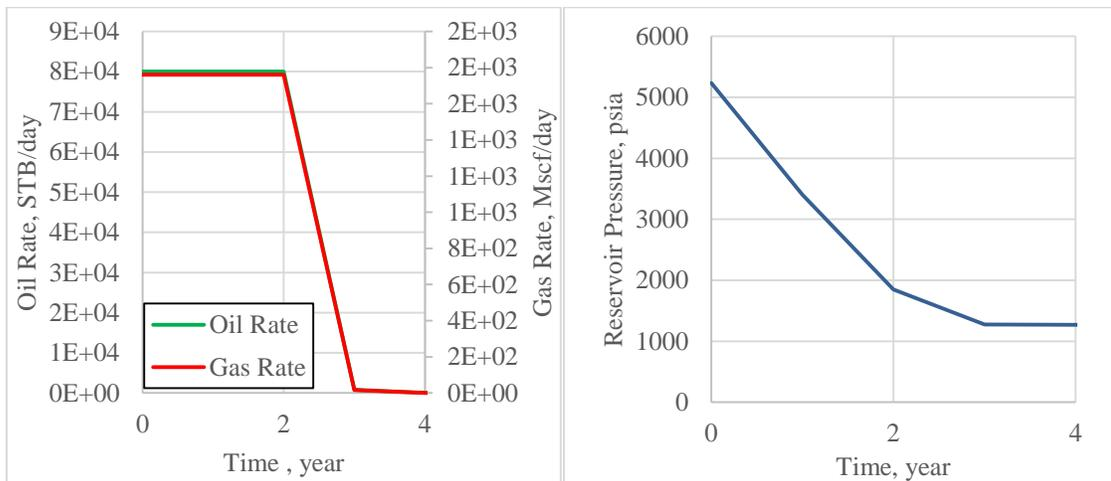


Figure 16 – Production rates and pressure of the heavy oil reservoir producing under natural depletion.

Compared to the light oil reservoir, the heavy oil reservoir has higher initial reservoir pressure, which is set at 5236 psia. However, higher initial reservoir pressure does not guarantee longer period of production under natural depletion. As soon as the production is initiated, both oil and gas are produced at constant rates. However, the

reservoir pressure drops significantly and soon approaches the minimum producer bottomhole pressure. Thus, the heavy oil reservoir is only able to produce for about 3 years under natural depletion even though significant portion of the heavy oil is still left within the reservoir. Therefore, CO₂-EOR is applied in both light and heavy oil reservoir to recover the hydrocarbon that is unable to be produced under natural depletion.

4.2 Injection Rate

To improve the recovery factor, CO₂ is injected into the reservoirs to enhance the oil mobility by achieving miscibility. CO₂ is injected at constant rate since the beginning till the end of the production. Different injection rates will lead to varying injection pore volumes, inducing significantly different reservoir responses. To study the effects of injection rates on reservoir behaviors, several injection rates have been applied while keeping other variables constant. Table 6 shows the operating conditions that have been kept constant for all injection rate cases.

Table 6 – Summary of the operating constraints for all injection rate cases.

Operating Constraints		
Injector BHP Max	7500	psia
Producer BHP Min	1200	psia
Producer Oil Target Rate (minimum)	20	MSTB/day
Producer Gas Rate Limit	No Limit	
Start of Injection	0	year
End of Injection	20 th	year

For light oil, the injection rates vary from 100 MMscf/day to 400 MMscf/day, with injection pore volumes range from 0.4 to 1.5. Several injection rates with their respective reservoir behaviors are summarized in Figure 17.

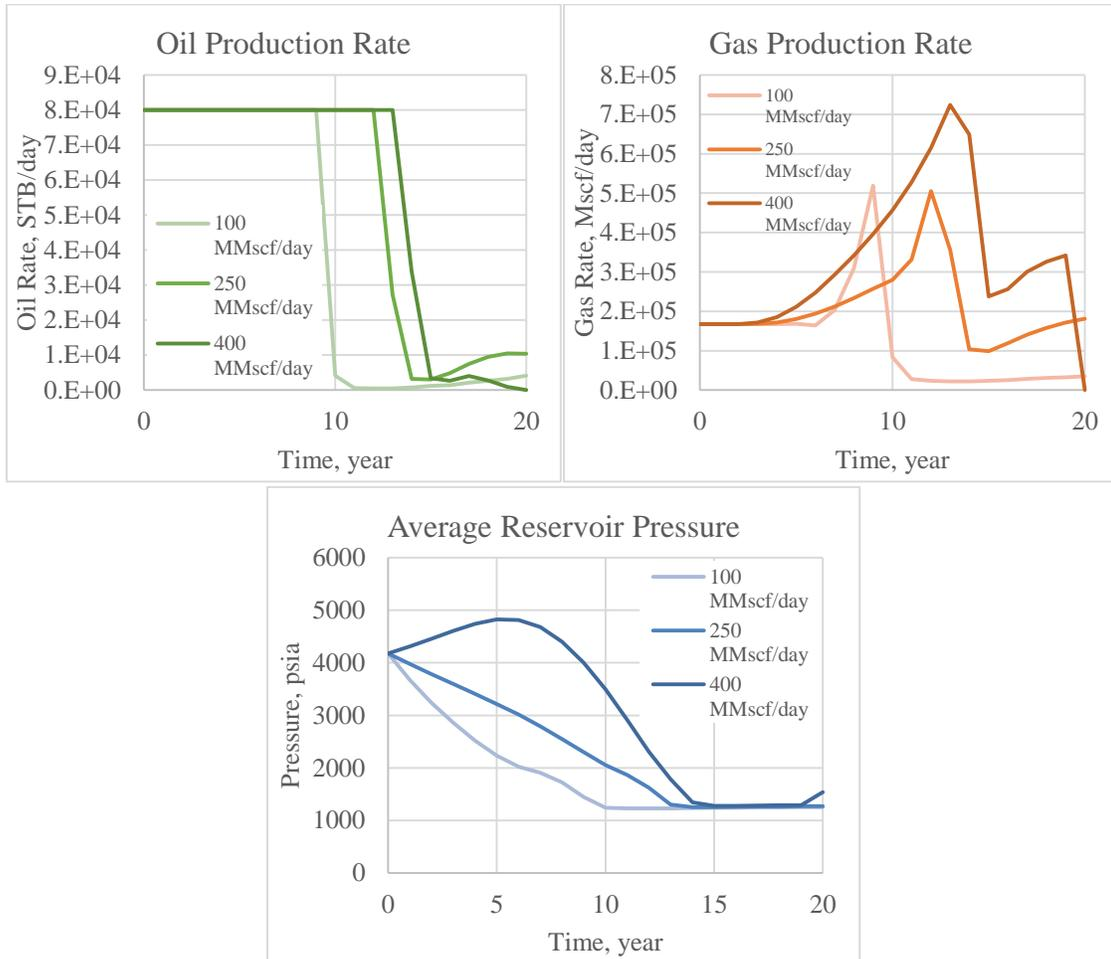


Figure 17 – Changes in oil production rate, gas production rate and reservoir pressure due to different injection rates in light oil reservoir.

The reservoir is able to produce for 20 years due to CO₂ injection. Higher injection rate will prolong the production period at target oil rate. However, the oil rates drop dramatically when the reservoir pressure hits the minimum operating bottomhole pressure

for producers. Apart from improving the oil mobility, the injected CO₂ provides additional pressure support to the reservoir, leading to higher oil production overall. High injection rate may even increase the pressure higher than the initial reservoir pressure. Thus, the injection will be constrained and paused if the reservoir pressure exceeds the maximum allowable bottomhole pressure for injector. Higher CO₂ injection rate will lead to higher gas production as CO₂ breakthrough occurs at the producers.

For heavy oil, the injection rates vary from 100 MMscf/day to 300 MMscf/day, with injection pore volumes range from 0.4 to 1.2. Several injection rates with their respective reservoir behaviors have been summarized in Figure 18. The reservoir responses to different injection rates in heavy oil reservoir differ slightly from the ones exhibited in light oil reservoir. The oil production rates are maintained at target rate in the beginning. However, as the reservoir pressure drops, the oil production rates drop steadily. The declines in oil production rates are not as sharp and dramatic as the ones illustrated in light oil cases. Similarly, as the CO₂ injection rate increases, the gas production rate also increases as more CO₂ will be produced after breakthrough. The changes in reservoir pressure are significant as the CO₂ injection rate increases. At a constant injection rate of 100 MMscf/day, the reservoir pressure declines steadily and reaches the minimum after 10 years of production. However, as the CO₂ injection rate increases, the reservoir pressure increases and hits the maximum at 7500 psia. CO₂ injection is paused as the reservoir pressure exceeds the maximum allowable BHP for injector. Continuous oil and gas production will then reduce the reservoir pressure as CO₂ injection is halted. The CO₂ injection is then reinitiated as the reservoir pressure reduces.

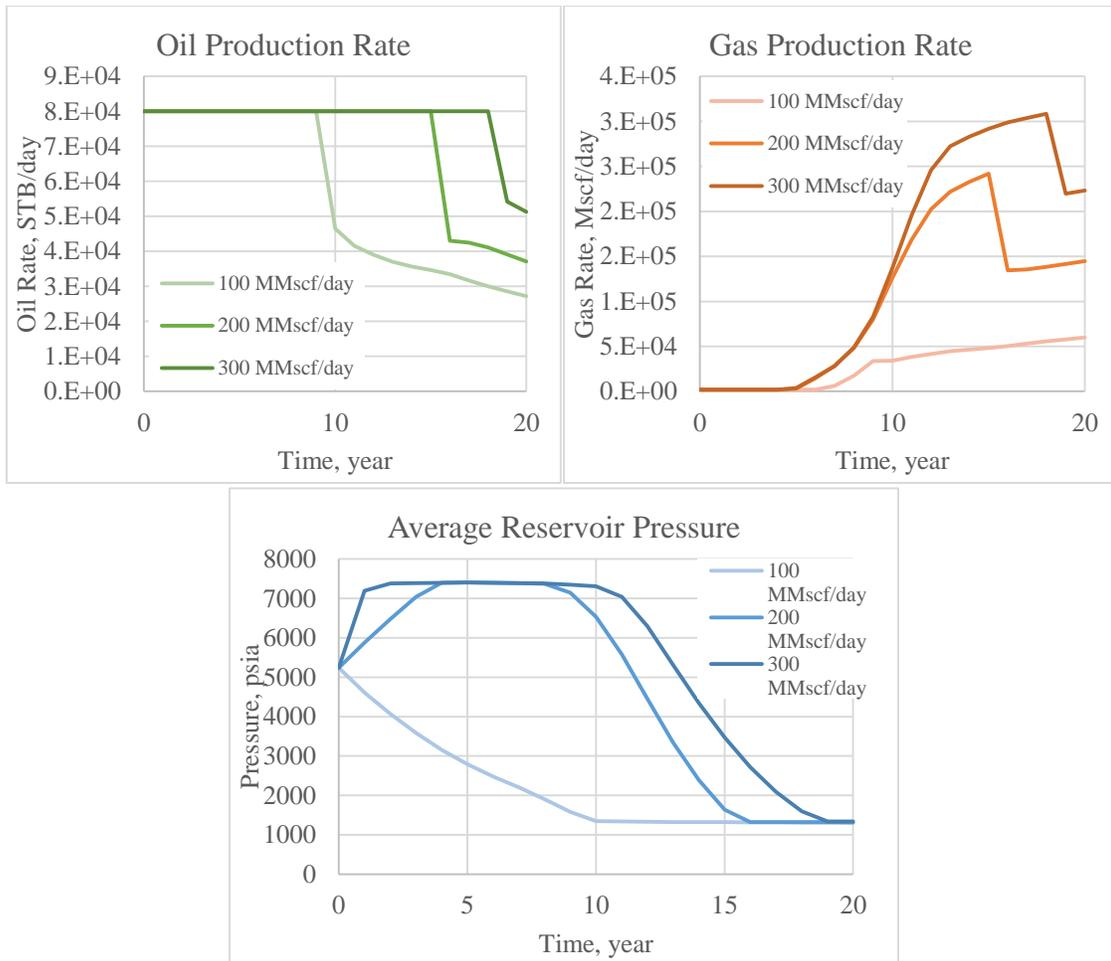


Figure 18 – Changes in oil production rate, gas production rate and reservoir pressure due to different injection rates in heavy oil reservoir.

4.3 CO₂ Recycling

As more CO₂ is injected into the reservoirs, the gas production at the producers will increase due to CO₂ breakthrough. The produced gas generally has high concentration of CO₂ with little hydrocarbon components. Large amount of CO₂ will be lost if the produced gas is not re-injected back into the reservoir. Figure 19 shows the molar composition of each component for the produced gas in light oil reservoir.

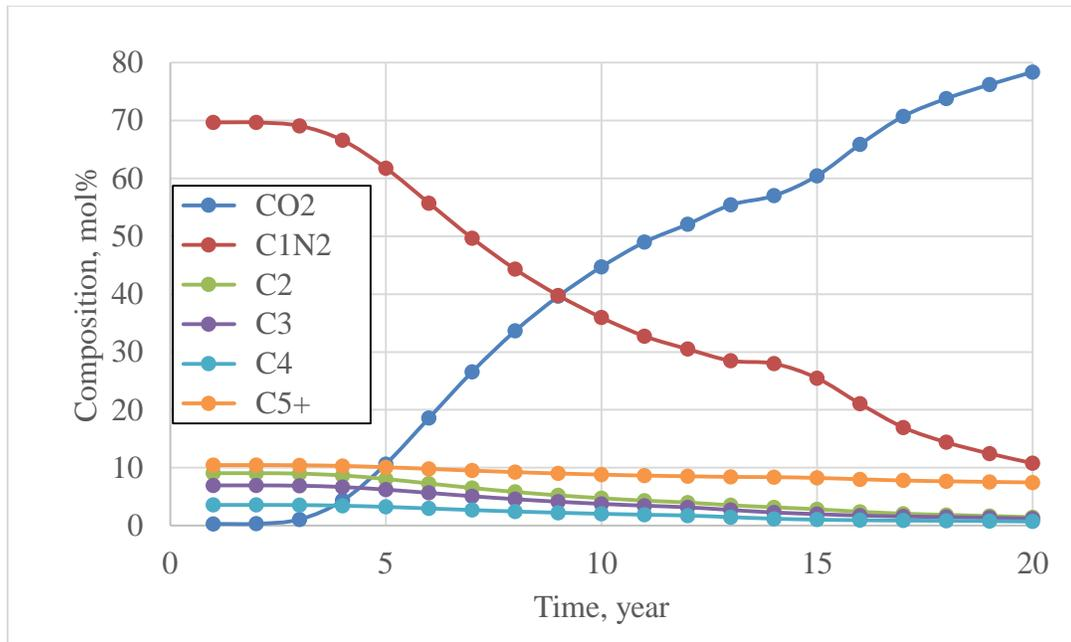


Figure 19 – Molar compositions of the gas produced for 20 years in light oil reservoir.

Initially, the gas produced consists mainly of light hydrocarbon and nitrogen. CO₂ breakthrough can be observed at the third year. After CO₂ breakthrough, the molar composition of CO₂ increases steadily. After 20 years of production, the molar composition of CO₂ in the gas produced can be as high as 78%. On the other hand, the molar composition of each component for the produced gas in heavy oil reservoir is shown in Figure 20.

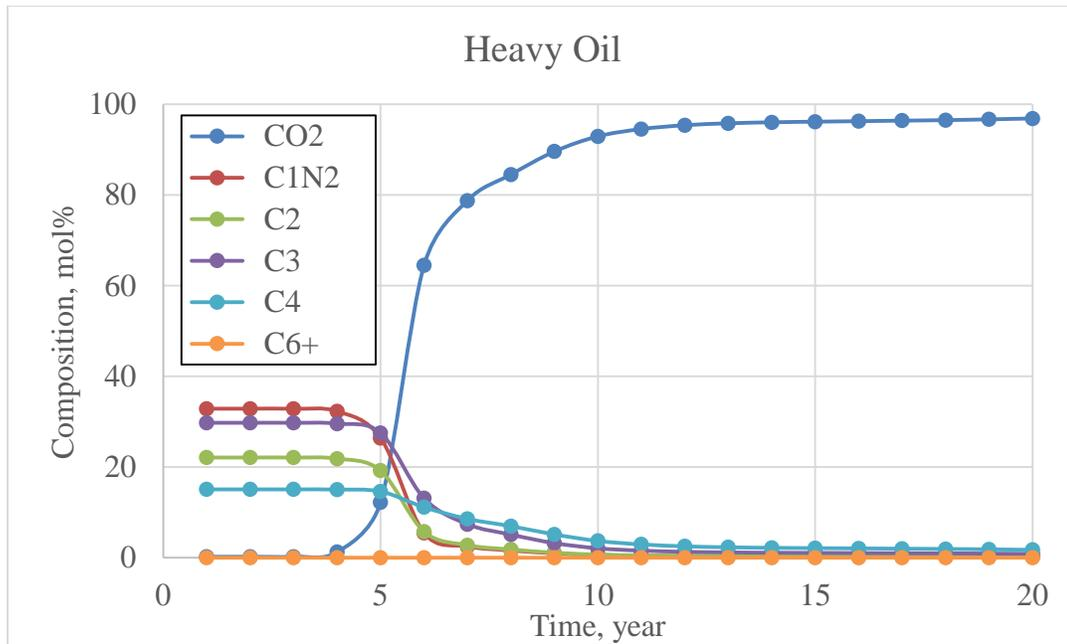


Figure 20 – Molar compositions of the gas produced for 20 years in heavy oil reservoir.

At the beginning of the production, the gas composition is mainly dominated by light hydrocarbon components. However, due to CO₂ breakthrough at the fourth year, the molar compositions of light hydrocarbon components reduce dramatically. After breakthrough, CO₂ composition increases dramatically and dominates the composition of the produced gas. At the end of the production, the molar composition of CO₂ can be as high as 97%.

Without recycling the produced gas, most of the CO₂ will be lost together with the produced gas. Thus, to maximize the utility of purchased CO₂, the gas produced, which is high in CO₂ concentration, is reinjected back into the reservoir. This is done by converting one of the existing producers into an injector when the CO₂ molar fraction in the produced gas exceeds 10%. All the produced gas will then be reinjected back into the reservoirs

through the converted producer while the middle injector will continue injecting pure CO₂ at a constant rate. Thus, the total amounts of pure CO₂ purchased in the cases with and without recycling are the same. The difference in production performance are solely due to the effect of recycling gas produced. The operating conditions for all cases with and without recycling in both light and heavy oil reservoir are summarized in Table 7. Figure 21 shows the reservoir responses to CO₂ recycling in light oil reservoir with a constant injection rate of 250 MMscf/day for the middle injector.

Table 7 – Operating constraints for all CO₂ recycling cases in light and heavy oil reservoir.

Operating Constraints		
Injector BHP Max	7500	psia
Producer BHP Min	1200	psia
Producer Oil Target Rate (minimum)	20	MSTB/day
Producer Gas Rate Limit	No Limit	
Start of Injection	0	year
End of Injection	20 th	year

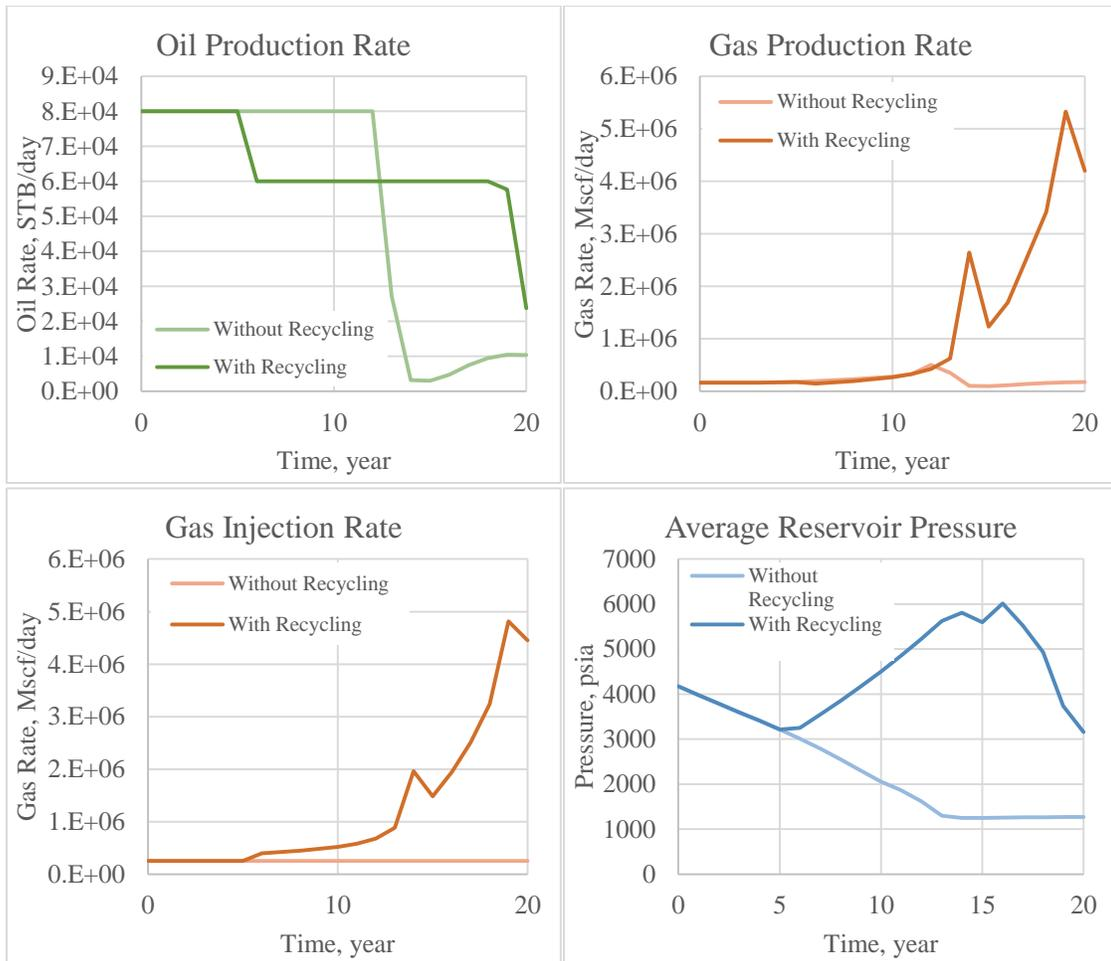


Figure 21 – Changes in oil production rate, gas production rate, gas injection rate and reservoir pressure due to CO₂ recycling in light oil reservoir.

There are significant differences between the case with and without recycling. First, the total gas injection rate increases tremendously as the produced gas is reinjected into the reservoir. For the case without recycling, the injection rate stays constant throughout. For the case with recycling, the gas injection rate follows the profile of gas production rate after the trigger of recycling produced gas is activated. The gas produced in the case with recycling is significantly larger than the one without recycling. As produced gas is reinjected back into the reservoir, more gas will achieve breakthrough at

the producer. The produced gas injected will not only enhance the miscibility, but also helps maintaining pressure. The reservoir pressure declines initially as gas and oil are being produced out of the reservoir. However, when the gas produced is reinjected, the reservoir pressure increases subsequently. The increase in reservoir pressure helps with the oil production. For the case without recycling, the oil production rate will maintain at target rate at first and reduce dramatically as the reservoir pressure hits the minimum limit. However, for the case with recycling, the oil production rate decreases in steps. The declines in oil production rate is more gradual if compared to the ones without recycling.

Similar runs have been conducted in heavy oil reservoir to identify the reservoir behaviors. Figure 22 shows the reservoir responses in heavy oil case when the injection rate of the middle injector is fixed at 100 MMscf/day. Similar reservoir responses are obtained from the heavy oil reservoir. The injection rate stays constant in the case without recycling. For the case with recycling, the injection rate stays constant at the beginning and then increases, following the gas production rate profile. As the gas molar fraction of CO₂ produced at the producer exceeds 10%, all the gas produced is recycled and reinjected back into the reservoir. Further recycling and reinjection cause the gas production rate to increase substantially. The case with recycling has better pressure maintenance if compared to the case without recycling. The pressure reduces due to production at the beginning. However, the reservoir pressure is maintained at higher pressure for the case with recycling due to the reinjection of produced gas. The increase in reservoir pressure will enhance the oil production, where the oil production rate decreases in steps instead of declining significantly over time.

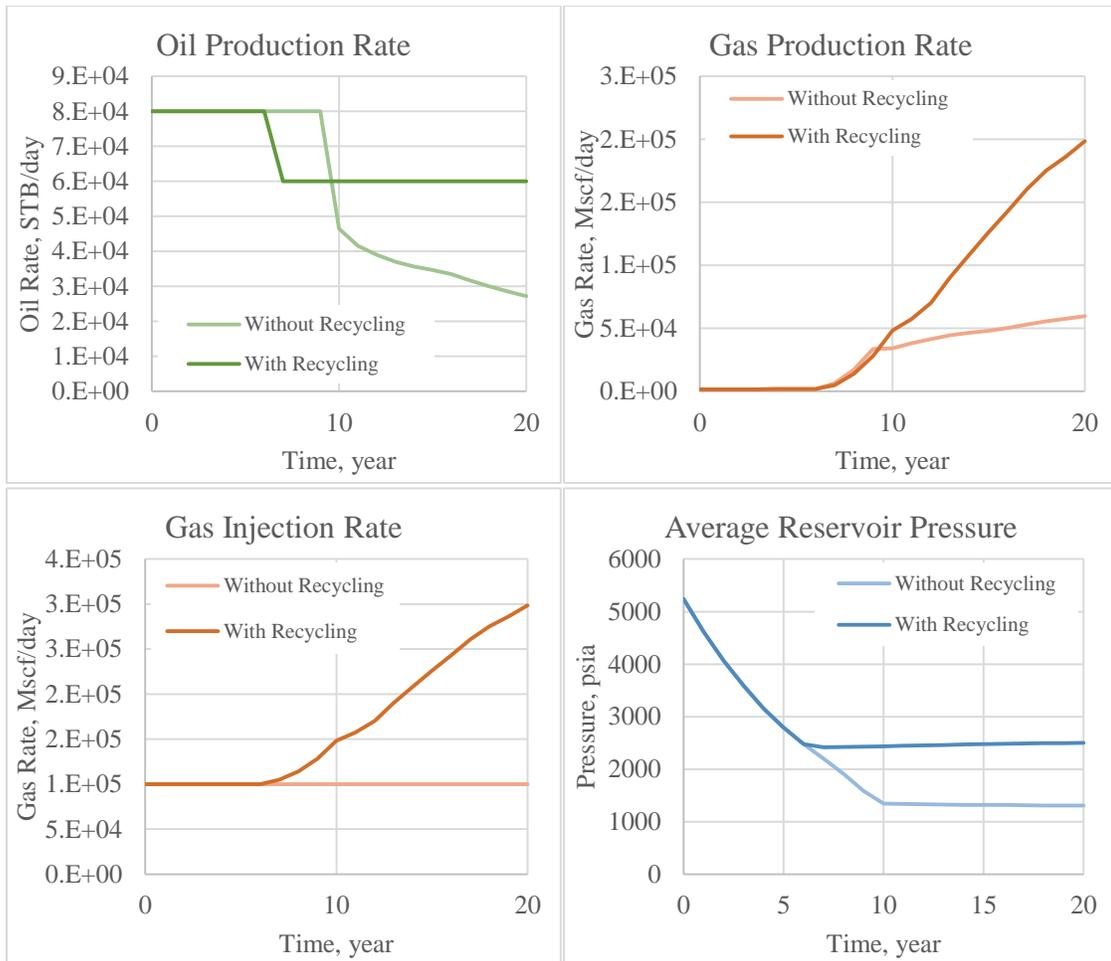


Figure 22 – Changes in oil production rate, gas production rate, gas injection rate and reservoir pressure due to CO₂ recycling in heavy oil reservoir.

4.4 Injection Initiation Timing

CO₂-EOR is considered a tertiary recovery, where it is generally applied after primary and secondary recovery. However, the injection initiation time may have effects on the production performances. Throughout production, reservoir pressure will continue to decline. Inject at later time might affect the miscibility of CO₂ and oil in the reservoir due to lower reservoir pressure. Reservoir oil might exist in two phases, causing a reduction in miscibility. Therefore, runs have been conducted to determine the effects of

injection initiation timing on the reservoir behaviors. The operating constraints for all the injection initiation timing cases in light oil reservoir are listed in Table 8. Figure 23 shows the reservoir behaviors for light oil reservoir when the injection initiation timing is delayed for 6 years.

Table 8 – Operating constraints for CO₂ injection initiation timing cases in light oil reservoir.

Operating Constraints		
Injector BHP Max	7500	psia
Producer BHP Min	1200	psia
Producer Oil Target Rate (minimum)	20	MSTB/day
Producer Gas Rate Limit	No Limit	
Injection Rate	300	MMscf/day
End of Injection	20 th	year

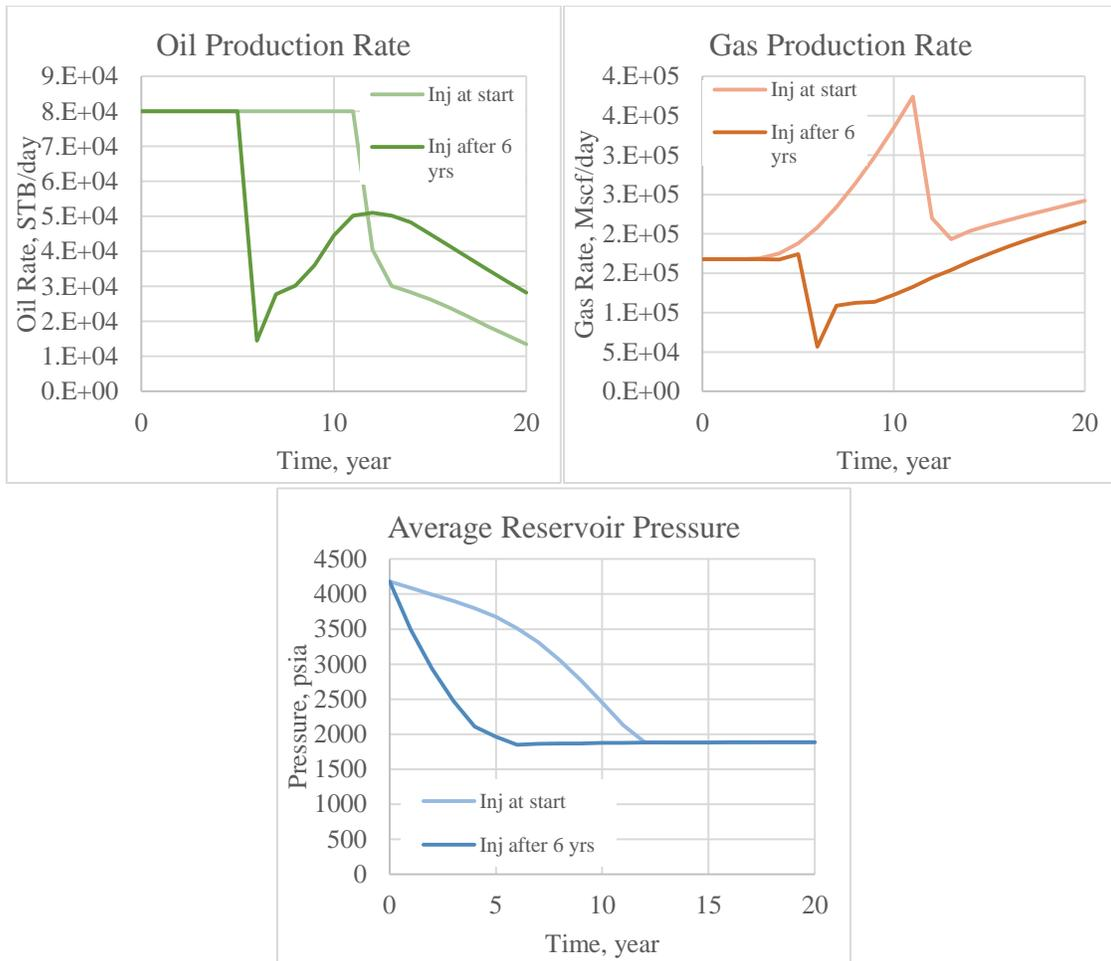


Figure 23 – Changes in oil production rate, gas production rate and reservoir pressure due to different injection initiation timing in light oil reservoir.

If the injection initiation timing is delayed, the reservoir pressure will start to drop. In this case, the reservoir pressure is very close to the minimum bottomhole pressure for the producers after six years of natural depletion. Thus, subsequent CO₂ injection will only help to maintain the reservoir pressure. If the minimum miscibility pressure is higher than the reservoir pressure, the subsequent CO₂ injection will lose its efficiency as the miscibility is reduced due to lower reservoir pressure. However, in this case, the performance of CO₂ injection is not influenced greatly as the MMP is around 2000 psia.

Thus, for the case with higher MMP, it is recommended to inject CO₂ at earlier time as the reservoir pressure is still sufficiently high. The oil production rate drops in the beginning as the pressure is decreasing. The oil rate increases as soon as CO₂ injection is initiated. However, the oil rate does not achieve the target oil rate during subsequent production period. Since the cumulative amount of CO₂ injected into the reservoir is less when the injection initiation timing is delayed, the gas production rate is constantly lower if compared to the case with injection initiation timing at the beginning.

For the heavy oil, the injection initiation timing can only be delayed up to 4 years. Initial reservoir pressure failed to provide adequate pressure support for production under natural depletion after 3 years. The operating constraints for all the injection initiation timing cases in heavy oil reservoir are listed in Table 9. Figure 24 shows the heavy oil reservoir response towards delayed CO₂ injection initiation timing.

Table 9 – Operating constraints for CO₂ injection initiation timing cases in heavy oil reservoir.

Operating Constraints		
Injector BHP Max	7500	psia
Producer BHP Min	1200	psia
Producer Oil Target Rate (minimum)	20	MSTB/day
Producer Gas Rate Limit	No Limit	
Injection Rate	175	MMscf/day
End of Injection	20 th	year

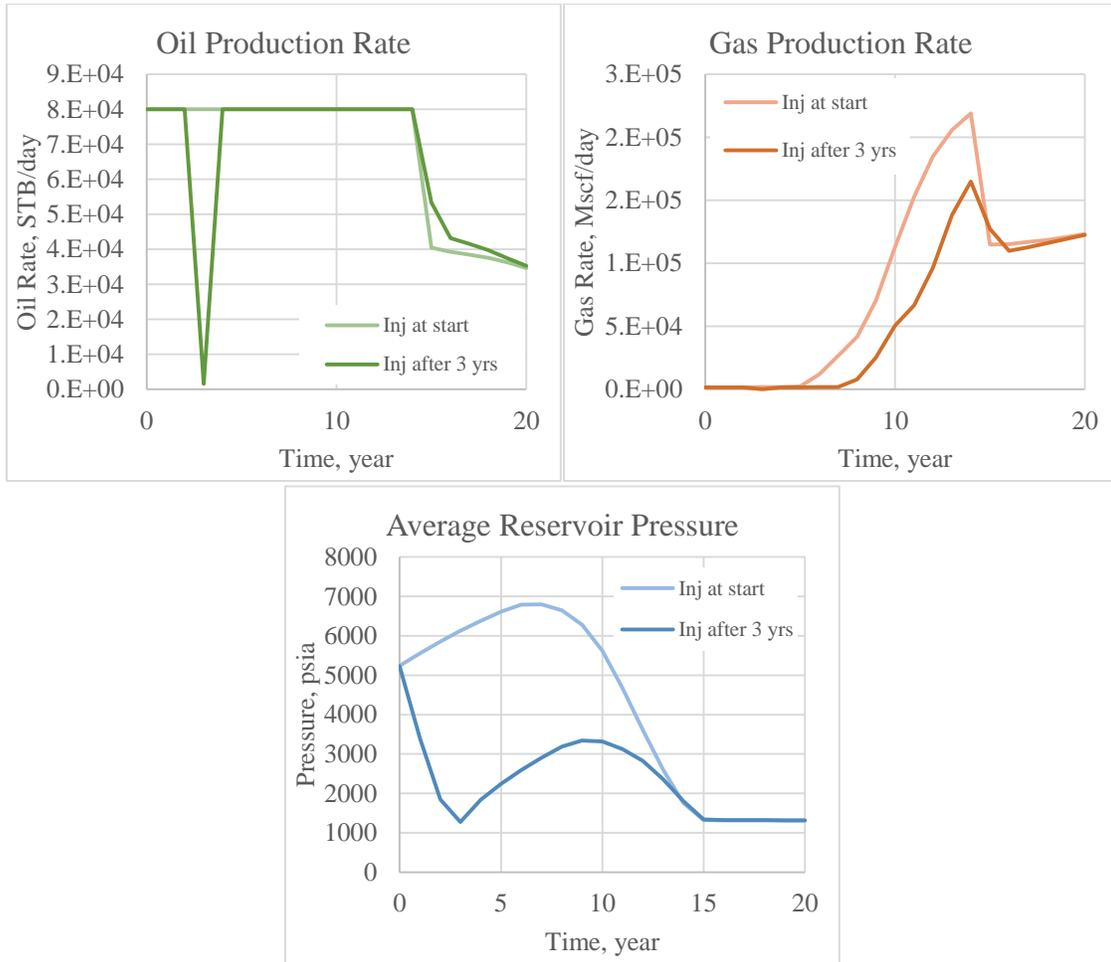


Figure 24 – Changes in oil production rate, gas production rate and reservoir pressure due to different injection initiation timing in heavy oil reservoir.

When CO₂ injection is initiated in the beginning, the reservoir pressure will increase. However, if the CO₂ injection timing is delayed, the reservoir pressure will decrease to a minimum. Reservoir pressure will only rise when the CO₂ is injected into the reservoir. Due to the decline in reservoir pressure, the oil production rate decreases to a minimum as reservoir is constantly losing pressure support due to subsequent production. The oil production rate will increase back to the target oil rate again when CO₂ injection is initiated. Towards the end of production, the oil production rate in the case

with delayed injection is slightly higher if compared with the one with injection timing at the beginning. Similarly, gas production rate is consistently lower in the case with delayed injection timing as the cumulative amount of CO₂ injected into the reservoir is less.

4.5 Producer BHP

After discussing the injection strategies, producer operating conditions will be investigated. One of the most important production strategies is by controlling producer BHP. Producer BHP will significantly influence the production by controlling the drawdown. If the producer BHP is too low, more oil is produced due to higher drawdown. However, the CO₂ injected may not be at sufficient rate to replace the oil produced, causing a decrease in reservoir pressure which will reduce the productivity. On the other hand, if the producer BHP is too high, less oil is produced and reservoir pressure will start increasing. This may not be economical as less oil is recovered while a huge amount of CO₂ is being injected.

For both light and heavy oil reservoir, producer BHP of 1200 psia and 300 psia are set to investigate the reservoir responses. The operating conditions for all cases conducted for both light and heavy oil reservoir by varying producer BHP are listed in Table 10. Figure 25 shows the light oil reservoir behaviors under different producer BHP.

Table 10 – Operating constraints for producer BHP cases in light and heavy oil reservoir.

Operating Constraints		
Injector BHP Max	7500	psia
Producer Oil Target Rate	20	MSTB/day
Producer Gas Rate Limit	No Limit	
End of Injection	20 th	year

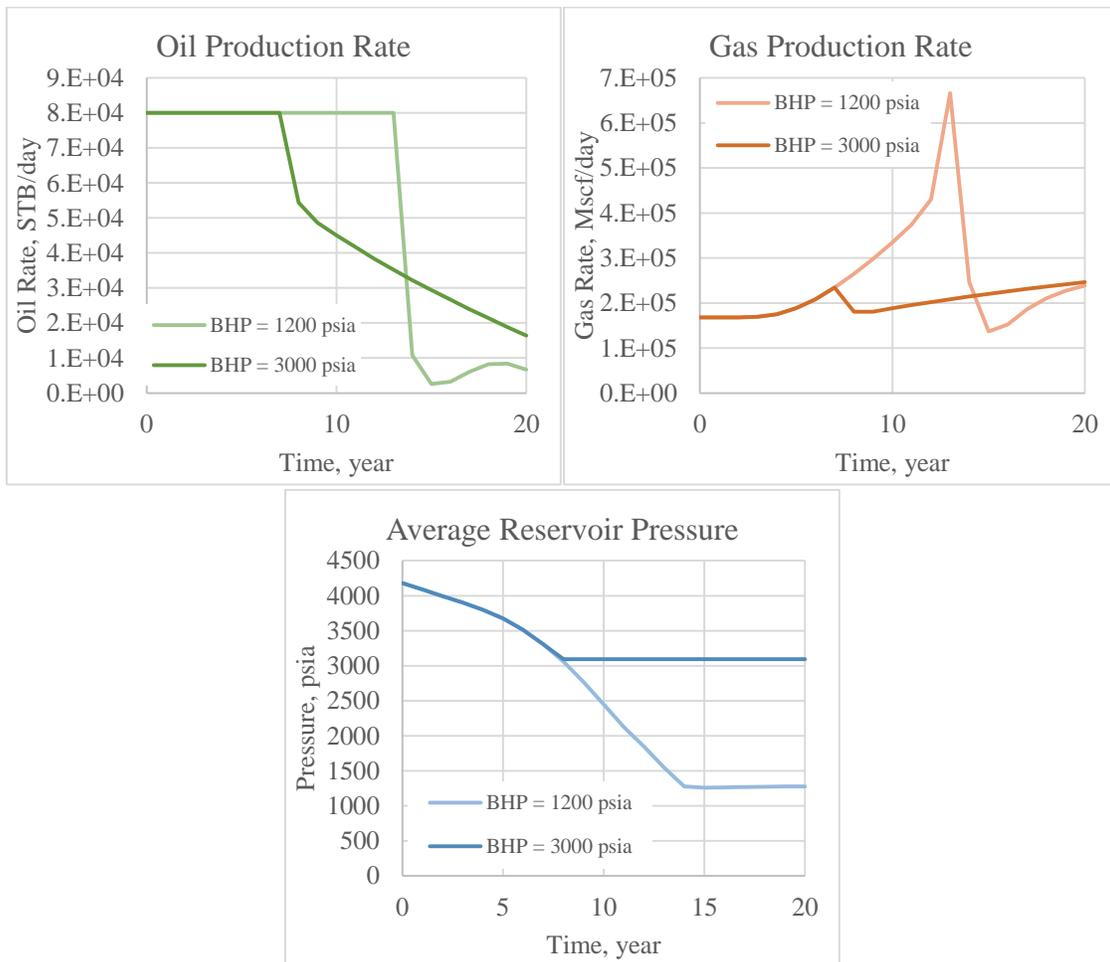


Figure 25 – Changes in oil production rate, gas production rate and reservoir pressure due to different producer BHP in light oil reservoir.

The decline in reservoir pressure is gradual since the CO₂ injection is initiated at the beginning. When the producer BHP is higher, the reservoir pressure will hit the minimum allowable producer BHP earlier, leading to the decline in oil production rate at earlier stage. However, the decline in oil production rate is gradual. On the other hand, the reservoir pressure will reach a minimum at later stage if lower minimum allowable producer BHP is used. However, once the reservoir hits the minimum, the oil production rate declines dramatically. Apart from oil production, the gas production rates for both scenario differ significantly. Since the producer BHP is set to be higher, less pressure drawdown leads to lower gas production rate. Thus, the gas production rates is consistently lower by a large margin in the case with higher producer BHP.

For heavy oil, the reservoir responses to different producer BHP can be summarized in Figure 26. Similar observations can be obtained from the heavy oil reservoir. The reservoir pressure will hit the minimum allowable producer BHP earlier if higher producer BHP is used. The oil production rate will decline as soon as the reservoir pressure hits the minimum. However, the declines in oil production rates in both cases are gradual. There is no crossover between the oil production rates in both scenarios. Gas production rates for the case with higher producer BHP are constantly lower than the one with lower producer BHP.

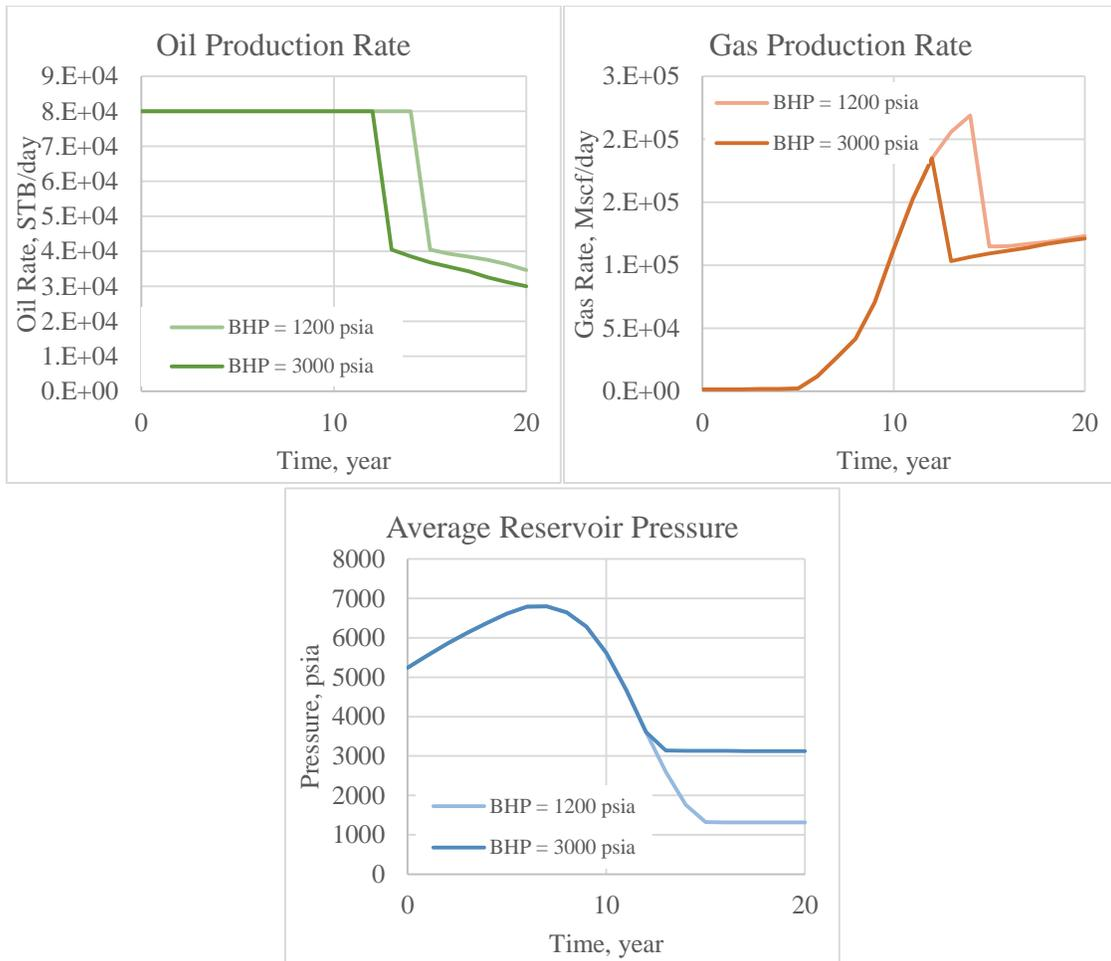


Figure 26 – Changes in oil production rate, gas production rate and reservoir pressure due to different producer BHP in heavy oil reservoir.

4.6 Producer Target Oil Rate

Producer target oil rate can be changed to get better reservoir production performance. Target oil rate is generally set based upon the surface facility capacities in handling the production volumes. However, setting different target oil rate might result in significant changes in the reservoir performances. If the oil is produced at higher rate, reservoir will soon lose its pressure support. Decline in reservoir pressure might deter the production performance significantly. Thus, oftentimes, production engineers have to

choke back the production of the wells to get better production performances in the long run. Different target oil rate can influence the reservoir behaviors significantly. The operating conditions for all target oil rates in both light and heavy reservoir are listed in Table 11. Figure 27 shows the light oil reservoir responses towards different target oil rates.

When a lower target oil rate is applied, less oil production is expected. Thus, the oil production rate at the beginning is lower if compared to the one with higher target oil rate. Since the oil production differs significantly, the changes in reservoir pressure also vary. Due to lower oil production rates in the case with low target oil rate, the reservoir pressure increases as the pressure is supported by continuous CO₂ injection. When the target oil rate is set higher, the CO₂ injection can no longer compensate with the pressure loss due to high production rates. Thus, reservoir pressure soon declines, inducing a dramatic decline in oil production rate in the late time. Oil production rate for the low oil target rate is maintained for a longer period of time, followed by a sharp decline towards the end. Since the reservoir pressure responds differently, the gas production rates peak at different period during the production. The gas production rate will decline when the reservoir pressure hits the minimum allowable producer BHP.

Table 11 – Operating constraints for constraints for producer target oil rate cases in light and heavy oil reservoir.

Operating Constraints		
Injector BHP Max	7500	psia
Producer BHP Min	1200	psia
Producer Gas Rate Limit	No Limit	
End of Injection	20 th	year

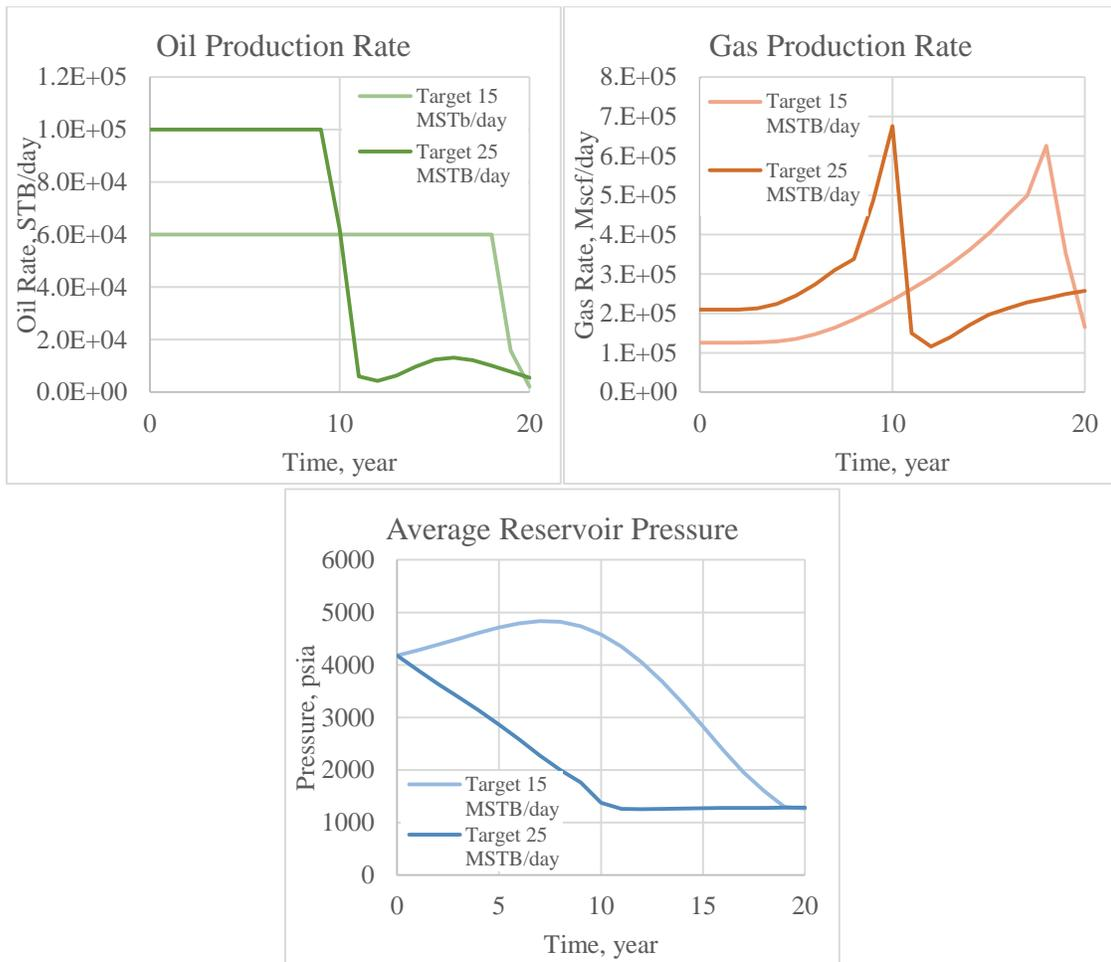


Figure 27 – Changes in oil production rate, gas production rate and reservoir pressure due to different producer target oil rate in light oil reservoir.

For heavy oil, similar observations can be obtained. Figure 28 shows the reservoir behaviors under different target oil rates. When low oil target rate is set, the oil production rate is maintained at lower rate but is kept constant for a longer production period. Reservoir pressure increases as the pressure is constantly replenished by continuous injection of CO₂ into the reservoir. The gas production rates peak at different period of the production due to the difference in reservoir pressure. Therefore, by changing the target oil rate, reservoir pressure can vary significantly. Since the miscibility of CO₂ in oil is highly sensitive towards the reservoir pressure, suitable target oil rate needs to be selected carefully to ensure the efficiency of the miscible flooding.

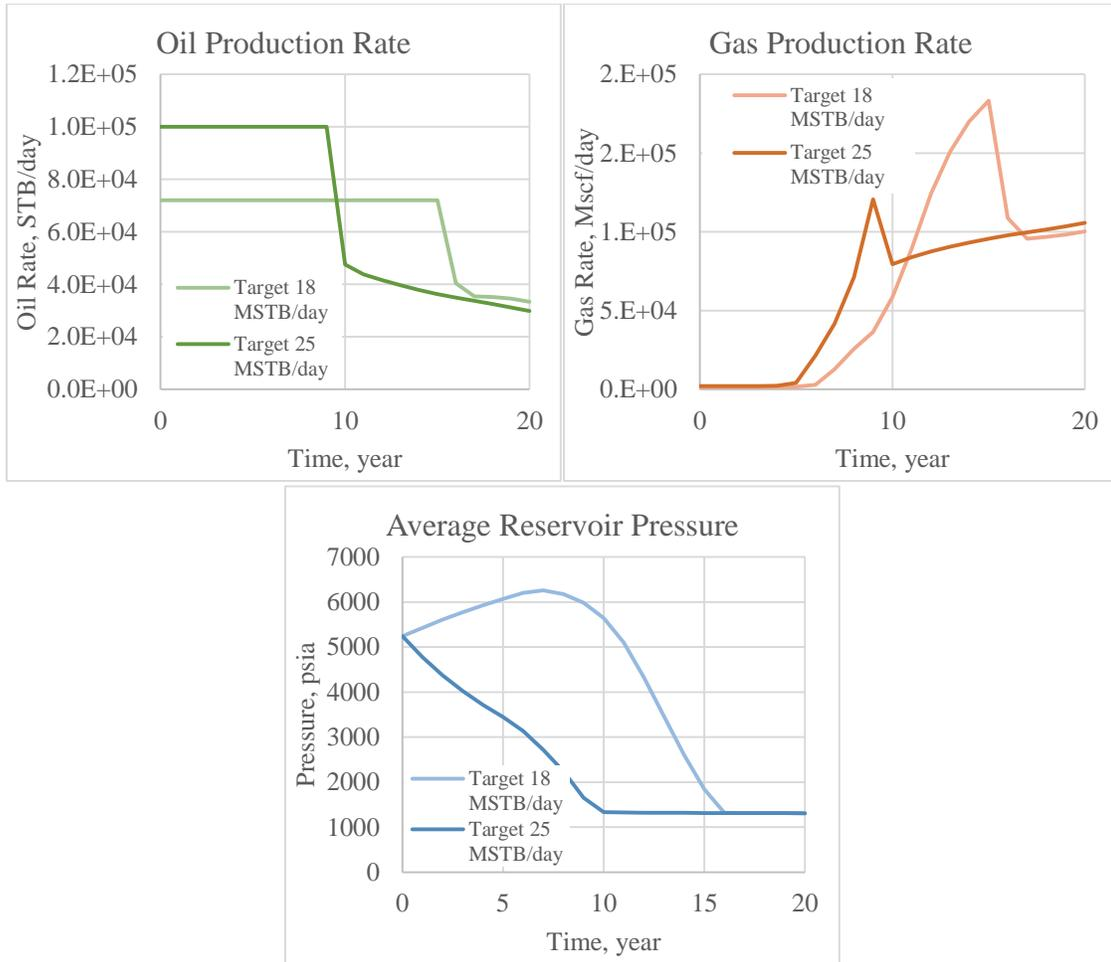


Figure 28 – Changes in oil production rate, gas production rate and reservoir pressure due to different producer target oil rate in heavy oil reservoir.

4.7 Producer Gas Rate Limit

Another useful strategies in rate control for optimization purpose is by manipulating the producer gas production rate limit. The CO₂ injected will sweep through the reservoir and reach the producer after several years of production. After breakthrough, gas production will dominate, leading to declining oil rate production as the relative permeability of oil decreases. By limiting the gas production, the CO₂ injected will remain

in the reservoir for a longer period before it is produced, resulting in better miscibility due to longer “soaking” period. Reservoir pressure can be maintained and regulated as most of the CO₂ injected is stored within the reservoir, instead of being vented out of the reservoir.

To determine the effects of gas rate limits on reservoir behaviors, runs with different gas rate limits have been conducted for both light and heavy oil reservoirs. The operating conditions for all gas production rate limit cases in both light and heavy reservoir are listed in Table 12. The reservoir responses towards different gas rate limits in light oil reservoir have been summarized in Figure 29 below.

Table 12 – Operating constraints for gas production rate limit cases in light and heavy oil reservoir.

Operating Constraints		
Injector BHP Max	7500	psia
Producer BHP Min	1200	psia
Producer Oil Target Rate (minimum)	20	MSTB/day
Start of Injection	0	year
End of Injection	20 th	year

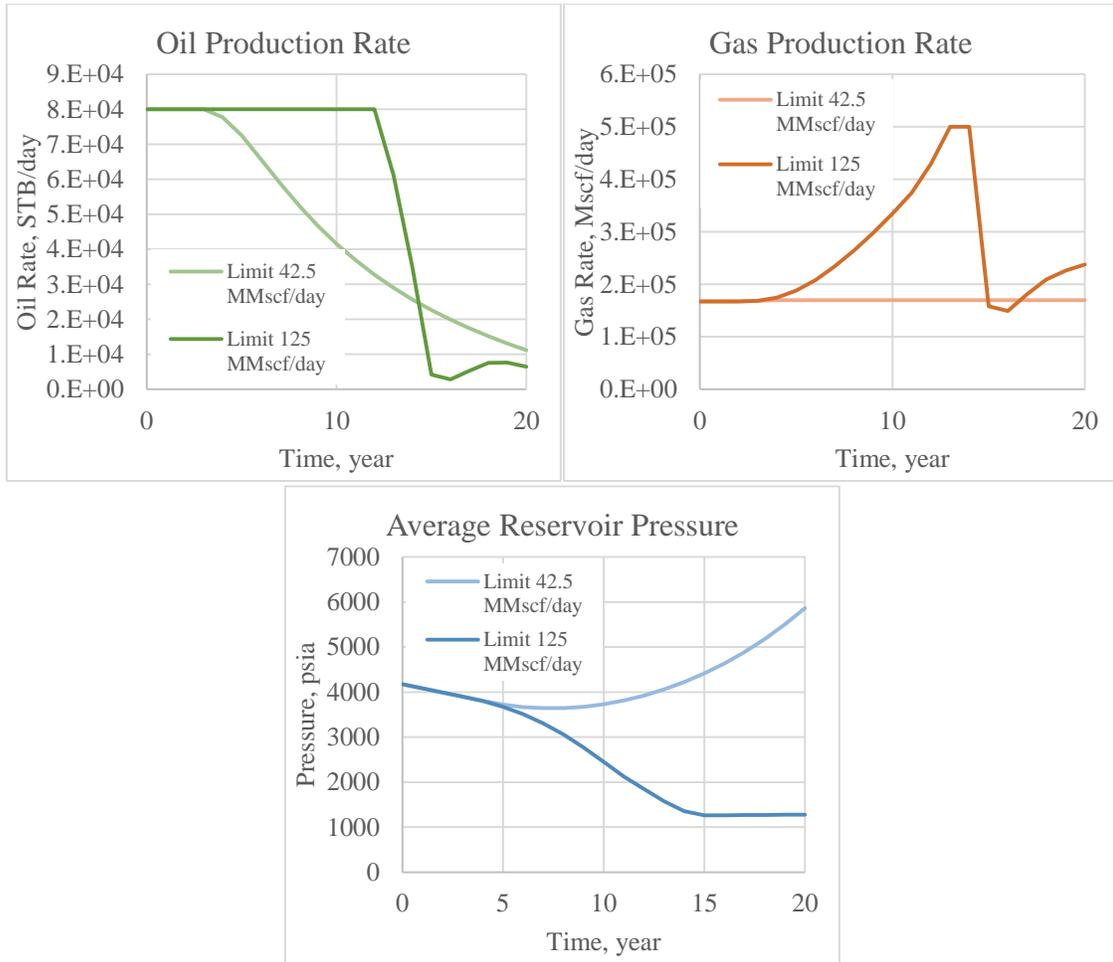


Figure 29 – Changes in oil production rate, gas production rate and reservoir pressure due to different producer gas rate limits in light oil reservoir.

When the gas production rate hits the maximum limit, the production control will be switched from oil target rate to gas rate limit. Due to the implementation of gas rate limit in the subsequent production, the oil production rate will be restricted as well. Gas production for lower rate limit will be maintained at a fairly constant manner throughout the production. Since gas production is restricted, most of the gas stays in the reservoir for pressure regulation. For low gas rate limit, the reservoir pressure actually increases as more gas is stored in the reservoir. Due to the additional pressure support provided, the oil

production rates differ significantly. For the case with high gas rate limit, the oil production was maintained at target oil rate, followed by a sharp decline as the reservoir pressure hits the minimum allowable pressure. However, for the case with low production rate, the oil production rate decreases gradually over time. This might lead to a better production overall by regulating the reservoir pressure more efficiently.

Heavy oil reservoir exhibits similar reservoir behaviors towards varying gas production rate limits, which is illustrated in Figure 30 below. Restriction in gas production will result in higher reservoir pressure as gas is stored within the reservoir instead of being vented out. Due to the additional pressure support, the oil production rate changes more gradually in the case with low gas rate limit. Consequently, the total gas production with low rate limit is significantly lower if compared with the case with high rate limit. More CO₂ can be stored within the reservoir if lower gas rate limit is applied.

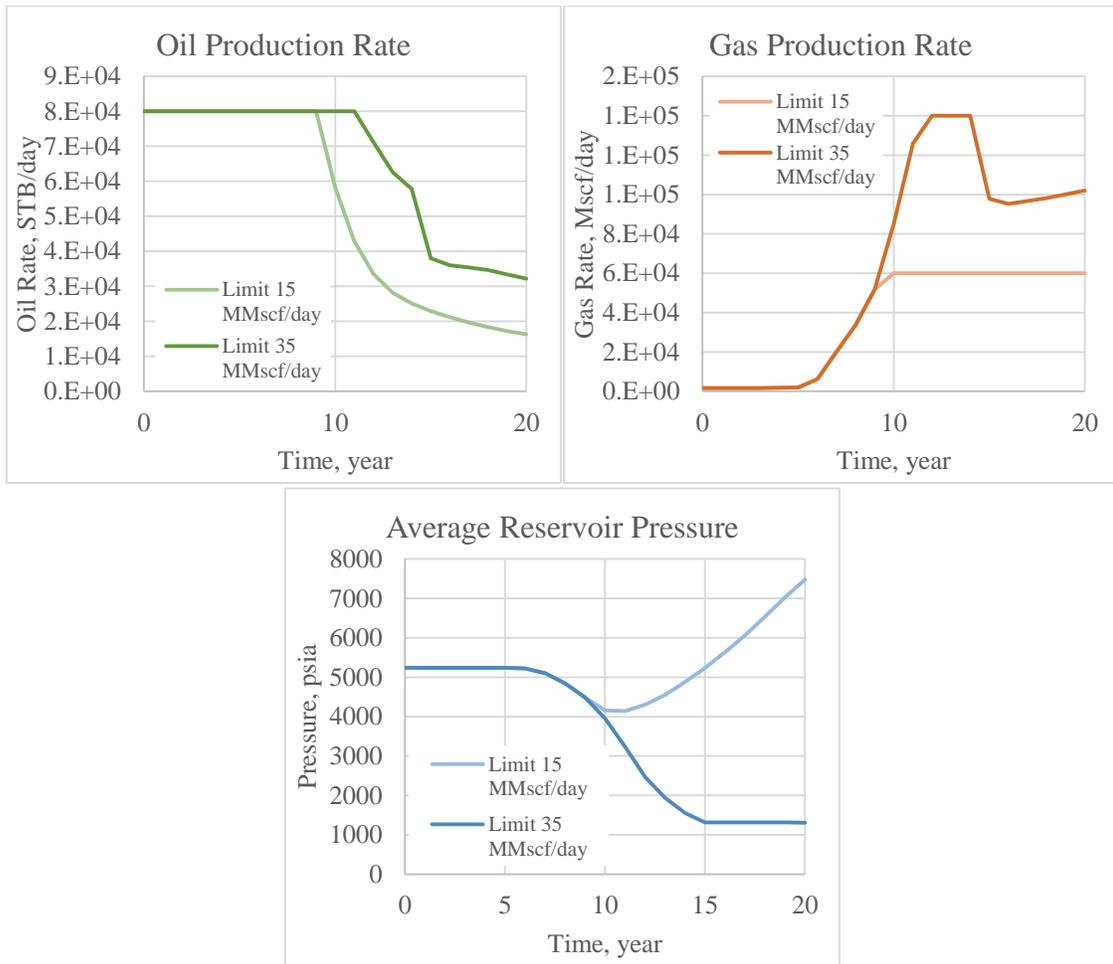


Figure 30 – Changes in oil production rate, gas production rate and reservoir pressure due to different producer gas rate limits in heavy oil reservoir.

CHAPTER V

LOCAL GRID REFINEMENT APPLICATION

To examine the effect of local grid refinement in reducing the numerical dispersion, a series of studies have been conducted. Simulation cases with and without local grid refinement are compared to determine the magnitude of numerical dispersion occurs within the large grid blocks. In every cases with LGR and without LGR, the total amounts of CO₂ injected, operating conditions for both injector and producers, and duration of the projects are the same. The percent errors of incremental recovery (over natural depletion), gas production and CO₂ stored, after 20 years of simulation, are calculated using the general equation below.

$$\text{Percent Error} = \left| \frac{\text{Results with LGR} - \text{Results without LGR}}{\text{Results with LGR}} \right| \dots\dots\dots (3)$$

Sensitivity analysis has been conducted over several injection and production variables.

The injection and production strategies investigated in this study include:

- Injection rate
- CO₂ recycling
- Injection initiation timing
- Producer bottomhole pressure (BHP)
- Producer target oil rate
- Producer surface gas production rate limit
- Completion location

It is important to note that in each sensitivity study, only the variable of interest will be changing while other parameters are kept constant.

5.1 Sensitivity to Injection Rate and Injection Pore Volume

Injection rate is one of the most important variables that needs to be investigated for CO₂-EOR miscible project. Different injection rate will result in different CO₂ breakthrough time, incremental recovery, gas production and CO₂ stored, which lead to different net present value (NPV) of the project. For every injection rate cases with LGR and without LGR, the total amounts of CO₂ injected and operating conditions for both injector and producers are the same. CO₂ injection is initiated at the beginning of the project and kept constant throughout 20 years of production. Injection pore volume can be calculated using the equation shown below.

$$Inj\ PV = \frac{FGIT \times B_g}{PV} \dots\dots\dots (4)$$

Even though the injected pore volumes are the same in the cases with LGR and without LGR, errors can be observed in the incremental recovery, gas production and CO₂ stored.

For light oil, the injection rates vary from 100 MMscf/day to 400 MMscf/day, with injection pore volumes range from 0.4 to 1.5. The percent differences due to LGR application in light oil reservoir are summarized in Table 13 below.

Table 13 – Errors resulted from LGR application by varying injection rate for light oil.

Injection Rate MMscf/day	Injection Pore Volume	Percent Error		
		Incremental Recovery	Gas Production	CO ₂ Stored
100	0.37	9.0%	0.9%	0.3%
150	0.55	4.8%	0.8%	2.2%
200	0.74	3.6%	1.8%	3.5%
225	0.83	7.3%	2.2%	4.2%
250	0.92	11.1%	2.4%	4.6%
300	1.10	16.4%	2.9%	5.4%
400	1.47	22.5%	0.2%	1.8%

Among all the parameters, incremental recovery shows the highest error if compared to gas production and amount of CO₂ stored. The errors resulted in incremental recovery are significant, range from 3.6% to 22.5%. Thus, the results signify that it is possible for compositional reservoir simulators to predict the incremental recovery with an inaccuracy as high as 20%. Apart from incremental oil recovery, the gas production and amount of CO₂ stored show slight inconsistency, with maximum errors of 2.9% and 5.4% respectively. Figure 31 shows the trends of percent error varying with injection pore volumes.

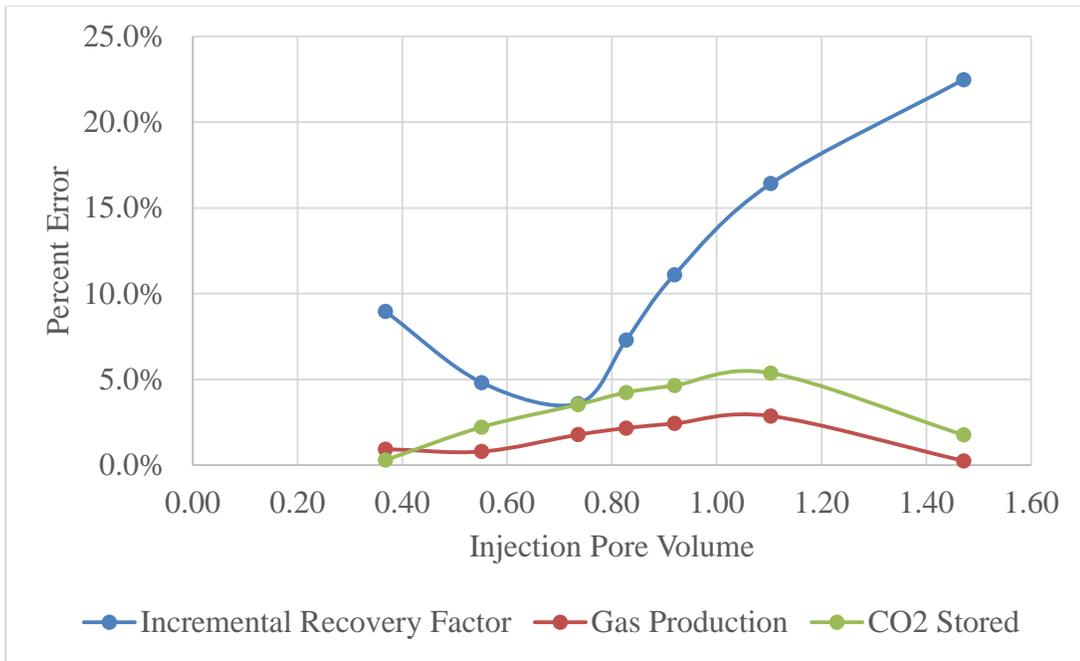


Figure 31 – Summary of error in incremental recovery, gas production and CO₂ stored by varying injection rate for light oil.

The errors of incremental recovery exhibits different trend if compared with those of gas production and CO₂ stored. It is important to note that, when the errors of incremental recovery is high, the errors of both gas production and CO₂ stored will be relatively low and vice versa. The errors of incremental recovery decreases to a minimum as the injection pore volume increases to about 0.7 and then increases dramatically as the injection pore volume continues to increase. On the other hand, both the errors of gas production and CO₂ stored increases to a maximum as the injection pore volume increases to 1.1. Then the errors start to reduce.

For heavy oil, the injection rates vary from 100 MMscf/day to 300 MMscf/day, with injection pore volumes range from 0.4 to 1.2. The percent differences due to LGR application in light oil reservoir are summarized in Table 14.

Table 14 – Errors resulted from LGR application by varying injection rate for heavy oil.

Injection Rate MMscf/day	Injection Pore Volume	Percent Error		
		Incremental Recovery	Gas Production	CO ₂ Stored
100	0.38	6.5%	16.5%	6.3%
125	0.48	10.9%	19.5%	10.7%
150	0.58	12.0%	15.9%	11.8%
175	0.67	12.2%	12.9%	11.9%
200	0.74	11.4%	13.4%	11.0%
225	0.80	10.7%	13.4%	11.0%
250	0.85	7.7%	17.4%	14.8%
300	1.15	2.7%	23.8%	20.2%

There are three major differences between the errors exhibited between heavy oil reservoir and light oil reservoir. First, the errors resulted in heavy oil case are higher if compared with light oil case. Second, gas production and CO₂ stored show relatively higher errors if compared with incremental recovery. Lastly, all the errors among incremental recovery, gas production and CO₂ stored are significant, range from 6% to 24%. The trends of errors in incremental recovery, gas production and CO₂ stored are summarized in Figure 32.

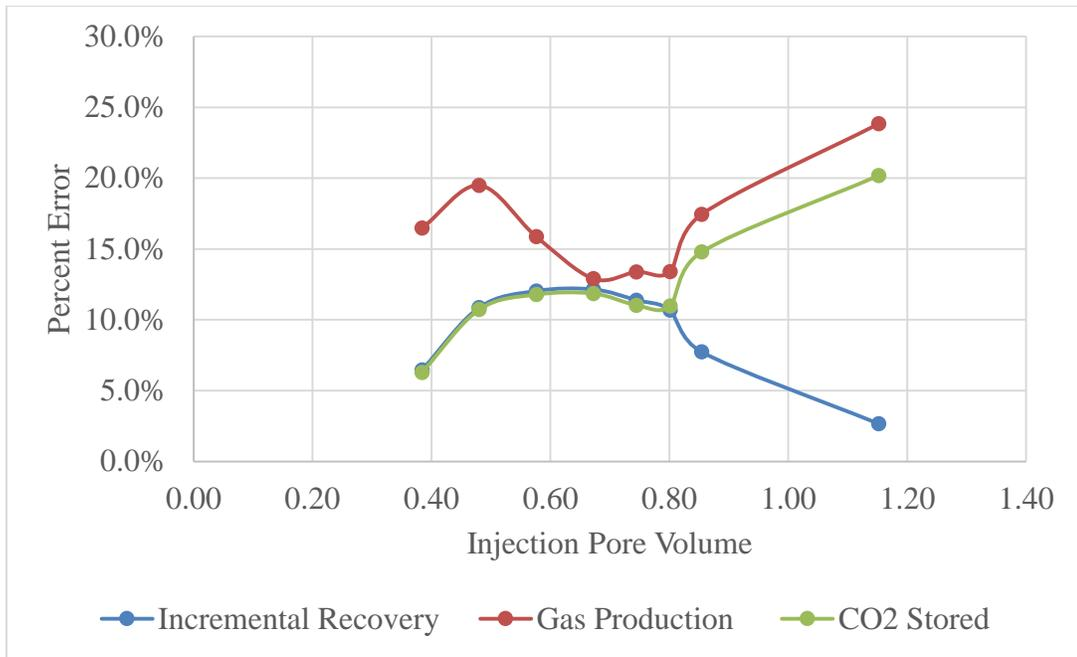


Figure 32 – Summary of error in incremental recovery, gas production and CO₂ stored by varying injection rate for heavy oil.

Similar to the light oil case, the error trend of incremental recovery is different from the ones exhibited by both gas production and CO₂ stored. The errors of both incremental recovery and CO₂ stored first increase with injection pore volume till they reach plateaus. The errors stay fairly consistent from injection pore volume of 0.5 to 0.8. For gas production, the errors increase at early stage and soon drop to a consistent value around 13%. However, as the injection pore volume continues increasing above 0.8, the errors of incremental recovery start to drop while the errors of both gas production and CO₂ stored increase dramatically to above 20%.

To further investigate the nature of the differences resulted from the application of LGR, the incremental recovery for each injection rate (with and without LGR application) is shown in Figure 33.

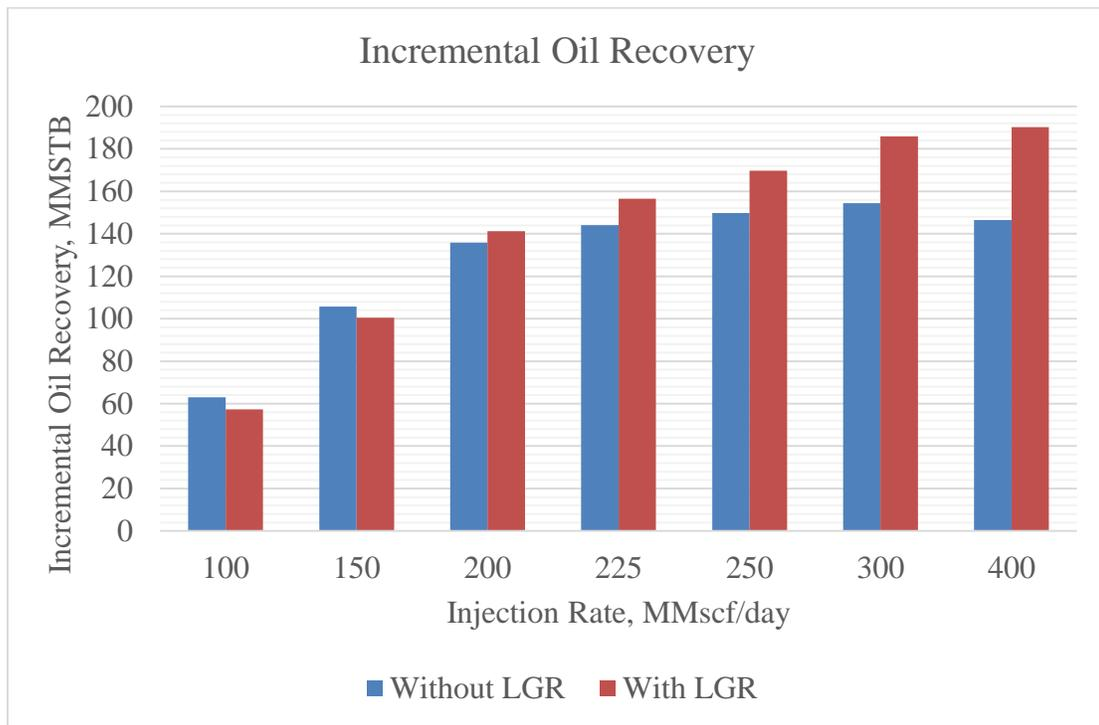


Figure 33 – Comparisons of incremental recovery obtained from cases with and without LGR for each injection rate.

There are two important observations concluded from the comparison chart above. First, the absence of LGR around injector and producers does not only contribute to significant errors, it also produces misleading results trends. According to the cases with LGR, the injection rate with highest incremental oil recovery is around 400 MMscf/day. However, without the application of LGR, the recommended injection rate is around 300 MMscf/day since it contributes to highest incremental recovery. Operators do not only predict the incremental recovery with high inaccuracy, they also determine the optimum or recommended development strategies wrongly. Second, the nature of errors due to LGR application is random. Most operators are worried that the incremental recovery predicted

using LGR will be lesser. However, the application of LGR can result in either lower or higher incremental recovery. There is no definite trend observed in the errors obtained due to the random nature of numerical dispersion.

5.2 Sensitivity to CO₂ Recycling

Without recycling produced gas, CO₂ will be lost together with the produced gas. Thus, to maximize the usage of purchased CO₂, the gas produced, which is high in CO₂ concentration, is reinjected back into the reservoir. This is done by converting one of the existing producers into an injector when the CO₂ molar fraction in the produced gas exceeds 10%. Although the middle injector will inject constant amount of CO₂, the cases with and without LGR will not have the same cumulative amount of CO₂ injected at the end due to the difference in CO₂ breakthrough time and amount of CO₂ reinjected back into the reservoir. However, both cases (with and without LGR) will have the same operating constraints like producer BHP, injector BHP and oil target rate. The percent differences due to the application of LGR for both light oil and heavy oil cases are summarized in Table 15 and Table 16 respectively.

Table 15 – Errors resulted from LGR application by recycling produced gas for light oil.

Injection Rate MMscf/day	Recycle	Percent Error		
		Incremental Recovery	Gas Production	CO ₂ Stored
250	No Recycle	11.1%	2.4%	4.6%
250	Recycle	3.9%	46.6%	0.7%
300	No Recycle	16.4%	2.9%	5.4%
300	Recycle	5.6%	46.0%	1.4%

For light oil, two different injection rates are used for the middle injector. The errors exhibited show dramatic changes when CO₂ is being recycled. The errors in both incremental recovery and CO₂ stored are reduced significantly. However, the gas production shows substantial error. The errors for both injection rates increase from 4% to about 46%.

Table 16 – Errors resulted from LGR application by recycling produced gas for heavy oil.

Injection Rate MMscf/day	Recycle	Percent Error		
		Incremental Recovery	Gas Production	CO ₂ Stored
100	No Recycle	6.5%	16.5%	6.3%
100	Recycle	1.8%	36.5%	0.1%
125	No Recycle	10.9%	19.5%	10.7%
125	Recycle	1.7%	34.3%	0.0%
150	No Recycle	12.0%	15.9%	11.8%
150	Recycle	1.5%	28.1%	1.2%

For heavy oil, three different injection rates are used for the middle injector. The errors show similar changes observed in light oil case. Both the errors in incremental

recovery and CO₂ stored has been reduced dramatically due to CO₂ recycling. However, the gas production errors increase substantially from around 16% to 37% depending on the injection rate of the main injector.

To further examine the errors observed, the average oil saturation and average CO₂ composition in both light and heavy oil reservoirs are monitored and recorded in Table 17 and Table 18 respectively.

Table 17 – Oil saturation and CO₂ composition comparison between models with LGR and without LGR for light oil.

Time year	Oil Saturation		CO ₂ Composition, mol%	
	Without LGR	With LGR	Without LGR	With LGR
0	1	1	0.237	0.237
5	1	1	17.08	19.724
10	0.89318	0.84628	32.809	37.253
15	0.99097	0.80951	47.507	48.615
20	1	0.99067	58.785	63.361

Table 18 – Oil saturation and CO₂ composition comparison between models with LGR and without LGR for heavy oil.

Time year	Oil Saturation		CO ₂ Composition, mol%	
	Without LGR	With LGR	Without LGR	With LGR
0	1	1	0.037	0.037
5	1	1	9.296	11.038
10	1	1	18.573	20.687
15	1	1	27.125	31.172
20	1	1	35.054	37.477

Without using LGR, the CO₂ composition over time will be tracked wrongly in the reservoir. In this particular situation, cases without LGR have higher CO₂ composition if

compared to the ones with LGR, resulting in early CO₂ breakthrough and conversion of producer into injector. The produced gas is reinjected earlier in the cases without LGR, compounding on the previous error due to early breakthrough. Additional recycled gas injected changes the composition of the hydrocarbon in the reservoir, leading to phase change especially in the light oil reservoir. Error in phase identification is observed when the oil saturations show significant differences over time, leading to the errors in reservoir oil density. Due to the errors in tracking hydrocarbon component composition and identifying fluid phases, the errors in gas production continue to compound and become larger over time.

5.3 Sensitivity to Injection Initiation Time

CO₂-EOR miscible flooding is usually performed when the reservoirs are not capable of producing at an economic rate by natural depletion. Thus, the CO₂ injection is generally initiated after several years of natural depletion where the average reservoir pressure is low. The reservoir pressure can sometimes be lower than the bubble point pressure, crossing into the two-phase region. Injecting CO₂ into a saturated reservoir might result in higher tendency for errors. Thus, injection initiation time is included in the study of LGR application. For every cases with LGR and without LGR, the cumulative amounts of CO₂ injected are the same since the injection rate is fixed. The operating conditions for both injector and producers are the same for every case compared. CO₂ injection is initiated at the beginning of the project and kept constant throughout 20 years of production.

For light oil case, the injection initiation timing ranges from 0 (start at the beginning) to 7th year. The runs are terminated at 7th year because the reservoir is not able to produce under natural depletion after 7 years. After 5 years of natural depletion, the reservoir pressure will reach the bubble point of the light oil, causing the fluids to exist as two phases in the reservoir. The percent errors due to the application of LGR are summarized in Table 19 below.

Table 19 – Errors resulted from LGR application by changing injection initiation time for light oil.

Injection Start Time, year	Percent Error		
	Incremental Recovery	Gas Production	CO ₂ Stored
0.0	14.9%	5.1%	8.6%
4.0	13.3%	5.2%	7.6%
6.0	13.5%	4.6%	6.6%
7.0	12.6%	4.4%	6.2%

As CO₂ is injected at later time, the percent errors decrease. Percent errors in incremental recovery, which is the highest percent errors among all, reduce from 15% to 13% when CO₂ is introduced into the reservoir 7 years later. Minor decrease can be observed in the errors of gas production and CO₂ stored as well. The results show that there is no additional percent differences when CO₂ is injected into saturated reservoirs (two-phase) due to the application of LGR. Figure 34 shows a summary of the error trends of incremental recovery, gas production and CO₂ stored varying with different injection initiation times for light oil.

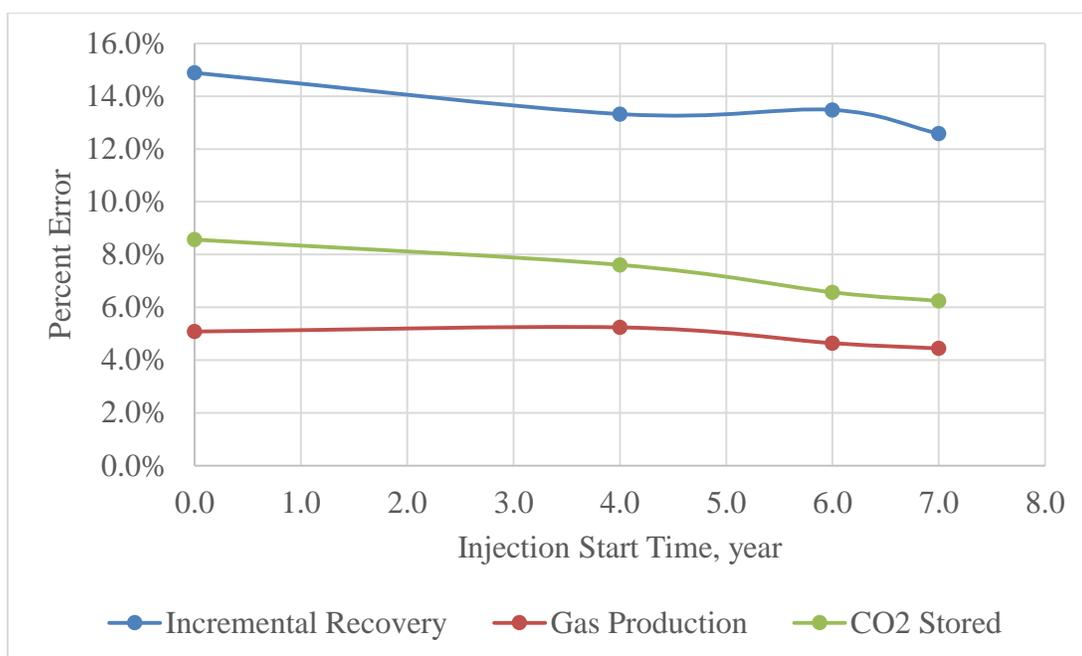


Figure 34 – Summary of error in incremental recovery, gas production and CO₂ stored by changing injection initiation time for light oil.

For heavy oil, the injection initiation times range from 0 (start at the beginning) to 4th year. The runs are terminated at 4th year because the reservoir is not able to produce under natural depletion after 4 years. It is important to note that heavy oil reservoir remains unsaturated throughout the project as the bubble point pressure of the heavy oil is extremely low. Thus, two-phase fluid flow will not exist within the reservoir. Table 20 summarizes the errors resulted from LGR application by changing the injection initiation time for heavy oil.

Table 20 – Errors resulted from LGR application by changing injection initiation time for heavy oil.

Injection Start Time, year	Percent Error		
	Incremental Recovery	Gas Production	CO ₂ Stored
0.0	12.2%	12.9%	11.9%
2.0	11.8%	13.8%	11.6%
3.0	11.1%	14.7%	10.9%
4.0	10.5%	15.3%	10.4%

Similarly, the errors in incremental recovery and CO₂ stored decrease slightly as the injection initiation time is delayed. However, the percent errors in gas production increase from 13% to 15% as the injection initiation time is delayed for 4 years. Throughout the duration of the project, the reservoir remains undersaturated. CO₂ injected is in the super-critical phase due to high injection pressure. CO₂ will mix and dissolve in the heavy oil. Miscibility and dissolution of CO₂ is highly sensitive to pressure. Pressure changes around the wells will cause significant changes to fluid behavior. Thus, when LGR is applied to the surroundings of the well, fluid behavior can be characterized more accurately. Gas is liberated as oil is produced and thus contributing to higher errors. Figure 35 shows a summary of the error trends.

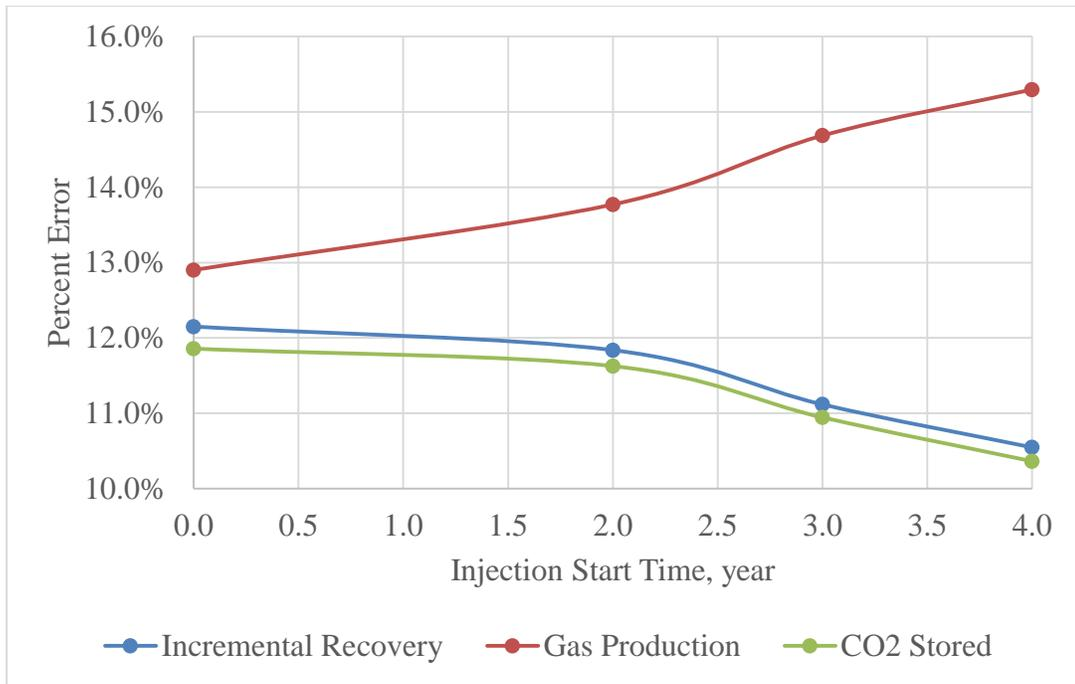


Figure 35 – Summary of error in incremental recovery, gas production and CO₂ stored by changing injection initiation time for heavy oil.

The changes in the errors for incremental recovery, gas production and CO₂ stored are minor, which is around 2% difference. Errors of incremental recovery and CO₂ stored decrease as the injection initiation time is delayed while the errors of gas production increase slightly. Although the percent error changes due to injection initiation time is minor, the percent errors are still considered significant, ranging from 10% to 16%.

5.4 Sensitivity to Producer BHP

Drastic changes in pressure can occur around the wells (injectors or producer). Since fluid behavior is highly dependent on the reservoir pressure, local grid refinement should be used around wells to reduce the numerical dispersion. To illustrate the ability of

local grid refinement to track the pressure around the wells, different producer BHPs are studied. For every case with LGR and without LGR, the total amounts of CO₂ injected and operating conditions for injector are the same. CO₂ injection is initiated at the beginning of the project and kept constant throughout 20 years of production.

For light oil, four different producer BHPs are used in this study. Lower producer BHP will result in higher pressure differential between the injector and producers, inducing a higher pressure change around producers. The percent differences for every producer BHP are recorded in Table 21.

Table 21 – Errors resulted from LGR application by changing producer BHP for light oil.

Producer BHP, psia	Percent Error		
	Incremental Recovery	Gas Production	CO ₂ Stored
1200	16.9%	2.7%	5.3%
1800	14.9%	5.1%	8.6%
2500	13.0%	5.6%	9.0%
3000	13.1%	5.9%	9.1%

As the producer BHP increases, the errors in incremental recovery decreases. High producer BHP will limit oil production due to smaller drawdown. Thus, as the producer BHP increases, the oil production decreases, contributing to lower margin of error. However, for gas production and CO₂ stored, the errors increase as the producer BHP increases. Figure 36 shows a summary of error trends varying with producer BHP.

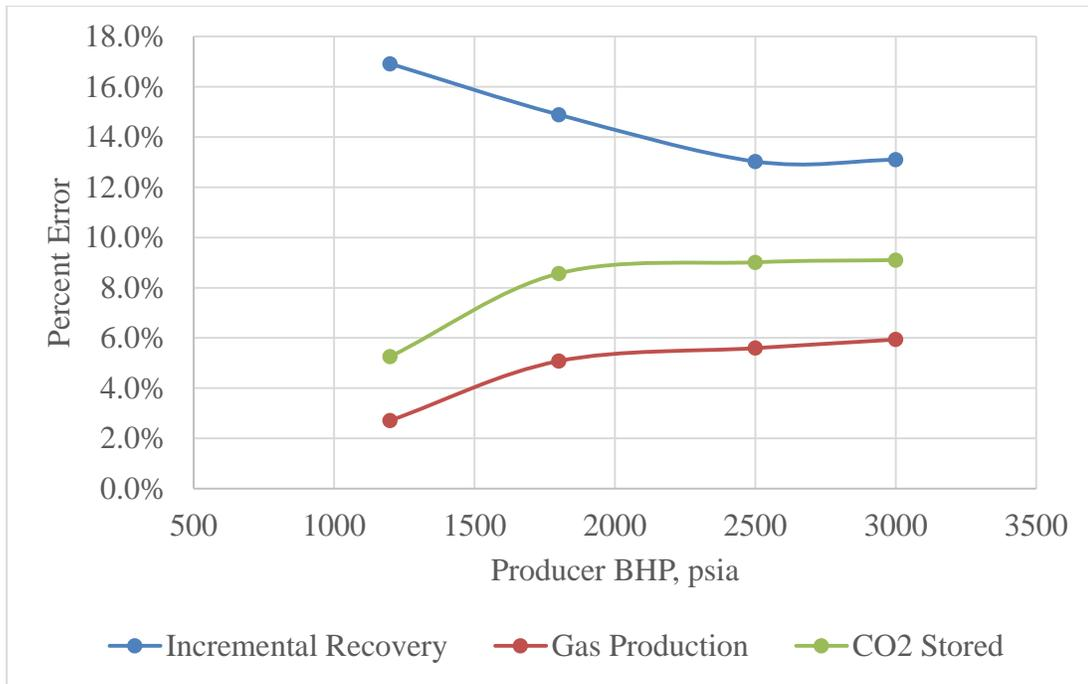


Figure 36 – Summary of error in incremental recovery, gas production and CO₂ stored by changing producer BHP for light oil.

As discussed previously, the errors in both gas production and CO₂ stored increase as the producer BHP increases while the errors in incremental recovery decrease as the producer BHP increases. One important thing to note is that the errors tend to stabilize at high producer BHP, causing the trends to reach plateaus.

For heavy oil, same set of producer BHPs is used. The percent errors resulted from the application of LGR are recorded in Table 22.

Table 22 – Errors resulted from LGR application by changing producer BHP for heavy oil.

Producer BHP, psia	Percent Error		
	Incremental Recovery	Gas Production	CO ₂ Stored
1200	12.2%	12.9%	11.9%
1800	12.1%	14.2%	11.5%
2500	12.2%	15.7%	11.4%
3000	12.2%	16.6%	11.4%

The errors shown in heavy oil case are slightly different from the ones observed in light oil. For incremental recovery and CO₂ stored, the errors stay relatively constant with minor changes. However, the errors in gas productions increases from 13% to 17% as the producer BHP increases. Figure 37 summarizes the error trends varying with producer BHP.

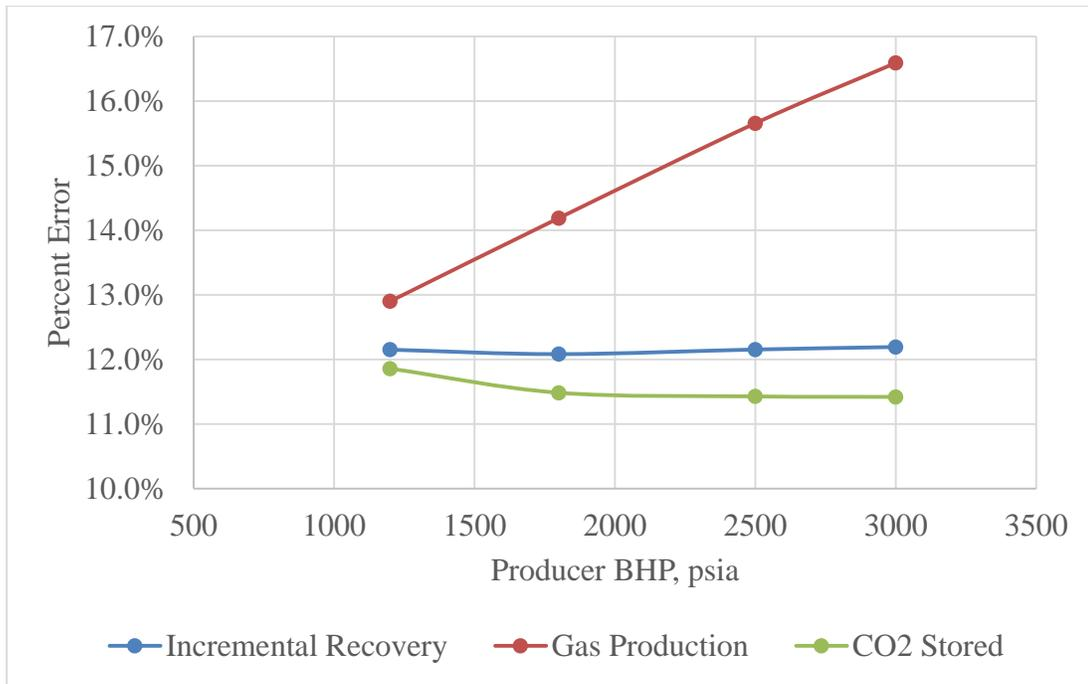


Figure 37 – Summary of error in incremental recovery, gas production and CO₂ stored by changing producer BHP for heavy oil.

Although there are only minor changes in the errors of both incremental recovery and CO₂ stored, the errors are significant. Regardless of the producer BHP used, there are always errors with magnitude of 11% to 12%. Errors in gas production increase linearly with producer BHP.

5.5 Sensitivity to Producer Target Oil Rate

In most EOR projects, producer target oil rate is controlled for various reasons. Target oil rate may be limited due to surface facilities limitation and pressure maintenance. If the amount of the oil produced is greater than the amount of CO₂ injected, the reservoir pressure will drop. Sometimes, pressure might drop below the minimum miscibility

pressure, resulting in lower oil recovery in miscible EOR operations. Thus, target oil rate is another variable of interest in this study. For every case with LGR and without LGR, the amount of CO₂ injected remains unchanged. The BHPs of injector and producers are kept constant. The CO₂ injection is initiated in the beginning and kept constant throughout the simulation.

For light oil, five different target oil rates are used, ranging from 15000 bbl/day to 25000 bbl/day for each well. The results showing the errors by varying producer target oil rate are recorded in Table 23.

Table 23 – Errors resulted from LGR application by changing producer target oil rate for light oil.

Target Oil Rate bbl/day/well	Percent Error		
	Incremental Recovery	Gas Production	CO ₂ Stored
15000	24.6%	2.4%	5.4%
18000	19.5%	3.1%	5.7%
20000	16.4%	2.9%	5.4%
22000	14.0%	2.5%	4.8%
25000	11.0%	1.9%	4.0%

The error trend of incremental recovery is significantly different from the ones exhibited by gas production and CO₂ stored. The errors in incremental oil recovery decrease substantially from 25% to 11% as the producer target oil rate increases. On the other hand, the errors for both gas production and CO₂ stored increase to a maximum and then decrease as the target oil rate increases. Figure 38 shows a summary of error trends resulted from varying producer target oil rate.

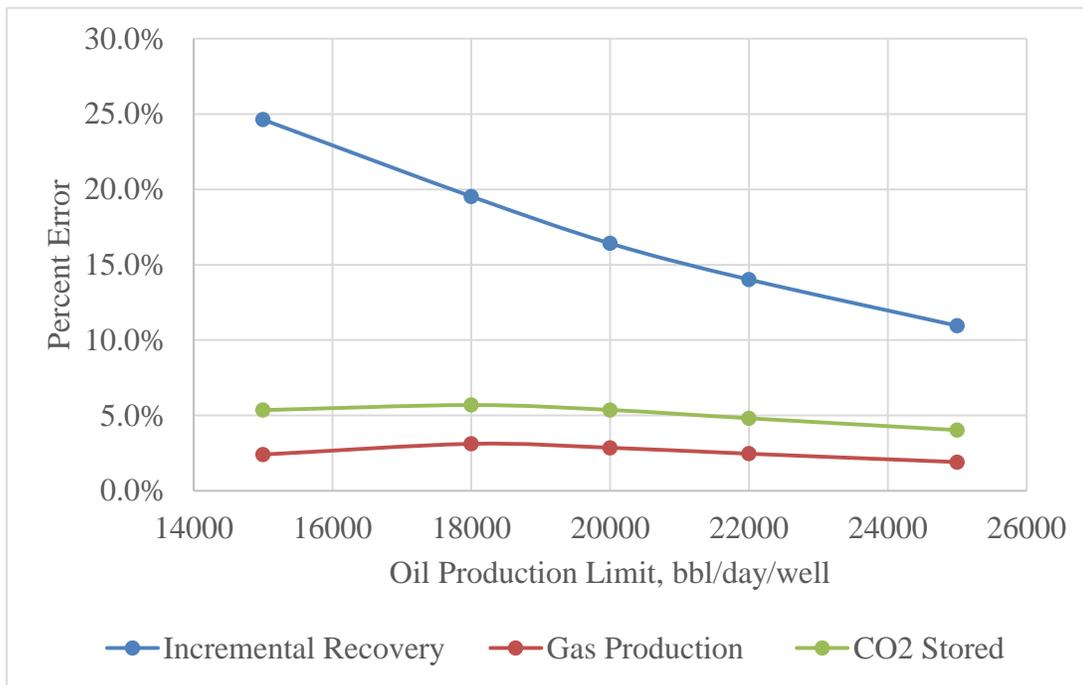


Figure 38 – Summary of error in incremental recovery, gas production and CO₂ stored by changing producer target oil rate for light oil.

The error changes in both gas production and CO₂ stored are not as significant as the one shown by incremental recovery. The errors in gas production stay relatively constant around 2-3% while the errors in CO₂ stored changes from 4-6%. However, the errors in incremental recovery decrease linearly with target oil rate.

For heavy oil, only four different target oil rates are used. Table 24 shows the error resulted from LGR application by varying the producer target oil rate.

Table 24 – Errors resulted from LGR application by changing producer target oil rate for heavy oil.

Oil Prod Limit bbl/day/well	Percent Error		
	Incremental Recovery	Gas Production	CO₂ Stored
18000	11.8%	14.7%	11.6%
20000	12.0%	15.9%	11.8%
22000	12.6%	17.0%	12.4%
25000	12.6%	17.7%	12.5%

The errors observed in heavy oil case are different from the ones in light oil case. All the errors in the incremental recovery, gas production and CO₂ stored increase as the target oil rate increases. Judging from the effect of errors due to LGR application, lower target oil rate should be used as it will result in lower errors in the simulation results. Figure 39 shows the error trends by varying producer target oil rate for heavy oil cases.

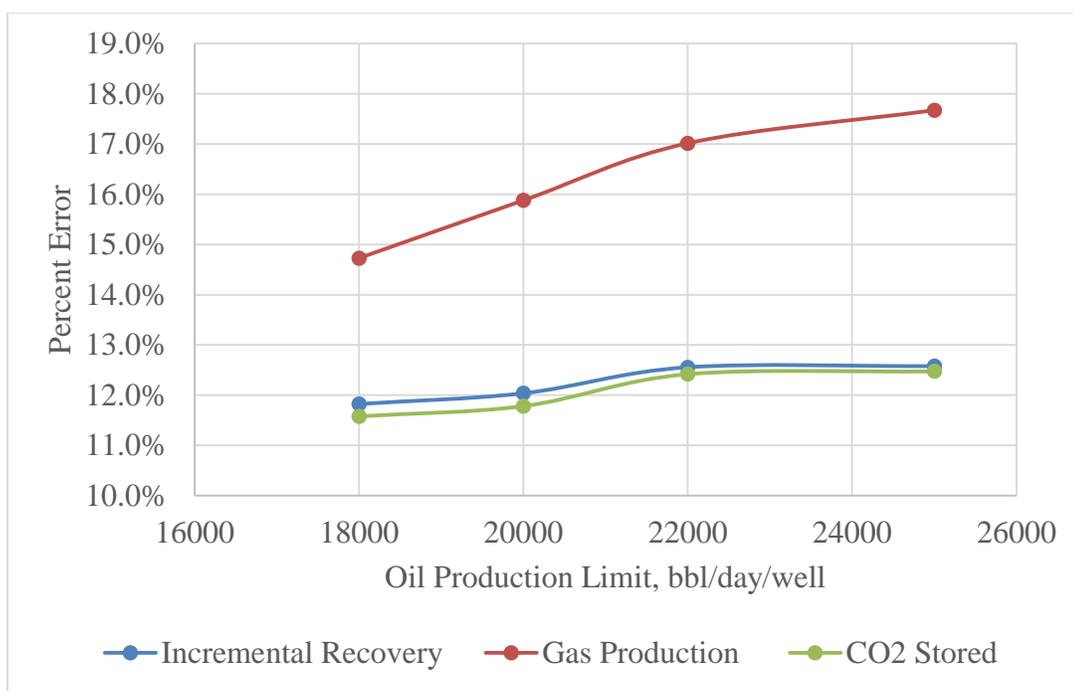


Figure 39 – Summary of error in incremental recovery, gas production and CO₂ stored by changing producer target oil rate for heavy oil.

Although all the errors increase with target oil rate, the error changes for each parameters are different. Incremental recovery and CO₂ stored show relatively smaller change in errors, ranging from 11% to 13%. The errors in both incremental recovery and CO₂ stored stay consistent at high target oil rate. However, the errors in gas production change dramatically from 14% to 18% as the target oil rate increases.

5.6 Sensitivity to Producer Gas Rate Limit

To regulate and maintain the reservoir pressure for a longer period, gas production can be limited. The gas injected will remain in the reservoir to help with pressure maintenance, instead of being vented out of the reservoir. Reservoir pressure can be

regulated to stay above MMP and sufficient drawdown can be obtained for longer period of production. For every case with LGR and without LGR, the amount of CO₂ injected remains unchanged. The operating conditions for both injector and producers are kept constant. The CO₂ injection is initiated in the beginning and kept constant throughout the simulation.

For light oil, seven different gas production rate limits have been imposed, ranging from 42500 Mscf/day to 150000 Mscf/day for each producer. The results obtained by changing producer gas production rate limit are recorded in Table 25.

Table 25 – Errors resulted from LGR application by changing producer gas production rate limit for light oil.

Gas Prod Limit Mscf/day/well	Percent Error		
	Incremental Recovery	Gas Production	CO ₂ Stored
42500	47.3%	0.0%	4.1%
50000	42.1%	0.2%	5.2%
75000	25.3%	1.8%	6.9%
100000	18.8%	3.4%	6.3%
125000	16.8%	3.0%	5.6%
150000	16.3%	2.9%	5.4%
No Limit	16.4%	2.9%	5.4%

Among all the parameters, incremental recovery shows the highest error if compared to gas production and amount of CO₂ stored. The errors resulted in incremental recovery are significant, range from 16% to 47%. Thus, the results signify that it is possible for compositional reservoir simulators to predict the incremental recovery with an inaccuracy as high as 47% if LGR is not applied. Apart from incremental oil recovery,

the gas production and amount of CO₂ stored show slight inconsistency, with maximum errors of 3.4% and 6.9% respectively. Figure 40 shows the trends of percent error varying with producer gas production rate limit.

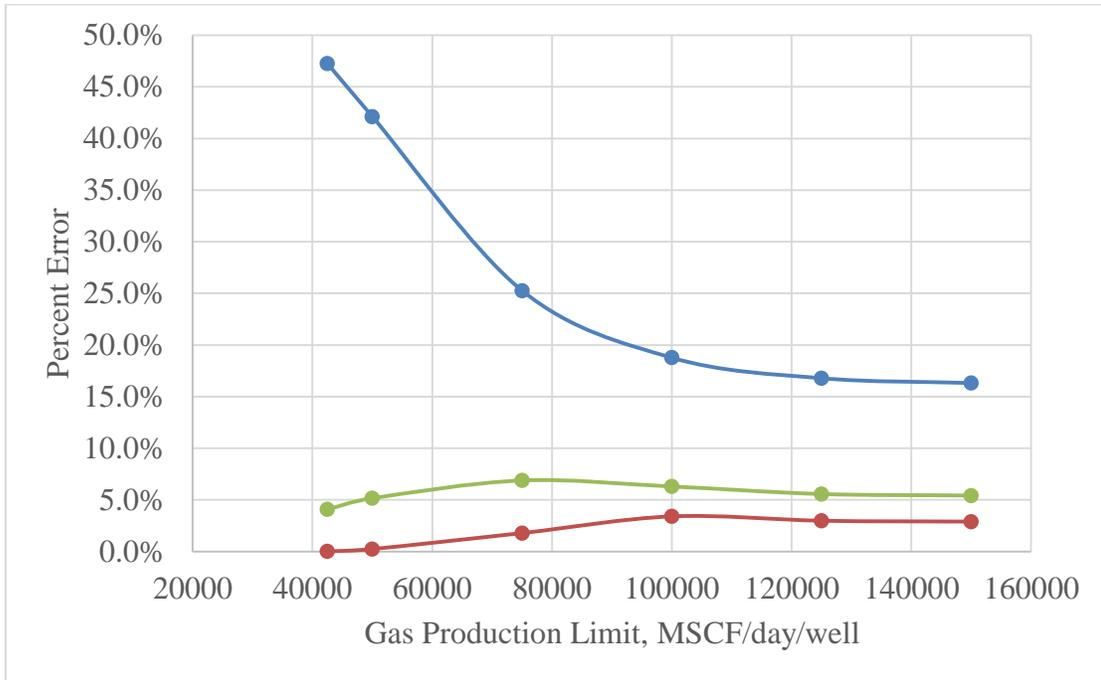


Figure 40 – Summary of error in incremental recovery, gas production and CO₂ stored by changing producer gas production rate limit for light oil.

The errors of incremental recovery exhibit different trend if compared with those of gas production and CO₂ stored. The errors of incremental recovery decrease dramatically and then stay relatively constant as the gas production limit exceeds 100000 Mscf/day. On the other hand, both the errors of gas production and CO₂ stored stay relative constant with minor changes.

For heavy oil, the gas production rate limits vary from 42500 Mscf/day to 125000 Mscf/day. The percent differences due to LGR application in light oil reservoir are summarized in Table 26.

Table 26 – Errors resulted from LGR application by changing producer gas production rate limit for heavy oil.

Gas Prod Limit Mscf/day/well	Percent Error		
	Incremental Recovery	Gas Production	CO ₂ Stored
42500	19.7%	11.5%	4.0%
50000	18.0%	12.7%	5.8%
75000	15.6%	14.1%	8.7%
100000	12.7%	16.5%	12.5%
125000	12.2%	16.1%	12.1%
No Limit	12.0%	15.9%	11.8%

Similar to the light oil case, the errors in incremental recovery decrease dramatically from 20% to 12% as the production gas rate limits increase. However, for the errors in both gas production and CO₂ stored, the errors increase to a maximum of 46.5% and 12.5% respectively and then stay relatively constant at higher production rate limit. The overall errors exhibited in heavy oil reservoir are significantly higher if compared to the ones shown in light oil reservoir. Figure 41 shows the trends of percent error varying with producer gas production rate limit.

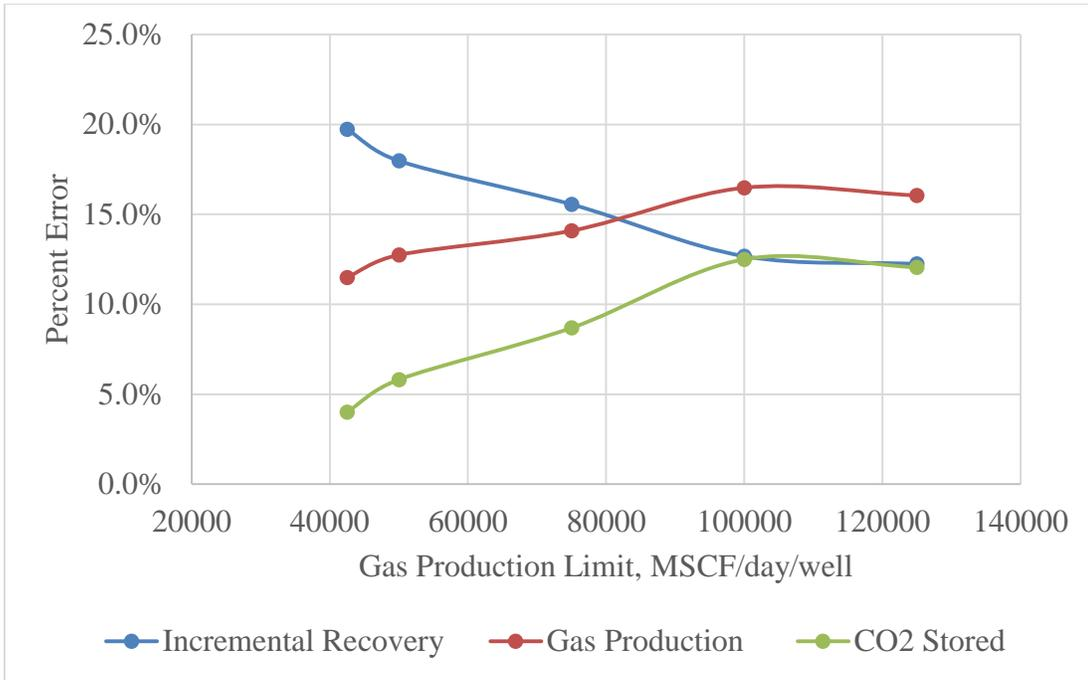


Figure 41 – Summary of error in incremental recovery, gas production and CO₂ stored by changing producer gas production rate limit for heavy oil.

Similar to the light oil case, the error trend of incremental recovery is different from the ones exhibited by both gas production and CO₂ stored. The errors of both gas production and CO₂ stored first increase with production rate limits till they reach plateaus. The errors stay fairly consistent when the gas production rate limit exceeds 100000 Mscf/day. For incremental recovery, the errors reduce substantially and stay constant as the gas production rate limit exceeds 100000 Mscf/day.

5.7 Computational Cost

The use of local grid refinement around the wells has been proven to be crucial in reducing the impacts of both numerical dispersion and non-linearity of flash calculations.

However, solving flash equilibrium equations in multi-component systems by using local grid refinement increases the computational costs greatly. The computation costs are extremely high especially in the cases with light oil reservoir where phase and saturation change significantly over the course of simulation. For light oil reservoir, the model without local grid refinement is coarse. Thus, it only takes 2 to 3 minutes to complete the simulation. However, the addition of static local grid refinement will increase the computational time up to 2 or 3 days. Since heavy oil reservoir requires less computational power as there is little change in phase behaviors, the computational time is lower. The coarse model without LGR application takes 1 to 2 minutes to run while the refined model with LGR application can take up to 2 to 3 hours for a single run. Therefore, the computational costs for LGR application is really high although it can provide results with higher accuracy.

CHAPTER VI

OPTIMUM DEVELOPMENT STRATEGIES

The performance of CO₂-EOR miscible flooding is highly dependent on the sweep efficiency of CO₂ in the reservoir. Unfavorable sweep efficiency will result in early breakthrough, decreasing the performance of the CO₂ flooding. Maximizing sweep efficiency can be done by employing several development strategies. One of the strategies is rate control, which involves allocating the injected fluids to the injectors and by adjusting the produced fluids from the producers. Optimization of the production-injection scheme is usually complicated due to reservoir heterogeneity and uncertainty. However, it can be done by conducting numerous runs of reservoir simulations to determine a reasonable scheme. Several variables have been included in this study so that their effects on the performance can be identified. Variables that are related to injection scheme include injection rate, injection initiation time and CO₂ recycling while the variables that are related to production scheme involve producer BHP, producer target oil rate and producer gas production rate limit.

Apart from sweep efficiency, gravity segregation is another major concern in conducting CO₂-EOR miscible flooding. Gravity override generally occurs in the reservoir as CO₂ is usually less dense than the reservoir oil. When the vertical communication is high, CO₂ tends to gravity segregate to the top of the reservoir unit and sweep the upper part of the reservoir. Thus, completion locations of both injector and producer wells have major impacts on the oil recovery in CO₂ flooding.

To evaluate and identify optimum injection and production strategies, two performance yardsticks have been used, namely CO₂ utilization factor and CO₂ storage efficiency. CO₂ utilization factor helps to determine the efficiency of the flood by measuring the amount of incremental oil that can be produced by every pound of CO₂ injected.

$$CO_2 \text{ Utilization Factor} = \frac{\text{Incremental Oil Produced (STB)}}{\text{Amount of CO}_2 \text{ Injected (MM lb)}} \dots\dots\dots (5)$$

According to Salem and Moawad (2013), for the CO₂-EOR miscible flooding to be economical, the utilization factor should be between 720 STB to 1080 STB per million pounds of CO₂ injected. Brock and Bryan indicates that most reservoirs flooded with CO₂ have a utilization factor of 500 STB to 1080 STB per million pounds of CO₂ injected. The higher the CO₂ utilization factor, the higher the efficiency of the CO₂ flooding.

On the other hand, CO₂ storage efficiency helps to determine the performance of CO₂ sequestration. It is defined by the cumulative amount of CO₂ stored in the formation over the cumulative amount of CO₂ injected throughout the study.

$$CO_2 \text{ Storage Efficiency} = \frac{\text{Total CO}_2 \text{ Stored}}{\text{Total CO}_2 \text{ Injected}} \dots\dots\dots (6)$$

The effects of each injection and production variable on CO₂ utilization factor and storage efficiency are studied and examined. These results obtained will be useful for more robust optimization study of injection-production scheme for CO₂-EOR miscible flooding based upon reservoir performance. Economic analysis will be included in the next chapter to determine the optimum development strategies based upon economic performance.

6.1 Injection Rate

For light oil, the injection rates vary from 100 MMscf/day to 400 MMscf/day, with injection pore volumes range from 0.4 to 1.5. The incremental recovery, gas production and CO₂ stored are recorded. CO₂ utilization factor and storage efficiency have been computed to evaluate the performance of CO₂ flooding. The results are summarized in Table 27.

Table 27 – Production performance at end of simulation by varying injection rate for light oil.

Injection Rate MMscf/day	Incremental Recovery	Gas Production MMMscf	CO₂ Stored MMM lb	CO₂ Utilization STB/MM lb	CO₂ Storage Efficiency
100	10.0%	883	78.5	676	92.7%
150	17.5%	1053	108.6	791	85.5%
200	24.6%	1289	128.9	834	76.1%
225	27.3%	1422	136.9	821	71.8%
250	29.6%	1565	143.7	801	67.8%
300	32.4%	1868	154.8	731	60.9%
400	33.1%	2429	180.3	561	53.2%

The incremental recovery increases as the injection pore volume increases. However, the increase in incremental recovery reduces as more and more CO₂ is injected into the reservoir. According to the CO₂ utilization factors calculated, the flooding performances at both low and high injection rate are not efficient. At low injection rate, small volume of CO₂ does not sweep the reservoir entirely, bypassing significant amount of oil in reservoir. However, high injection rate will result in early CO₂ breakthrough, leading to lower CO₂ utilization factor. Thus, based upon CO₂ utilization factors, the

optimum injection rate is around 200 MMscf/day, resulting in an injection pore volume of 0.7. The CO₂ utilization factors also indicate that injection pore volumes of 0.4 and 1.5 are not economical as their CO₂ utilization factors are lower than the 720 STB/MM lb. Apart from incremental recovery, both gas production and amount of CO₂ stored increases as more CO₂ is injected. Thus, to determine the amount of CO₂ retained in the reservoir, CO₂ storage efficiency has been evaluated. The CO₂ storage efficiency reduces significantly as the injection pore volume increases. This is due to earlier CO₂ breakthrough time in cases with high injection rates. Figure 42 shows the summary of trends of CO₂ utilization factor and storage efficiency.

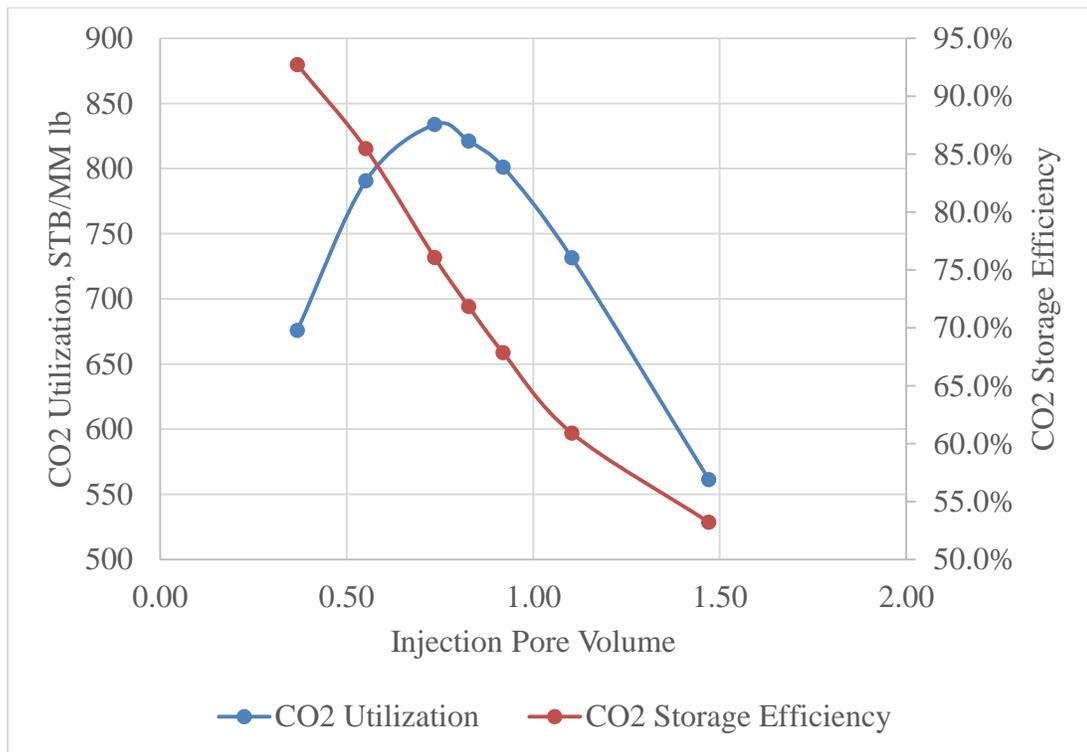


Figure 42 – CO₂ utilization factor and storage efficiency trend by varying injection rate for light oil.

From the trends exhibited, there is a trade-off in CO₂ utilization factor and storage efficiency. The injection pore volume with the highest CO₂ utilization factor will not result in the best storage efficiency. Thus, optimum injection pore volume based upon reservoir performance ranges from 0.5 to 0.8, depending on the priority and purpose of the CO₂ flooding projects.

For heavy oil, the injection rates vary from 100 MMscf/day to 300 MMscf/day, with injection pore volumes range from 0.4 to 1.2. The results are summarized in Table 28.

Table 28 – Production performance at end of simulation by varying injection rate for heavy oil.

Injection Rate MMscf/day	Incremental Recovery	Gas Production MMMscf	CO₂ Stored MMM lb	CO₂ Utilization STB/MM lb	CO₂ Storage Efficiency
100	25.8%	209	61.3	4060	72.3%
125	28.8%	331	68.5	3625	64.7%
150	30.7%	475	73.1	3216	57.5%
175	32.4%	622	77.4	2912	52.2%
200	33.8%	731	80.7	2738	49.2%
225	34.8%	817	83.3	2623	47.2%
250	35.8%	897	85.8	2529	45.5%
300	37.6%	1048	90.3	1968	35.5%

Similar to light oil, the incremental recovery of heavy oil increases as the injection pore volume increases. However, the increase in incremental recovery reduces as the injection pore volume increases. Both the incremental recovery and CO₂ utilization factor of heavy oil are higher if compared to light oil. According to the CO₂ utilization factors

calculated, the flooding performance at all injection rates are efficient and economical. However, optimum injection pore volume can still be determined. Higher injection rate will result in early CO₂ breakthrough, leading to lower CO₂ utilization factor. Thus, based upon CO₂ utilization factors, the optimum injection rate is around 100 MMscf/day, resulting in an injection pore volume of 0.4. Apart from incremental recovery, both gas production and amount of CO₂ stored increases as more CO₂ is injected. The CO₂ storage efficiency reduces significantly as the injection pore volume increases. This is due to earlier CO₂ breakthrough time in cases with high injection rates. Figure 43 shows the summary of trends of CO₂ utilization factor and storage efficiency.

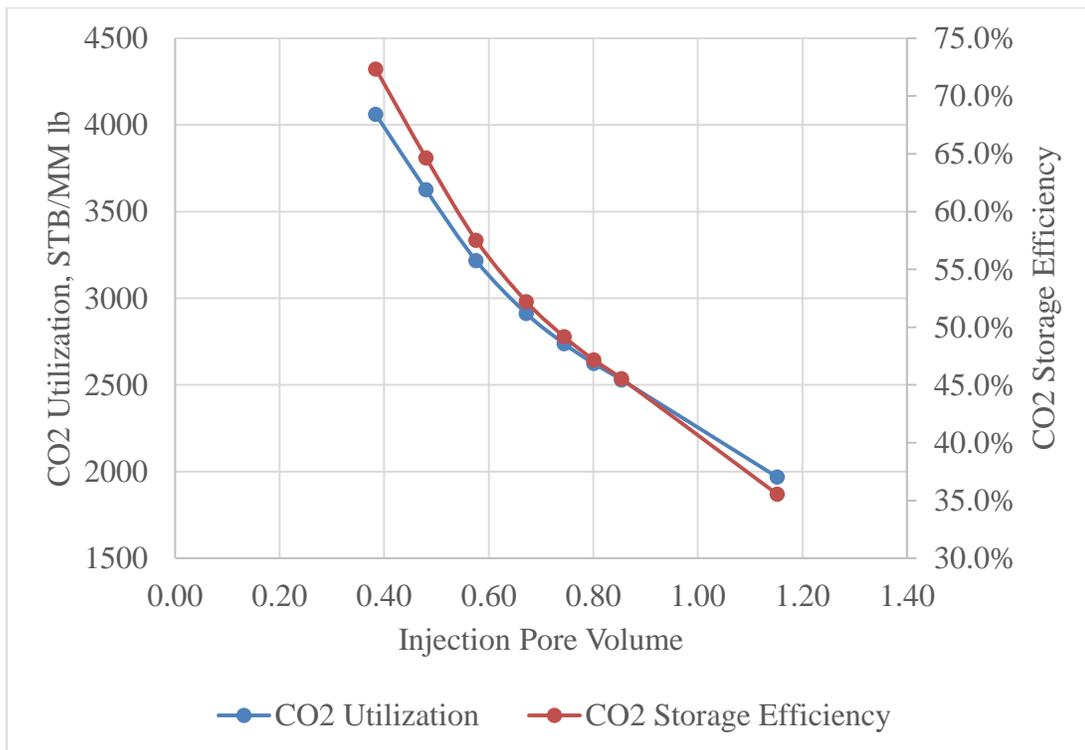


Figure 43 – CO₂ utilization factor and storage efficiency trend by varying injection rate for heavy oil.

Heavy oil cases show significant differences in the trends of CO₂ utilization factor and storage efficiency if compared to light oil cases. From the trends exhibited, there is no trade-off in CO₂ utilization factor and storage efficiency. Both CO₂ utilization and storage efficiency show similar trends, which reduce with increasing injection pore volume. Thus, optimum injection pore volume based upon reservoir performance is around 0.4, which results the highest CO₂ utilization factor and storage efficiency.

6.2 CO₂ Recycling

For light oil, the injection rates of the middle injector investigated range from 250 MMscf/day to 350 MMscf/day. The results of the production performance are summarized in Table 29.

Table 29 – Production performance at end of simulation by recycling produced gas for light oil.

Injection Rate MMscf/day	Recycle	Incremental Recovery	Gas Production MMMscf	CO ₂ Stored MMM lb	CO ₂ Utilization STB/MM lb	CO ₂ Storage Efficiency
250	No Recycle	29.6%	1565	143.7	801	67.8%
250	Recycle	52.7%	8074	148.7	1428	70.2%
300	No Recycle	32.4%	1868	154.8	731	60.9%
300	Recycle	50.3%	9274	163.8	1137	64.5%

By recycling the gas produced, the incremental recovery increases dramatically. For example, the incremental recovery for recycling case with injection rate of 250 MMscf/day increases nearly twice if compared to the one without recycling. Reinjecting

produced gas will not only help enhancing oil mobility, but also help with maintaining reservoir pressure for production. The significant increase in incremental recovery results in higher CO₂ utilization factor in the cases with recycling. The gas production also increases substantially in the case with recycling as more gas is produced when the produced gas is recycled. Simultaneously, more CO₂ can be stored in the reservoir at the end of the simulation if CO₂ is recycled. The CO₂ storage efficiency of the cases with recycling improves slightly if compared to the ones without recycling. Thus, in terms of reservoir performance, recycling produced gas is highly recommended as it will give better production performance.

For light oil, the injection rates of the middle injector investigated range from 100 MMscf/day to 150 MMscf/day. The results of the production performance are summarized in Table 30.

Table 30 – Production performance at end of simulation by recycling produced gas for heavy oil.

Injection Rate MMscf/day	Recycle	Incremental Recovery	Gas Production MMMscf	CO₂ Stored MMM lb	CO₂ Utilization STB/MM lb	CO₂ Storage Efficiency
100	No Recycle	25.8%	209	61.3	4060	72.3%
100	Recycle	31.0%	483	81.8	4874	96.5%
125	No Recycle	28.8%	331	68.5	3021	53.9%
125	Recycle	30.7%	597	102.8	3219	80.9%
150	No Recycle	30.7%	475	73.1	2412	43.1%
150	Recycle	30.5%	681	111.6	2396	65.9%

There are two major differences in the production performance for heavy oil reservoir due to recycling if compared to light oil reservoir. First, although the incremental

recovery increases, the improvement in incremental recovery is not as significant as the ones in light oil cases. The largest improvement occurs in the case with injection rate of 100 MMscf/day, where the incremental recovery increases from 26% to 31%. Second, at high injection rate, recycling produced gas does not contribute to better reservoir performance. The incremental recovery actually declines slightly when the injection rate is fixed at 150 MMscf/day. When the injection rate of the middle injector is high, the additional positive effect due to recycling produced gas is diminished. Generally, the CO₂ utilization factor shows improvement in all cases other than the case with an injection rate of 150 MMscf/day. Apart from the incremental recovery, the gas production and the amount of CO₂ stored increase when the produced gas is recycled. The storage efficiency increases significantly when CO₂ is recycled. The increase in storage efficiency due to recycling is more prominent in heavy oil reservoir if compared to light oil reservoir. Therefore, it is highly recommended to recycle produced gas, especially if the constant injection rate of pure CO₂ is low, as this will improve the incremental recovery and CO₂ storage efficiency substantially.

6.3 Injection Initiation Time

Since the injection initiation time differs, the cumulative amount of CO₂ injected in each case vary. For light oil, the injection initiation time ranges from 0 (beginning) to 7th year. The injection initiation time cases are terminated at 7th year because the reservoir is not able to produce under natural depletion after 7 years. After 5 years of natural depletion, the reservoir pressure will start decreasing below the bubble point of the light

oil, causing the fluids to exist as two phases in the reservoir. The results of production performance are summarized in Table 31.

Table 31 – Production performance at end of simulation by changing injection initiation time for light oil.

Injection Rate MMscf/day	Injection Start Time, year	Incremental Recovery	Gas Production MMMscf	CO₂ Stored MMM lb	CO₂ Utilization STB/MM lb	CO₂ Storage Efficiency
300	0.0	43.1%	1668	166.9	974	65.7%
300	4.0	41.9%	1379	159.4	1112	73.8%
300	6.0	37.7%	1227	147.0	1135	77.1%
300	7.0	35.0%	1152	140.4	1130	78.9%

As the injection initiation time is delayed, the incremental recovery drops from 43% to 35% as the amount of CO₂ injected into the reservoir decreases. However, this does not suggest that injecting CO₂ at later time is not recommended. CO₂ utilization factor exhibits a different trend if compared to incremental recovery. CO₂ utilization factor increases at first and then starts to decrease. This suggests that there is an optimum injection initiation timing for CO₂-EOR project, which is at the 6th year in the cases with light oil. Injection at the beginning does not contribute to additional benefits as the reservoir is capable at producing under natural depletion. After 5 years of natural depletion, the reservoir pressure reduces to about 2000 psia, which is around the MMP for the CO₂-EOR project. Injection at later time around MMP results in the most optimum CO₂ utilization factor. If the injection is initiated at a pressure lower than the MMP, the CO₂ utilization factor starts to drop, which is exhibited by the case with injection initiation time at 7th year. Apart from incremental recovery, the gas production decreases as the CO₂

injection initiation time is delayed. Delayed CO₂ injection initiation time will result in later breakthrough time. Thus, gas production will be reduced. The amount of CO₂ stored in the reservoir decreases as the injection initiation time is delayed as less CO₂ is injected throughout the simulation. However, the CO₂ storage efficiency increases linearly with injection initiation time. Figure 44 shows the trends of CO₂ utilization factor and storage efficiency by changing the CO₂ injection initiation time in light oil reservoir.

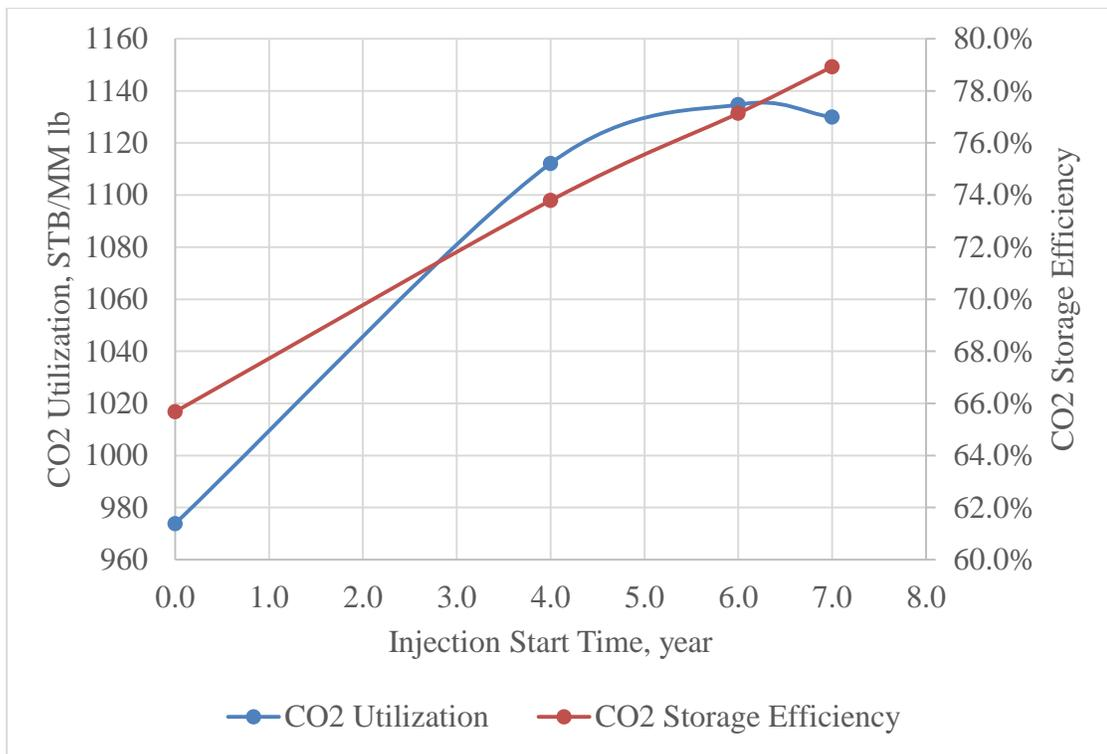


Figure 44 – CO₂ utilization factor and storage efficiency trend by changing injection initiation time for light oil.

For heavy oil, the injection initiation time ranges from 0 (beginning) to 4th year. The injection initiation time cases are terminated at 4th year because the reservoir is not

able to produce under natural depletion after 4 years. The reservoir pressure will never drop below the bubble point because the bubble point of the heavy oil is extremely low. Thus, the fluid in the reservoir will always remain in single phase. The results of production performance are summarized in Table 32.

Table 32 – Production performance at end of simulation by changing injection initiation time for heavy oil.

Injection Rate MMscf/day	Injection Start Time, year	Incremental Recovery	Gas Production MMMscf	CO₂ Stored MMM lb	CO₂ Utilization STB/MM lb	CO₂ Storage Efficiency
175	0.0	32.4%	622	77.4	2912	52.2%
175	2.0	32.2%	563	76.2	3042	54.1%
175	3.0	32.2%	499	76.3	3216	57.1%
175	4.0	31.7%	447	74.9	3345	59.4%

Unlike in light oil reservoir, the incremental recovery drops slightly when the injection initiation time is delayed. However, the CO₂ utilization factor in heavy oil case increases significantly as the injection initiation time is delayed. Although injection initiation time is delayed in some cases, however the reservoir pressure is still well above the MMP of CO₂ in heavy oil. Thus, as long as the reservoir pressure is maintained above MMP, delay in injection initiation time will result in higher CO₂ utilization factor. Similar trend can be observed in the gas production as it decreases with delayed injection initiation time. For CO₂ storage efficiency, it increases with injection initiation time although less amount of CO₂ is stored in the reservoir at later injection time. Figure 45 summarized the trends of CO₂ utilization factor and storage efficiency by changing the CO₂ injection initiation time in heavy oil reservoir.

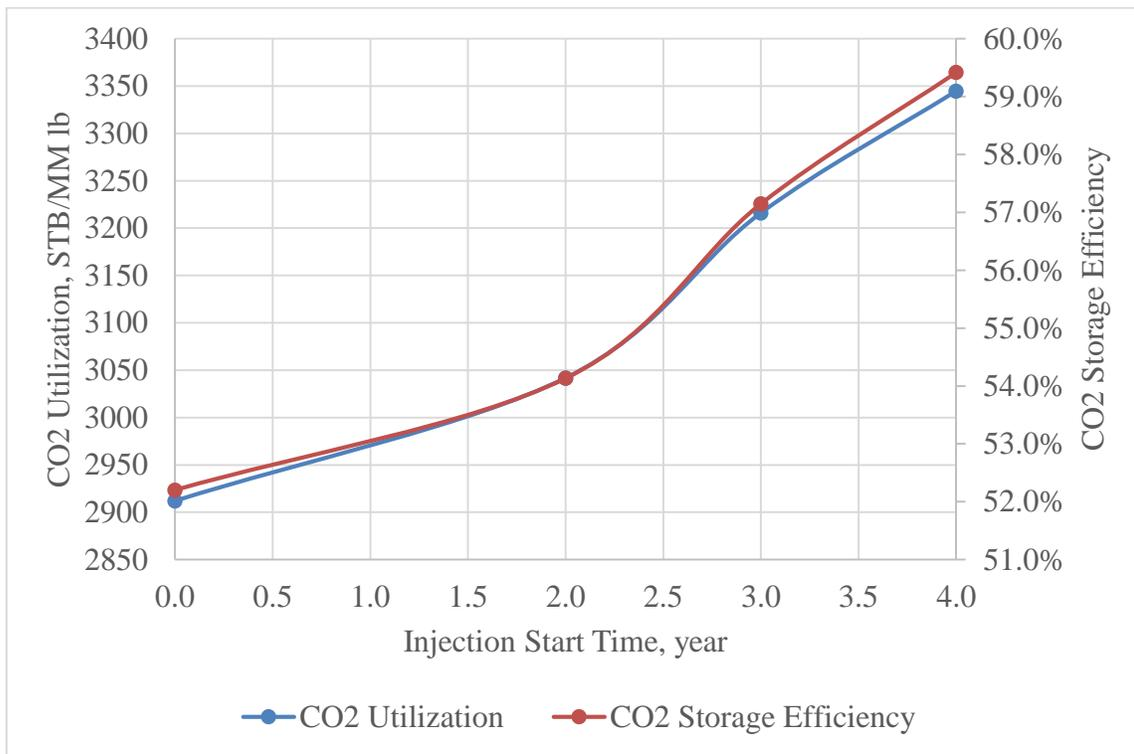


Figure 45 – CO₂ utilization factor and storage efficiency trend by changing injection initiation time for heavy oil.

6.4 Producer BHP

For light oil cases, the producer BHPs used range from 1200 psia to 3000 psia. Constant injection rate of 300 MMscf/day has been applied in light oil reservoir. The production performance of light oil reservoir by changing producer BHP is summarized in Table 33.

Table 33 – Production performance at end of simulation by changing producer BHP for light oil.

Producer BHP, psia	Incremental Recovery	Gas Production MMMscf	CO₂ Stored MMM lb	CO₂ Utilization STB/MM lb	CO₂ Storage Efficiency
1200	26.9%	1868	154.8	731	60.9%
1800	36.7%	1668	166.9	974	65.7%
2500	46.8%	1547	174.2	1217	68.6%
3000	49.2%	1486	177.6	1279	69.9%

The incremental recovery for light oil reservoir increases significantly from 27% to 49% by increasing the producer BHP. High producer BHP induce smaller drawdown. Thus the CO₂ injected will be able to stay in the reservoir for a longer time to achieve miscibility, lengthening the “soaking” period. Besides, by increasing the producer BHP, the reservoir pressure will be maintained for a longer time as we “choke” back our production. Therefore, the CO₂ utilization factor increases substantially as the producer BHP increases. For example, the CO₂ utilization suggests that the flooding is not economical if the producer BHP is set at 1200 psia. However, if the producer BHP is raised to 3000 psia, the CO₂ utilization factor improves considerably. This will result in better economic outcomes for the flooding. Furthermore, the gas production decreases as the producer BHP increases. The amount of CO₂ stored also increases due to better storage efficiency. Therefore, for light oil, it is recommended to use higher producer BHP as it will give a better overall performance in incremental recovery, gas production and CO₂ stored. Figure 46 summarizes the trends of CO₂ utilization factor and storage efficiency for light oil case by varying the producer BHP.

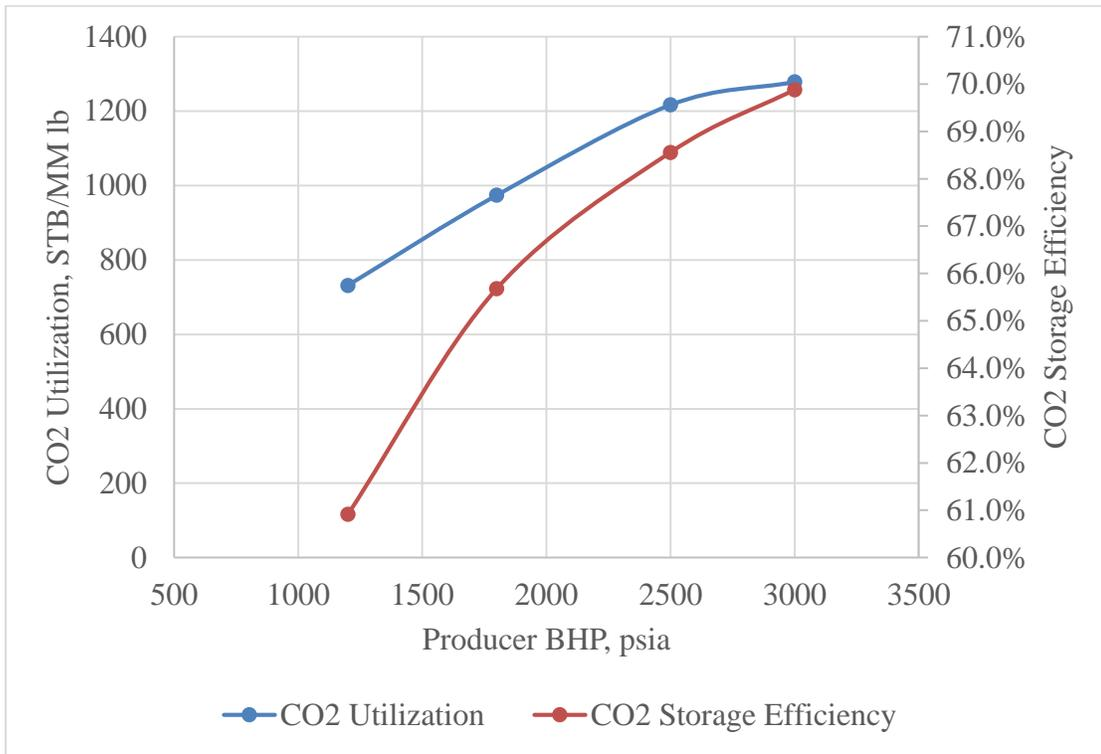


Figure 46 – CO₂ utilization factor and storage efficiency trend by changing producer BHP for light oil.

Similarly, for heavy oil, the producer BHPs used range from 1200 psi to 3000 psi. CO₂ has been injected at a constant rate of 150 MMscf/day since the beginning of the simulation. The production performances for all the cases in heavy oil reservoir are summarized in Table 34.

Table 34 – Production performance at end of simulation by changing producer BHP for heavy oil.

Producer BHP, psia	Incremental Recovery	Gas Production MMMscf	CO₂ Stored MMM lb	CO₂ Utilization STB/MM lb	CO₂ Storage Efficiency
1200	36.4%	622	77.4	1699	30.5%
1800	36.1%	580	81.7	1687	32.1%
2500	36.0%	548	85.4	1680	33.6%
3000	35.9%	529	87.5	1677	34.4%

There are two main differences observed from the production performance in heavy oil reservoir if compared to the ones in light oil reservoir. First, the incremental recovery decreases as the producer BHP increases. This contrasts with the trends exhibited by light oil reservoir. CO₂ utilization factor reduces as the producer BHP increases. Second, the influence of producer BHP is not as significant as the ones observed in light oil reservoir. The incremental recovery reduces from 36.4% to 35.9%, suggesting that producer BHP is not an important variable in optimizing the development strategies. Apart from the incremental recovery, heavy oil reservoir exhibits similar trends in terms of gas production and CO₂ storage. The gas production decreases with increasing producer BHP as less gas is produced together with the oil due to smaller pressure drawdown. For CO₂ storage, the storage efficiency increases with increasing producer BHP. More CO₂ is retained in the reservoir as the hydrocarbon is produced with small pressure drawdown. Figure 47 shows the trends of CO₂ utilization factor and storage efficiency by changing producer BHP in heavy oil reservoir. The trends suggest that there is a trade-off between the CO₂ utilization factor for production and CO₂ storage efficiency for sequestration

purposes. Thus, determination of producer BHP in heavy oil reservoir is highly dependent on the priority and purpose of the flooding projects.

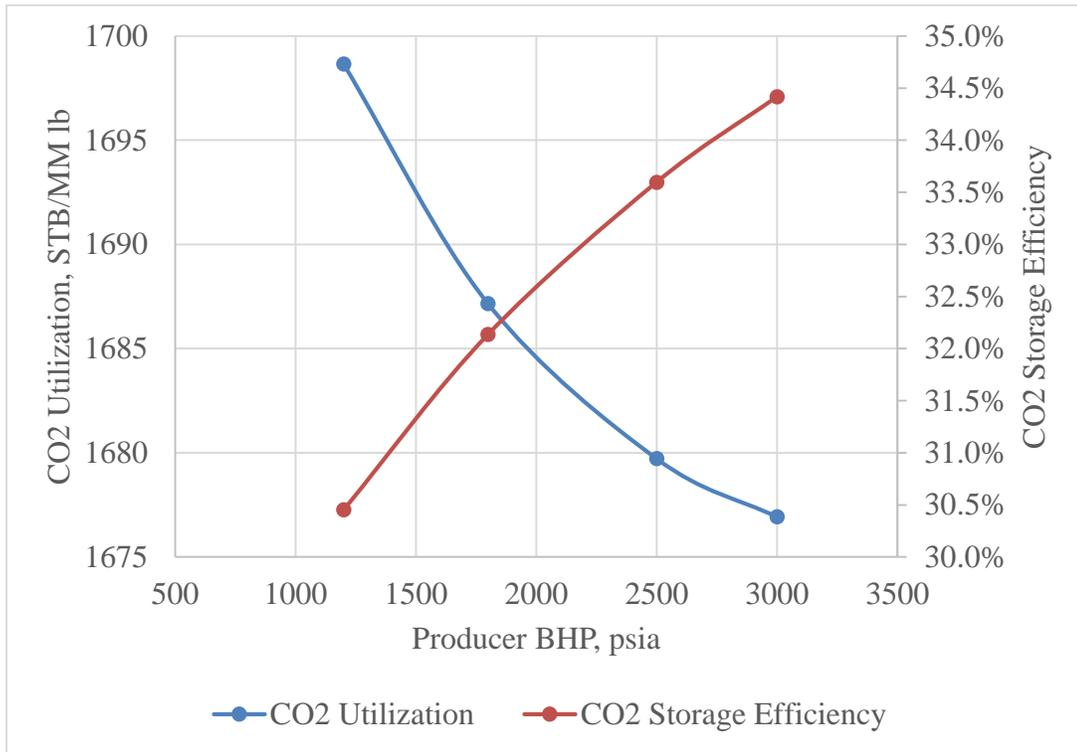


Figure 47 – CO₂ utilization factor and storage efficiency trend by changing producer BHP for heavy oil.

6.5 Producer Target Oil Rate

For light oil, the target oil rates are set from 15 Mstb/day to 25 Mstb/day for each producer. CO₂ is injected at a constant rate of 300 MMscf/day since the beginning of the simulation. The results are summarized in Table 35.

Table 35 – Production performance at end of simulation by changing producer target oil rate for light oil.

Target Oil Rate, bbl/day/well	Incremental Recovery	Gas Production MMMscf	CO₂ Stored MMM lb	CO₂ Utilization STB/MM lb	CO₂ Storage Efficiency
15000	33.0%	1974	137.2	745	54.0%
18000	32.9%	1887	150.7	743	59.3%
20000	32.4%	1868	154.8	731	60.9%
22000	31.7%	1860	157.1	717	61.8%
25000	30.8%	1857	159.0	695	62.6%

First, incremental recovery decreases as the producer oil target rate increases. When the target oil rate is low, the production is limited, which helps with the pressure maintenance. Similar outcome has been observed in the cases where the producer BHP is varied. Better reservoir performance can be achieved if the light oil production is limited. Limiting production does not only help with pressure maintenance, it also helps to achieve better miscibility between CO₂ and reservoir oil. Thus, CO₂ utilization factor decreases as the producer BHP increases. Therefore, production engineers should not plan on building surface facility to handle large production volumes as this does not benefit reservoir performance in this case. Apart from incremental recovery, gas production decrease as the target oil rate increases. More CO₂ can be stored in the reservoir at the end of the simulation if high target oil rate is used. More voids in the reservoir are available if more oil is produced, enhancing the space for CO₂ sequestration. Figure 48 shows the trend of CO₂ utilization factor and storage efficiency by varying oil target rate. Trade-off in CO₂ utilization factor and storage efficiency can be observed.

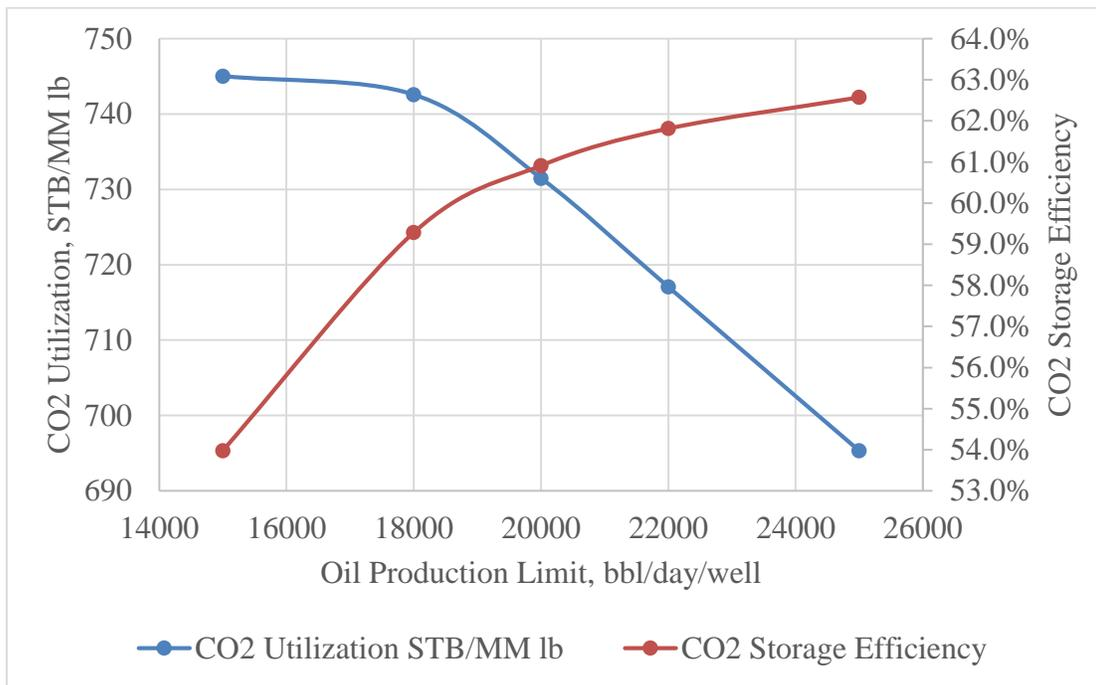


Figure 48 – CO₂ utilization factor and storage efficiency trend by changing producer target oil rate for light oil.

For heavy oil, the target oil rates are fixed from 18 Mstb/day to 25 Mstb/day for each producer. CO₂ is injected at a constant rate of 150 MMscf/day since the beginning of the simulation. The results are summarized in Table 36.

Table 36 – Production performance at end of simulation by changing producer target oil rate for heavy oil.

Target Oil rate, bbl/day/well	Incremental Recovery	Gas Production MMMscf	CO ₂ Stored MMM lb	CO ₂ Utilization STB/MM lb	CO ₂ Storage Efficiency
18000	30.0%	488	71.1	1572	28.0%
20000	30.7%	475	73.1	1608	28.8%
22000	31.1%	468	73.4	1628	28.9%
25000	31.6%	459	74.5	1653	29.3%

The incremental recovery of heavy oil shows different trend if compared to the light oil cases. The incremental recovery increases slightly from 30% to about 32% when the target oil rate increases. CO₂ utilization factor also increases with increasing target oil rate. However, since the changes in both incremental recovery and utilization factor are minor, optimizing target oil rate will not improve the production considerably. Apart from the incremental recovery, the gas production decreases as the target oil rate increases. CO₂ storage efficiency also improves slightly as more oil is produced from reservoir, leaving more pore spaces for CO₂ sequestration. Figure 49 summarizes the trends of CO₂ utilization factor and storage efficiency by changing producer target oil rate. Both performance yardsticks show similar trends, suggesting that high target oil rate is highly recommended for heavy oil reservoir as it will give better CO₂ utilization factor and storage efficiency.

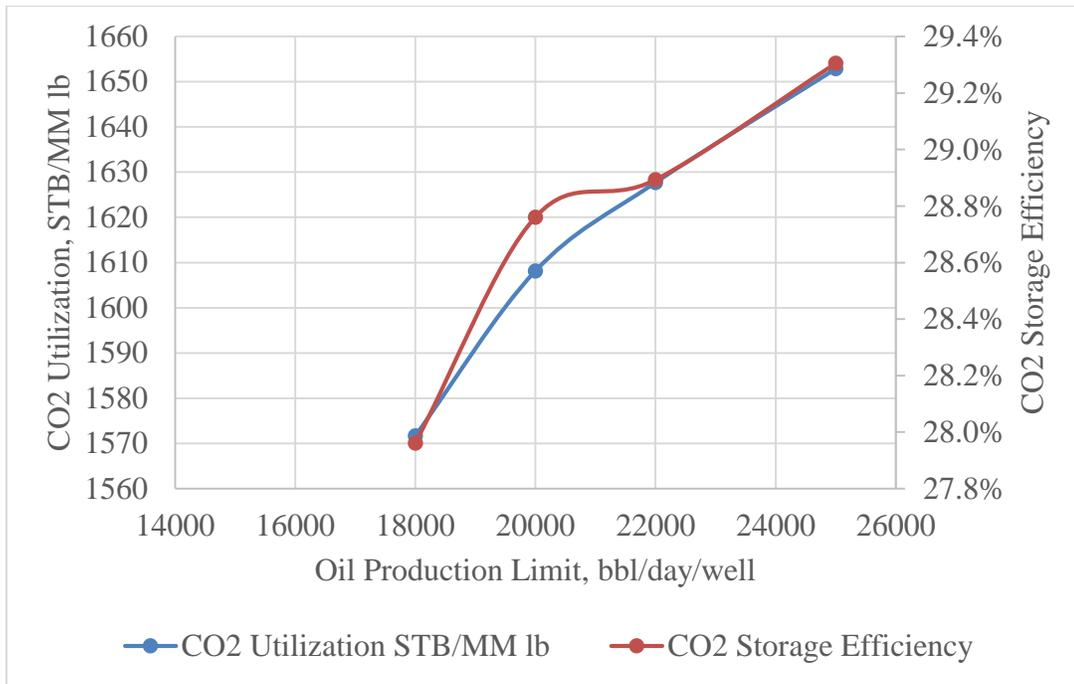


Figure 49 – CO₂ utilization factor and storage efficiency trend by changing producer target oil rate for heavy oil.

6.6 Producer Gas Rate Limit

For light oil, the gas production rate limits are set from 42.5 Mscf/day to 150 Mscf/day for each producer. CO₂ is injected at a constant rate of 300 MMscf/day since the beginning of the simulation. The results are summarized in Table 37.

Table 37 – Production performance at end of simulation by changing producer gas production rate limit for light oil.

Gas Prod Limit Mscf/day/well	Incremental Recovery	Gas Production MMMscf	CO₂ Stored MMM lb	CO₂ Utilization STB/MM lb	CO₂ Storage Efficiency
42500	19.0%	1239	194.5	430	76.5%
50000	24.7%	1407	183.6	557	72.2%
75000	35.2%	1864	151.7	796	59.7%
100000	32.8%	1871	153.9	740	60.6%
125000	32.5%	1869	154.5	734	60.8%
150000	32.4%	1868	154.7	732	60.9%
No Limit	32.4%	1868	154.8	731	60.9%

The trend of the incremental recovery shows there is an optimum value for the gas production rate in which will recover the highest amount of oil. The incremental recovery increases to a maximum value and then decreases as the gas production rate limit increases. At high gas production rate limit, the incremental recovery stays relatively constant as the high rate limit does not contribute to any significant effects as if there is no limit on gas production. Comparing the case with no rate limit and the case with optimum rate limit, the incremental recovery can increase by about 3% just by imposing a gas production rate limit. The CO₂ utilization factor increases till an optimum value and then decreases with increasing rate limit. Apart from the incremental recovery, the gas production increases with increasing rate limit. Higher rate limit will allow more gas to be produced, leading to high gas production. The amount of CO₂ stored decreases when high gas rate limit is imposed. At high rate limit, most of the CO₂ injected will be produced together with the hydrocarbon. Less CO₂ will remain in the reservoir, leading to poor

storage efficiency. Figure 50 shows the trends of CO₂ utilization factor and storage efficiency by changing the gas production rate limit for light oil reservoir. From the trend shown, there is a significant trade-off between the CO₂ utilization factor and storage efficiency at low gas production rate limit. Low gas rate limit should be imposed if the project focuses on CO₂ sequestration in the reservoir. However, if the project focuses on the economic benefits due to oil production, optimum gas rate limit of 75 MMscf/day should be used as it will result in the best CO₂ utilization factor.

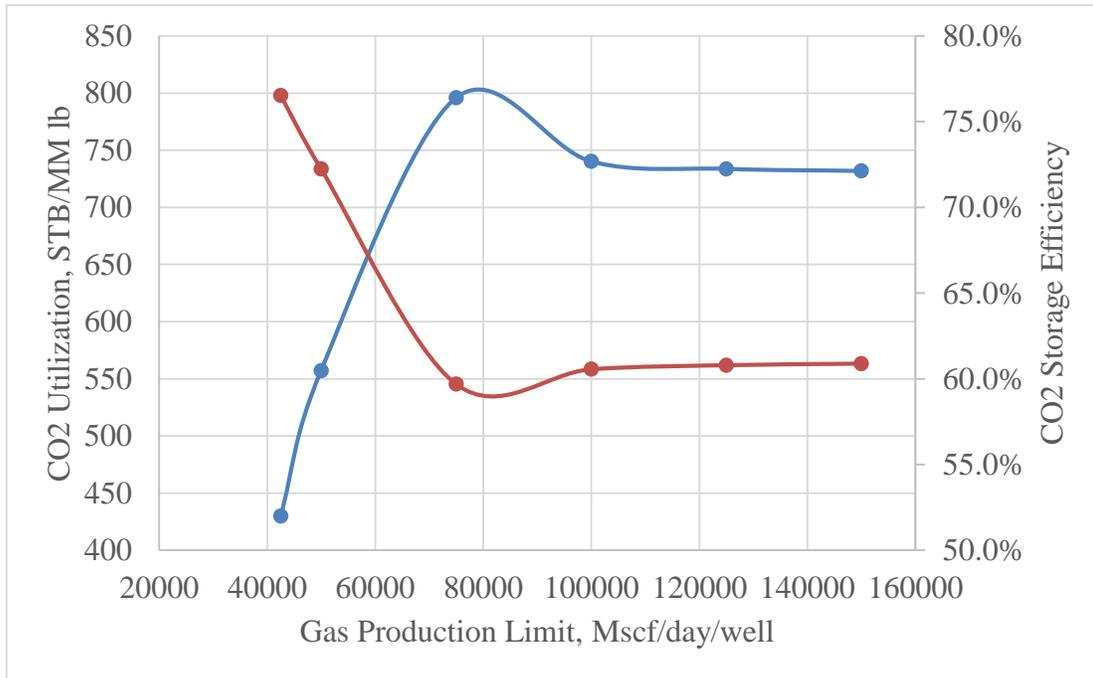


Figure 50 – CO₂ utilization factor and storage efficiency trend by changing producer gas production rate limit for light oil.

For heavy oil, the gas production rate limit range from 15 MMscf/day to 35 MMscf/day. Since the gas production rate is low in heavy oil reservoir, the gas production

rate limits imposed are relatively lower if compared to the ones in light oil reservoir. The production performances due to the change in gas production rate limit are summarized in Table 38.

Table 38 – Production performance at end of simulation by changing producer gas production rate limit for heavy oil.

Gas Prod Limit Mscf/day/well	Incremental Recovery	Gas Production MMMscf	CO₂ Stored MMM lb	CO₂ Utilization STB/MM lb	CO₂ Storage Efficiency
15000	23.6%	275	95.2	2484	75.1%
20000	26.2%	351	86.8	2740	68.3%
25000	28.6%	423	78.5	2991	61.8%
30000	30.5%	480	72.0	3191	56.7%
35000	30.6%	476	72.5	3209	57.0%
No Limit	30.7%	475	73.1	3216	57.5%

The incremental recovery shows significantly different trend if compared to the one in light oil reservoir. The incremental recovery increases as the gas production rate limit increases. Essentially, the results suggest that the incremental recovery will be better if no rate limit is imposed on the gas production. At high gas rate limit, the incremental recovery does not show significant change and stays relatively constant. For the gas production, it is expected that the gas production will increase as the rate limit increases. The amount of CO₂ stored also decreases as the imposed gas rate limit increases. Most of the CO₂ injected is produced at higher rate limit, leading to a decline in the amount of CO₂ stored in the reservoir. Therefore, the CO₂ storage efficiency reduces with increasing gas rate limit. Figure 51 summarizes the trends of CO₂ utilization factor and storage efficiency as the gas rate limit increases. Similar observation can be obtained if compared to the light

oil cases as trade-off exists between the CO₂ utilization factor and storage efficiency. Compromise between CO₂ utilization factor and CO₂ sequestration has to be made according to the priority and purpose of the project.

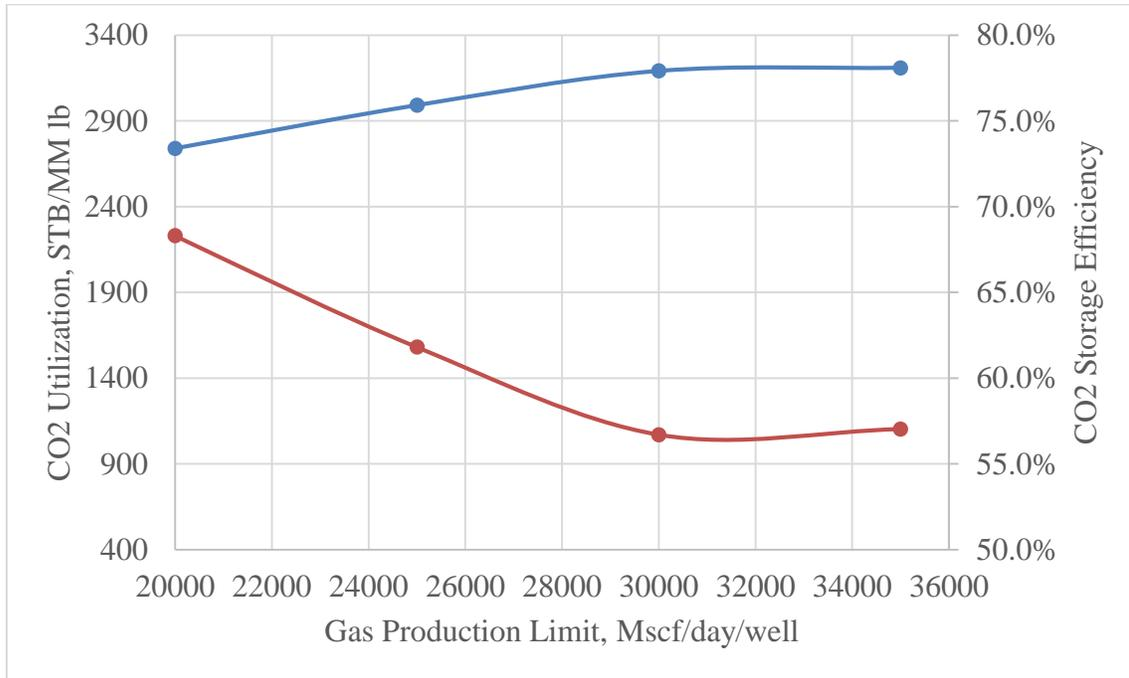


Figure 51 – CO₂ utilization factor and storage efficiency trend by changing producer gas production rate limit for heavy oil.

6.7 Completion Location

Due to the effect of gravity segregation, completion locations play an important role in dictating the reservoir performance for CO₂-EOR miscible flooding. Apart from completion location of the well, the effect of completion interval is also included in this study. Early breakthrough of CO₂ due to inappropriate completion design may create a preferential path for CO₂ to flow through the reservoir, leaving significant portions of the

reservoir unswept. For both light and heavy oil reservoirs, two completion heights have been considered, namely, half or one-third of the pay zone. The completion locations have been divided into two main categories, which are top and bottom. The reservoir performance of the light oil reservoir by varying the completion design are summarized in Table 39 and Table 40 below.

Table 39 – Production performance at end of simulation by changing completion location for light oil (completed half of net pay).

Completion Location		Incremental Recovery	Gas Production MMMscf	CO ₂ Stored MMM lb	CO ₂ Utilization STB/MM lb	CO ₂ Storage Efficiency
Injector	Producer					
Whole	Whole	28.5%	1921	146.5	644	57.6%
Bottom	Bottom	37.3%	1915	143.3	842	56.4%
Bottom	Top	40.5%	1769	169.7	914	66.8%
Top	Bottom	38.8%	1846	156.3	876	61.5%
Top	Top	32.5%	1851	155.7	734	61.3%

Table 40 – Production performance at end of simulation by changing completion location for light oil (completed one-third of net pay).

Completed Interval		Incremental Recovery	Gas Production MMMscf	CO ₂ Stored MMM lb	CO ₂ Utilization STB/MM lb	CO ₂ Storage Efficiency
Injector	Producer					
Whole	Whole	28.5%	1921	146.5	644	57.6%
Bottom	Bottom	36.9%	1870	146.5	833	57.6%
Bottom	Top	41.4%	1726	174.0	935	68.5%
Top	Bottom	38.5%	1789	162.1	869	63.8%
Top	Top	32.8%	1821	157.4	741	61.9%

There are several important observations from the results presented. First, partial completions perform better if compared to full completion. Completion interval of half or one-third of the pay zone has absolutely better production performance in every aspect

even after considering the partial completion skins. Second, when the completion locations of the injector and producer are inversed, the reservoir performance is better. When the completion locations are inversed, CO₂ will need travel longer path to reach producer, leading to longer stay in the reservoir. CO₂ breakthrough can be delayed and the shorter preferential path for subsequent continuous flow of CO₂ will not be created. Lastly, the completion design with injector at the bottom and producer at the top is the most optimum completion design in light oil reservoir. Since CO₂ is less dense than the oil, CO₂ will tend to segregate to the top of the reservoir. Thus, by injecting CO₂ at the bottom, the CO₂ will displace from the bottom to the top of the reservoir, enhancing the sweep efficiency. Since the producer is completed at the top, the CO₂ has to travel the longest distance. Light oil with dissolved CO₂ will then be produced at the top of the producer. By practicing the optimum completion design, gas production can be reduced to a minimum while storing maximum amount of CO₂. CO₂ storage efficiency improves significantly if the optimum completion design is adopted. Figure 52 shows a comparison of CO₂ concentration for two different completion designs at the end of simulation. Completion design with bottom injector and top producer shows better sweep efficiency. CO₂ concentration is higher in most regions if compared to the ones on the right with bottom injector and bottom producer. This proves that CO₂ storage efficiency and utilization factor can be improved significantly if correct completion designs are implemented.

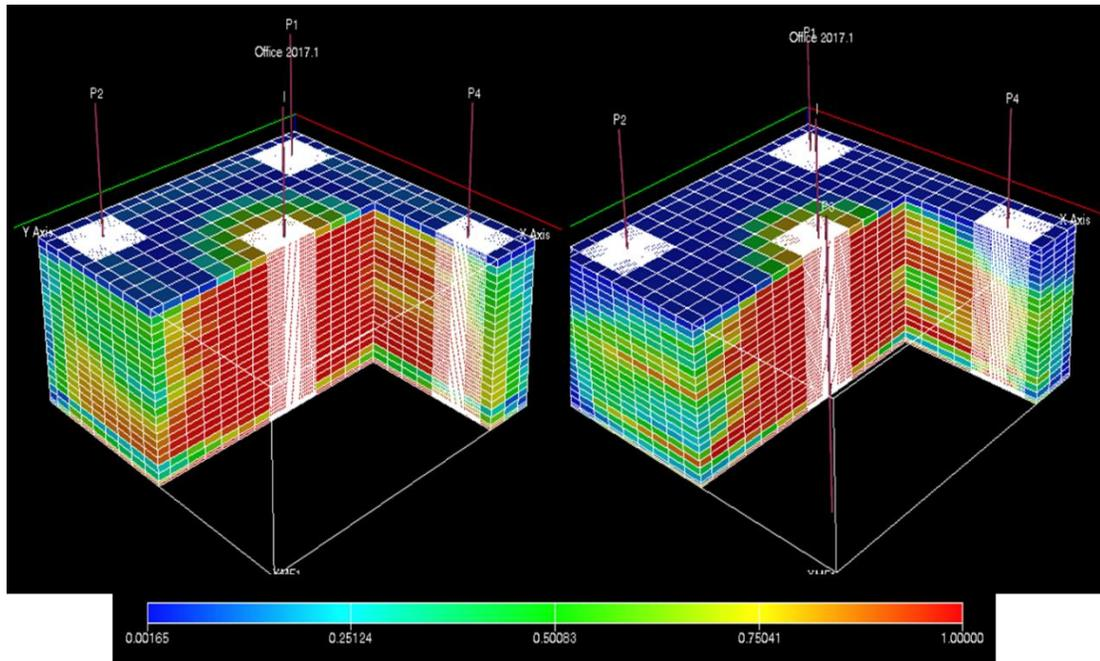


Figure 52 – Comparison of CO₂ concentration at the end of simulation for two different completion designs. (Left – Bottom injector and top producer; right – Bottom injector and bottom producer)

For heavy oil reservoir, two completion intervals have been considered, which include completion zone with half and one-third of the net pay. The results for both scenario have been summarized in Table 41 and Table 42.

Table 41 – Production performance at end of simulation by changing completion location for heavy oil (completed half of net pay).

Completion Location		Incremental Recovery	Gas Production MMMscf	CO ₂ Stored MMM lb	CO ₂ Utilization STB/MM lb	CO ₂ Storage Efficiency
Injector	Producer					
Whole	Whole	34.1%	406	81.2	3567	63.9%
Bottom	Bottom	34.3%	350	87.5	3591	68.9%
Bottom	Top	36.2%	350	87.7	3796	69.1%
Top	Bottom	38.5%	266	97.4	4030	76.6%
Top	Top	30.6%	471	73.5	3202	57.9%

Table 42 – Production performance at end of simulation by changing completion location for heavy oil (completed one-third of net pay).

Completed Interval		Incremental Recovery	Gas Production MMMscf	CO ₂ Stored MMM lb	CO ₂ Utilization STB/MM lb	CO ₂ Storage Efficiency
Injector	Producer					
Whole	Whole	34.1%	406	81.2	3567	63.9%
Bottom	Bottom	31.8%	375	84.6	3335	66.6%
Bottom	Top	36.5%	331	89.9	3822	70.8%
Top	Bottom	38.5%	222	102.6	4037	80.7%
Top	Top	30.5%	464	74.4	3190	58.5%

There are several similarities and differences between the reservoir performances of heavy oil and light oil reservoirs. One of the similarities is the production performance of completion design with inversed completed locations is superior if compared to the completion design with the same completion locations. However, full completion in heavy oil reservoir is not necessarily the worst case scenario. It is better if compared to the cases with same completion locations. If the net pay is completed half, it will result in better production performance. The optimum completion design for CO₂-EOR process in heavy oil reservoir is completely opposite from the one exhibited in light oil reservoir. The optimum completion design is the one with its injector completed at the bottom and producer completed at the top of the reservoir. The difference in trend is mainly due to the density difference between light and heavy oil. The density difference between CO₂ solvent and heavy oil is large, inducing serious gravity segregation effects. Thus, heavy oil preferably stays at the bottom of the reservoir due to gravity. Hence, producer completed at the bottom will result in better production performance. To improve the sweep efficiency, CO₂ will be injected at the top. CO₂ will start accumulating at the top of

the reservoir and displace the heavy oil downward by achieving miscibility by mixing. With this completion design, CO₂ can stay in the reservoir for longer period time to achieve miscibility with the reservoir oil. Apart from the incremental recovery, optimum completion design will result in lowest gas production and highest amount of CO₂ stored. This is due to the significant delay in CO₂ breakthrough when the optimum completion design is adopted.

CHAPTER VII

ECONOMIC ANALYSIS OF CO₂-EOR PROJECT

Apart from optimizing the reservoir performance, economic performance of the projects has to be evaluated. Oil and gas companies generally focus on the economic performance more than the reservoir performance. Projects are usually ranked using economic performance yardsticks such as net present value (NPV) discounted at the hurdle rate, rate of return, payback period and cost to develop. Thus, economic analysis is also included in this study. Detailed cost analysis has been carried out and sensitivity of economic performance of CO₂-miscible EOR project to variables such as prices have been conducted.

7.1 General Cost Functions

General cost functions include costs involved in general oil and gas exploration activities, which are not specific to CO₂-EOR projects.

7.1.1 Drilling Costs

To understand the costs of upstream drilling and production activity, U.S. Energy Information Administration (EIA) commissioned HIS Global Inc. to study the costs on a per well basis in 2015. The study was conducted based upon data collected from 2006 to 2015, with forecasts of cost to 2018. The report mainly emphasizes on five onshore regions, namely Eagle Ford, Bakken, Marcellus, Midland and Delaware. The drilling costs

per well has been increasing steadily from 2006 to 2012 due to the rapid growth in drilling activities. However, since 2012, the costs of drilling starts to decline due to reduced drilling activities and increasing drilling efficiencies (EIA, 2016). According to drilling cost correlations developed by Heddle et al. (2003), the drilling cost is highly correlated with the oil price (shown in Figure 53). The decline of drilling costs has been reported by EIA in their recent publication “Trends in U.S. Oil and Natural Gas Upstream Costs”. Although the report mainly focuses on the costs associated with drilling horizontal wells in the regions mentioned above, the drilling costs reported are useful as they were reported as costs per vertical depth and horizontal length. The drilling costs per vertical depth reported by EIA are shown in Figure 54 (EIA, 2016).

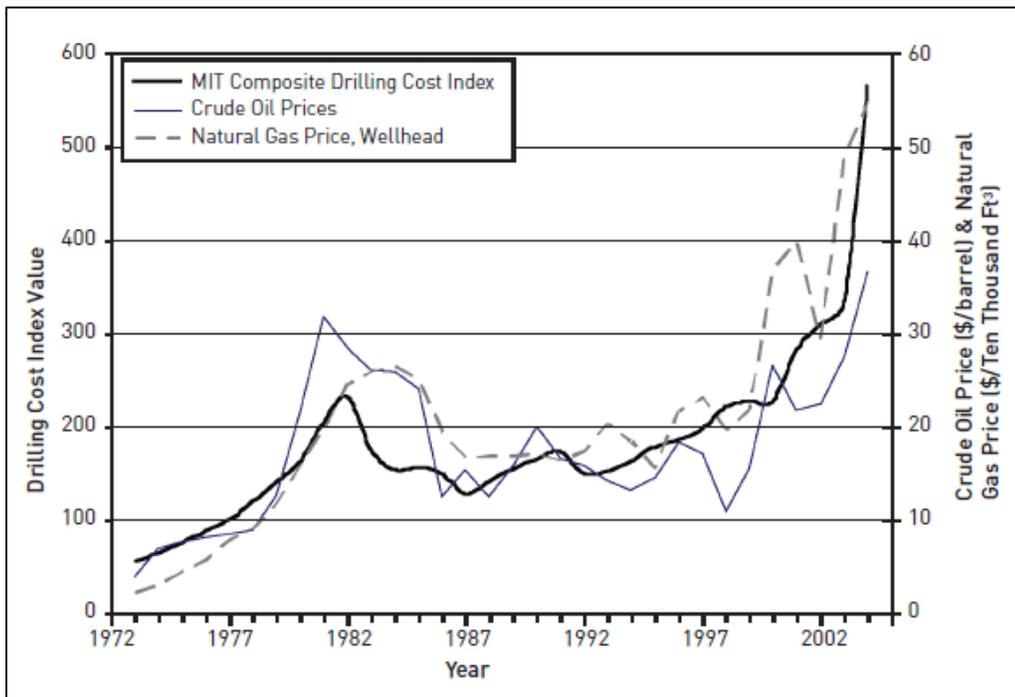


Figure 53 – Crude oil and natural gas prices compared to MIT Composite Drilling Index (Reprinted from Heddle et al., 2003).

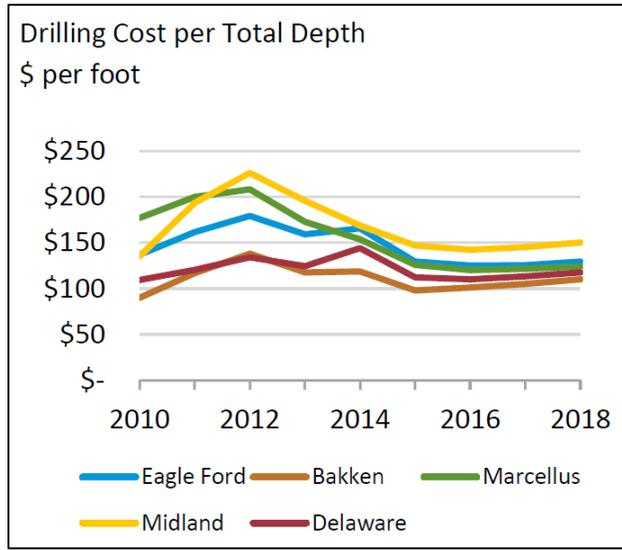


Figure 54 – Drilling cost per vertical depth surveyed from 2010 to 2015, with forecast to 2018 (Reprinted from EIA, 2016).

Apart from the drilling costs reported by EIA, the correlation by Heddle et al. (2003), which is also cited by McCollum and Ogden (2006), is adjusted. The scaled-up correlation is shown below, where C_{drill} is the cost of drilling and d is the vertical drilling depth in feet.

$$C_{Drill} = 125,000 \times \exp(2.44 \cdot 10^{-4} \times d) \quad \dots\dots\dots (7)$$

Drilling costs obtained from both the forecasts by EIA and the correlation show consistency. Since the reservoir depth in the simulation is about 10,000 ft, the drilling cost estimated is around \$1.3 to \$1.5 million per well.

7.1.2 Completion Costs

For completion cost, tubing cost, C_{tubing} , will make up large portion of the completion costs in CO₂-EOR project. Study has been conducted by EIA (2010) to gather

the costs of oil wells in the United States from 1976 to 2009. Regression analysis for the tubing costs and the correlation for tubing cost have been derived. The correlation is shown below, where $index_t$ is the cost index and d is the reservoir depth in feet.

$$C_{Tubing} = Index_t \times 17,646 \times \exp(2.47 \cdot 10^{-4} \times d) \dots\dots\dots (8)$$

The cost index used in this case is the average of the cost index over the last 5 years old data. After applying the correlation, the completion cost per well is around \$4.9 million. The completion costs for the makeover of existing wells such as converting a producer to an injector are estimated at \$3 million.

7.1.3 Surface Facilities Costs

For CO₂-EOR projects, the capital expenditure for surface facilities mainly includes the cost of installing production and injection equipment and cost of construction of surface pipeline network. According to Algharaib and Al-Soof (2008), the capital cost of surface facilities required for CO₂-EOR projects with 5-spot pattern can be estimated using the correlation below, where $C_{facilities}$ is cost of surface facilities and d is the reservoir depth in feet.

$$C_{Facilities} = 1,000,000 + 310.36 \times d \dots\dots\dots (9)$$

7.1.4 Fixed Operating Costs

Normal operating costs cover normal daily operation, surface and subsurface repair, maintenance and services. According to Zekri et al. (2000), the conventional operating costs reported is around \$1.37/bbl of oil produced. According to the study

conducted by EIA in 2010, the average fixed operating costs for the oil wells in the United States are around 0.5% of the drilling costs associated.

$$OPEX_{fixed} = 0.005 \times C_{Drill} \dots\dots\dots (10)$$

The correlation shown helps to estimate the fixed operating costs per well per month by using the costs of drilling, C_{drill} .

7.1.5 Variable Costs - Production

The variable costs due to production may include oil production, gas production and water disposal costs. Since there is no water production associated, water disposal cost is omitted from the study. The variable costs of oil and gas production are summarized in Table 43 below based on the data gathered from EIA (2010).

Table 43 – Variable costs for oil and gas production.

Variable Costs – Production	
Oil Variable Costs	\$0.50 per bbl
Gas Variable Costs	\$0.05 per Mscf

7.1.6 Variable Costs - Injection

CO₂ is injected at a constant rate into the reservoir throughout the project. Besides, in the case of recycling, gas produced will be reinjected back into the reservoir as well. Thus, injection costs will account for the gas compression needed for injection. For the range of pressure used in this project, the injection costs are shown in Table 44.

Table 44 – Gas or CO₂ injection costs.

Parameter	Value
Gas/CO ₂ Injection Costs	\$0.80 /Mscf

7.2 Cost Functions Specific to CO₂-EOR

There are several specific costs that needs to be considered in CO₂-EOR projects. CO₂ market price, compression costs and recycling costs will be included in this study. This section does not discuss about CO₂ generation costs and transportation costs. Detailed economic model developed for CO₂-EOR projects have been published by Algharaib and Al-Soof (2008), Heddle et al. (2003) and Dahowski et al. (2012).

7.2.1 CO₂ Market Price

Despite huge number of CO₂ uses have been identified, most of the CO₂ utilization are on relatively small scale. According to global CCS institute, the global demand for CO₂ is estimated to be around 80 million tons per year. More than 50% of the CO₂ demand, which is around 50 million tons per year, comes from oil and gas industry for EOR purposes (GCI, 2011). Other small scale uses of CO₂ include food industry, beverage carbonation and much more. Although CO₂ is purchased regularly, there is no established bulk price for public scrutiny. CO₂ price is typically negotiated and agreed upon by the parties involved. The price of CO₂ is highly dependent on the supply and also regulatory constraints on CO₂ emission by the government. Intercontinental Exchange Inc. has tracked the price of CO₂ closely and the data is published on California Carbon Dashboard

website. The CO₂ price is shown in Figure 55. The price of CO₂ has been relatively stable at \$12 to \$13 per ton since 2014.



Figure 55 – CO₂ price published on California Carbon Dashboard website (data from Intercontinental Exchange Inc.)

Since CO₂ price is highly dependent on the government regulations, Synapse Energy Economics Inc. has conducted a series of forecast on future CO₂ prices depending on the regulations (Luckow et al., 2015). The company established 3 scenarios of price forecast for CO₂, namely low case, mid case and high case. Low case involves lenient policy on controlling CO₂ emission while high case represents stringent regulations on CO₂ emissions (Luckow et al., 2015). The price forecast is shown in Figure 56. Thus, in this study, the CO₂ market price is fixed at \$15/metric ton, which is about \$0.80/Mscf.

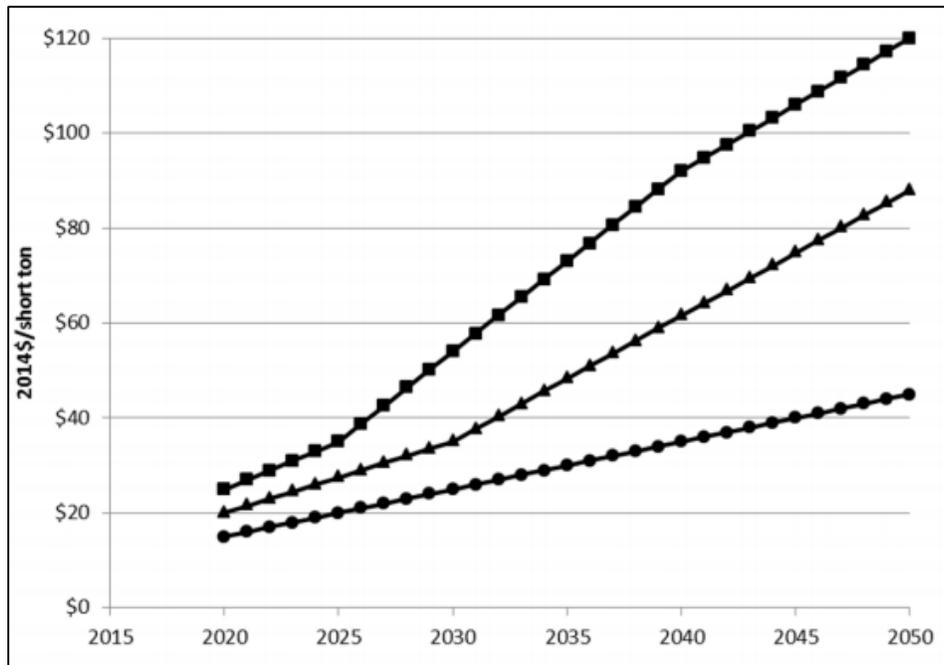


Figure 56 – Forecast of CO₂ price depending on different levels of regulations (Reprinted from Luckow et al., 2015).

7.2.2 Recycling Costs

Gas recycling costs contribute to significant impacts on the costs of performing CO₂-EOR miscible process as the CO₂ that has achieved breakthrough at the producers will be captured and reinjected back into the reservoir. The CO₂ recycling costs can be estimated based on the work presented by Heddle et al. (2003) with an assumption that the recycling plant should be sized to the average annual CO₂ flow rate into the field. The correlation used to estimate the capital costs of recycling facility are shown below, where $C_{recycling}$ is capital cost of recycling facilities and Q is the annual mass flow rate of CO₂ in tons.

$$C_{recycling} = 23.66 \times Q \quad \dots\dots\dots (11)$$

According to Heddle’s work, the annual operating and maintenance costs for CO₂ recycling are assumed to be 16% of the capital costs (Heddle et al., 2003). As a results, the costs of CO₂ recycling estimated are around \$0.4/Mscf in this case, which is comparable to the published estimates of 0.35/Mscf (Dahowski et al., 2012; Ghomian et al., 2008; KGS, 2002).

7.3 Summary of the Economic Model

A summary of the equations and costs used in the economic analysis is shown in Table 45.

Table 45 – Summary of the equations and costs used in economic analysis.

Model element	CapEx	OpEx
Producers	$C_{Drill} = 125,000 \times \exp(2.44 \cdot 10^{-4} \times d)$ $C_{Tubing} = Index_t \times 17,646 \times \exp(2.47 \cdot 10^{-4} \times d)$	$OPEX_{Fixed} = 0.005 \times C_{Drill}$ $OPEX_{oil} = 0.50 \text{ \$/stb}$ $OPEX_{gas} = 0.05 \text{ \$/Mscf}$
Injectors	$C_{Drill} = 125,000 \times \exp(2.44 \cdot 10^{-4} \times d)$ $C_{Tubing} = Index_t \times 17,646 \times \exp(2.47 \cdot 10^{-4} \times d)$	$OPEX_{Fixed} = 0.005 \times C_{Drill}$ $OPEX_{gas} = 0.80 \text{ \$/Mscf}$
Surface Facilities	$C_{Facilities} = 1,000,000 + 310.36 \times d$	
CO ₂ Market Price		$OPEX_{CO_2} = 15 \text{ \$/mton}$
CO ₂ Recycling	$C_{Recycling} = 23.66 \times Q$	$OPEX_{Recycling} = 0.16$ $\times C_{Recycling}$

7.4 Sensitivity Study

Economic analysis is extremely sensitive towards the economic inputs used such as oil price, CO₂ price, capital costs and operating expenses. In this chapter, the sensitivity

of the economical outputs towards these inputs will be discussed. Net present value (NPV) of the project, with mid-year discounting of 10%, has been evaluated in each scenario.

7.4.1 Oil Price

Undeniably, the single most influential variable in economic analysis is the oil price. Oil price has been known to be the one of the commodities with the most fluctuation in its prices. Figure 57 provides an overview of the oil price from 1984 to 2017 (EIA).

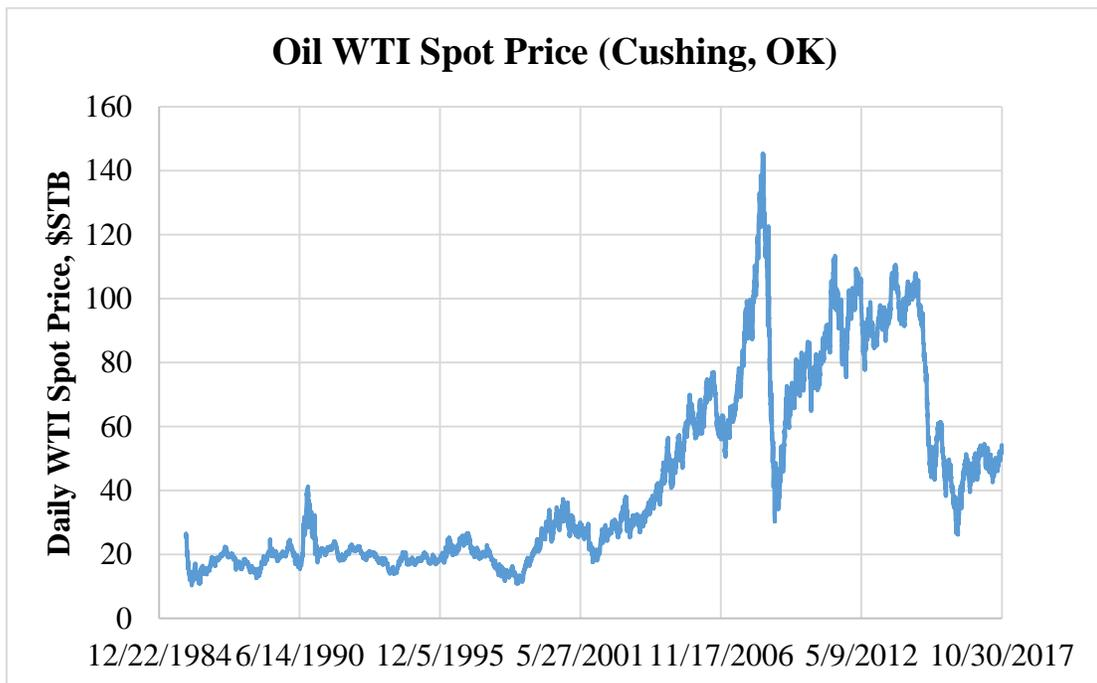


Figure 57 – Overview of oil price from 1984 to 2017 (data source from EIA).

The base oil price used in this study is taken from the average oil price of the past year, which is around \$45/bbl. However, to determine the effect of oil price on NPV value of the project, economic analysis with oil price ranges from \$20/bbl to \$100/bbl is

conducted. Figure 58 shows the incremental NPV (based upon reference case with natural depletion) of the light oil reservoir at different injection pore volume.

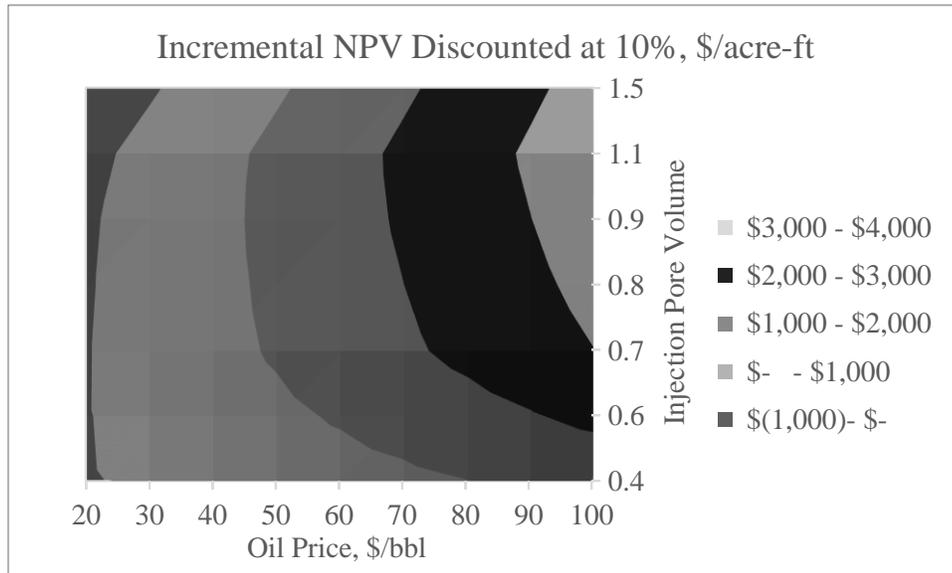


Figure 58 – Incremental NPV of the light oil reservoir at different injection pore volumes with varying oil prices.

There are several significant observations based on the trends of the incremental NPV. First, CO₂ miscible EOR project might not be economical under low oil price environment. Losses may occur at low oil price as the revenue generated is not adequate to cover the cost of CO₂ injection. Second, the optimum injection pore volume changes under different oil price environment. For example, if the oil price is \$45/bbl, the optimum injection pore volume is around 0.9. However, if the oil price is at \$90/bbl, the optimum injection pore volume changes to 1.1. The higher the oil price, the higher the optimum injection pore volume based upon the economic performance. The optimum injection pore volume determined from economic analysis may differ from the one obtained from

reservoir performance. This is due to the diminishing economic return from the additional CO₂ injected at higher injection pore volume. Figure 59 shows the incremental NPV of heavy oil reservoir under varying oil prices and injection pore volumes.

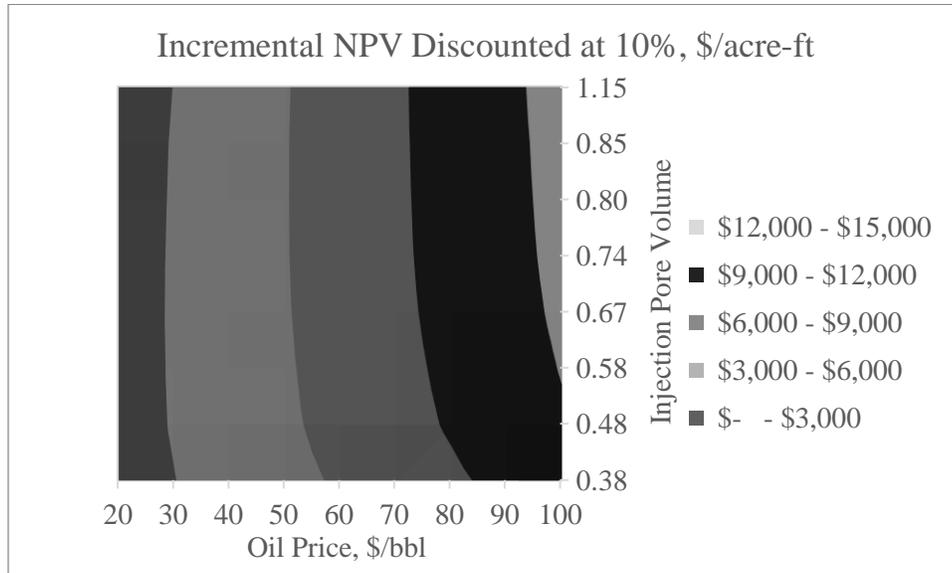


Figure 59 – Incremental NPV of the heavy oil reservoir at different injection pore volume with varying oil prices.

The trends of incremental NPV in heavy oil reservoir differs significantly from the ones exhibited in light oil reservoir. First, the optimum injection pore volume is not extremely sensitive towards the oil price if compared to the light oil case. Second, the incremental NPV in heavy oil reservoir is significantly higher, with incremental NPV up to \$15,000/acre-ft. Under natural depletion, heavy oil reservoir is not capable of producing substantial amount of oil. Thus, by implementing CO₂ injection, the economic performance improves significantly, which is reflected by higher incremental NPV.

7.4.2 CO₂ Price

Although the CO₂ price does not fluctuate as much as the oil price, changes in CO₂ price may influence the economics of the project significantly. The current CO₂ price is around \$0.80/Mcf. Therefore, sensitivity analysis with CO₂ price ranging from \$0.50/Mscf to \$2.50/Mscf has been conducted. Figure 60 shows the incremental NPV of light oil reservoir under varying CO₂ prices.

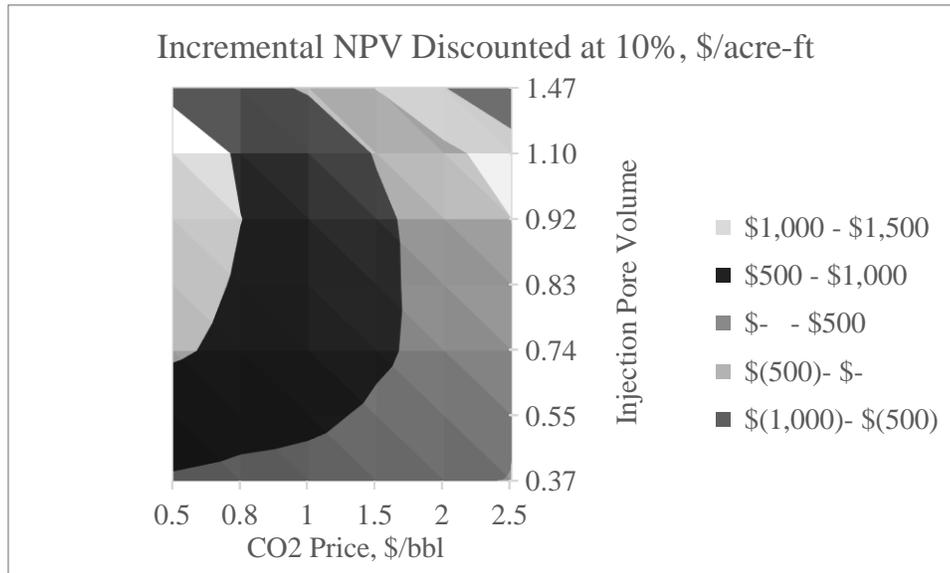


Figure 60 – Incremental NPV of the light oil reservoir at different injection pore volumes with varying CO₂ prices.

For light oil reservoir, CO₂ price can influence the incremental NPV significantly. When the CO₂ price is around \$1.50/Mcf, losses may occur at high injection pore volume. The optimum injection pore volume is also influenced by the price of CO₂. The lower the price of CO₂, the higher the optimum injection pore volume based upon the economic

performance. More CO₂ can be purchased at lower price and injected into the reservoir to recover more oil. Figure 61 shows the incremental NPV obtained from heavy oil reservoir subjected to different CO₂ prices.

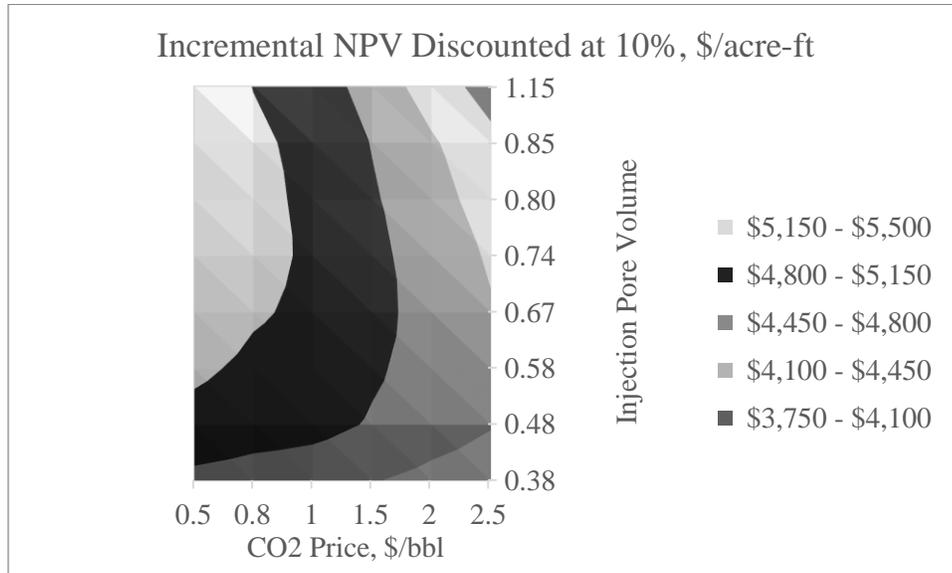


Figure 61 – Incremental NPV of the heavy oil reservoir at different injection pore volumes with varying CO₂ prices.

Similarly, the incremental NPV of the heavy oil reservoir is influenced greatly by the price of CO₂. The impact of CO₂ prices on the optimum injection pore volume can be identified clearly in this case. If the CO₂ price is around \$1.00/Mcf, the optimum injection pore volume is around 0.74. However, the optimum injection pore volume reduces to 0.65 when the CO₂ price increases to about \$1.50/Mcf.

7.4.3 Recycling Costs

Without recycling produced gas, CO₂ will be lost together with the produced gas. Thus, to maximize the usage of purchased CO₂, the gas produced, which is high in CO₂ concentration, is reinjected back into the reservoir. Current cost of recycling CO₂ is estimated at \$0.40/Mcf, which is half of the current CO₂ price. To evaluate the economic benefits from CO₂ recycling, the incremental NPV of the recycling case is reevaluated using the CO₂ price as if the recycled CO₂ is being purchased from the market. Figure 62 shows the incremental NPV resulted from recycling CO₂ while Figure 63 shows the incremental NPV obtained from purchasing the similar amount of CO₂ from the market.

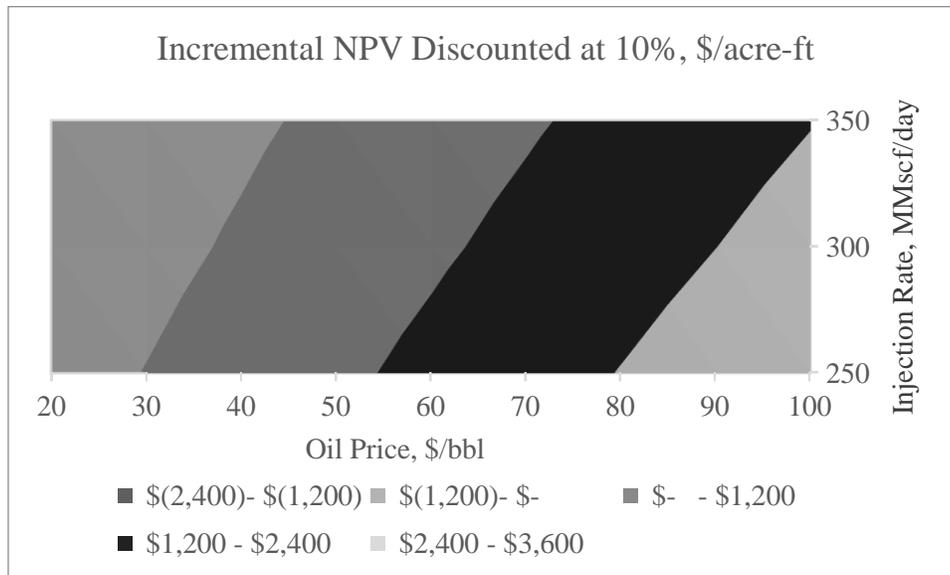


Figure 62 – Incremental NPV resulted from recycling CO₂ in light oil reservoir.

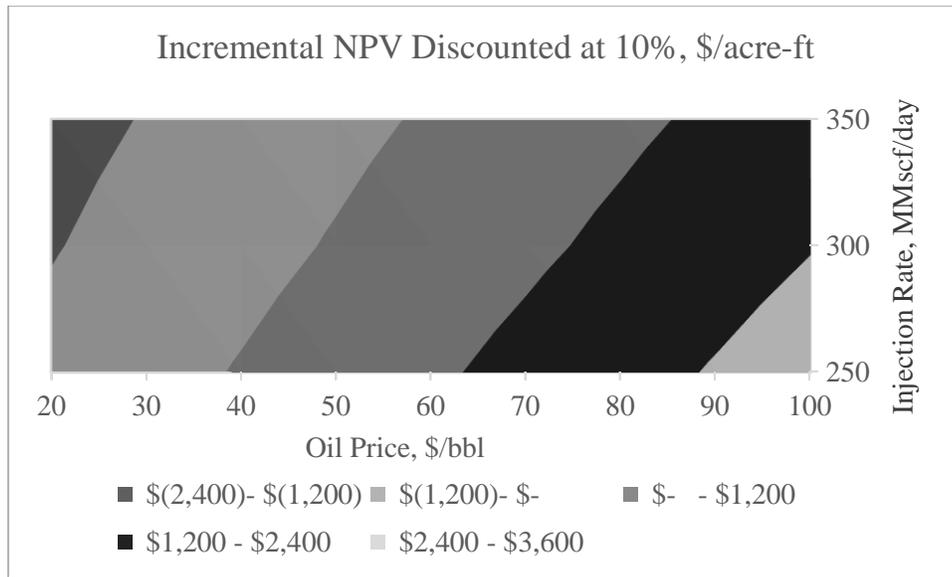


Figure 63 – Incremental NPV resulted from purchasing similar amount of recycled CO₂ at market price in light oil reservoir.

Significant improvement in incremental NPV can be observed. Higher incremental NPV can be achieved by recycling and reinjecting produced CO₂ back into the reservoir. For example, at a constant injection rate of 250 MMscf/day, the incremental NPV in the recycling case is around \$995/acre-ft when the oil price is at \$50/bbl. However, if similar amount of CO₂ had to be purchased, the incremental NPV reduces to \$563/acre-ft under similar oil price. Therefore, it is economically beneficial to recycle CO₂ produced since the cost of recycling is lower than the costs of purchasing fresh CO₂ stream from the market.

For heavy oil reservoir, similar runs have been conducted to evaluate the benefits obtained from recycling produced CO₂. Figure 64 shows the incremental NPV resulted from recycling CO₂ while Figure 65 shows the incremental NPV obtained from purchasing the similar amount of CO₂ from the market.

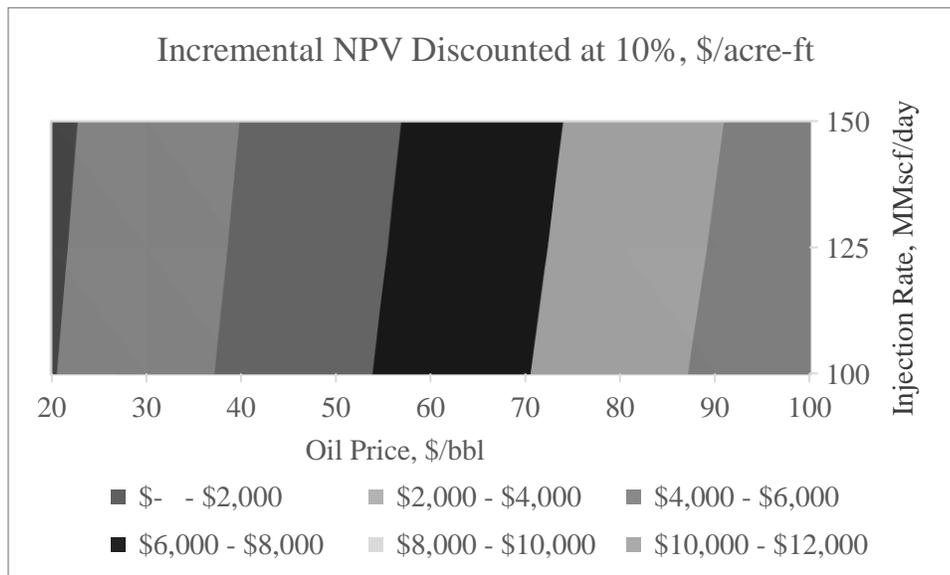


Figure 64 – Incremental NPV resulted from recycling CO₂ in heavy oil reservoir.

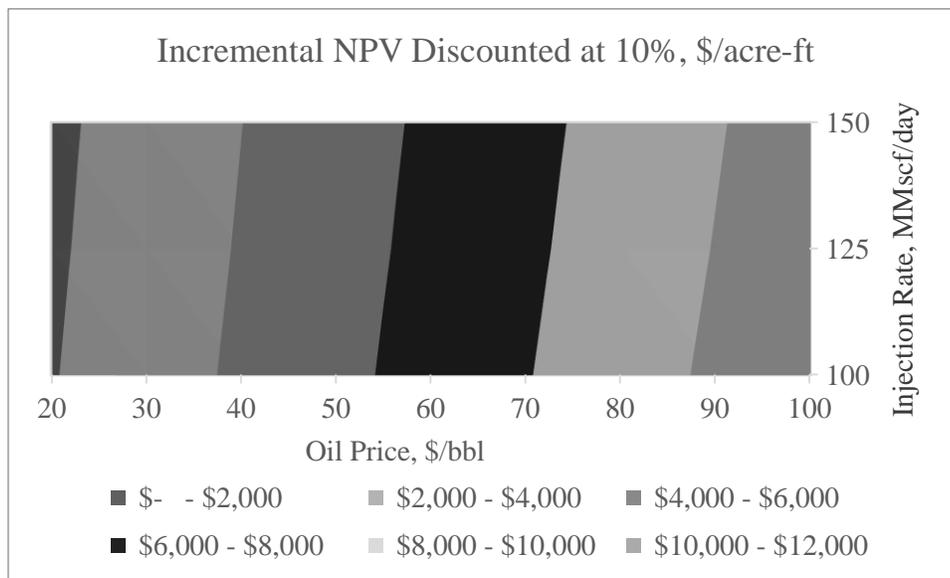


Figure 65 – Incremental NPV resulted from purchasing similar amount of recycled CO₂ at market price in heavy oil reservoir.

The improvement in incremental NPV for the heavy oil case is not as apparent as the one in light oil reservoir. This is because the incremental NPV in heavy oil reservoir is largely dominated by the immense incremental revenue obtained from improved oil recovery. Furthermore, the gas production from heavy oil reservoir is low if compared to the gas production in light oil reservoir. Thus, less CO₂ is recycled and reinjected back into the reservoir in the heavy oil case. The contour plot exhibited is not sensitive enough to capture the slight improvement in the incremental NPV due to CO₂ recycling. The incremental NPV improves from \$5,510/acre-ft to \$5,549/acre-ft at an oil price of \$50/bbl if the CO₂ produced is recycled and reinjected back into the reservoir.

7.4.4 Tax Incentives

Apart from prices of commodities such as oil and CO₂, the tax incentives offered by the government can influence the economic performance of CO₂-EOR project significantly. Under the Section 45Q, a per-ton credit for CO₂ stored in secure geological formation is offered by the government. After accounting for inflation, the section 45Q credit has been adjusted to \$11.24 per metric ton of qualified CO₂ through EOR projects (KPMG, 2017). Thus, Section 45Q credits have been taken into the consideration to evaluate its impact on the economic performance of the project. Figure 66 and Figure 67 show comparisons of the incremental NPV resulted from the cases with and without the Section 45Q tax incentive program in light oil and heavy oil reservoir respectively.

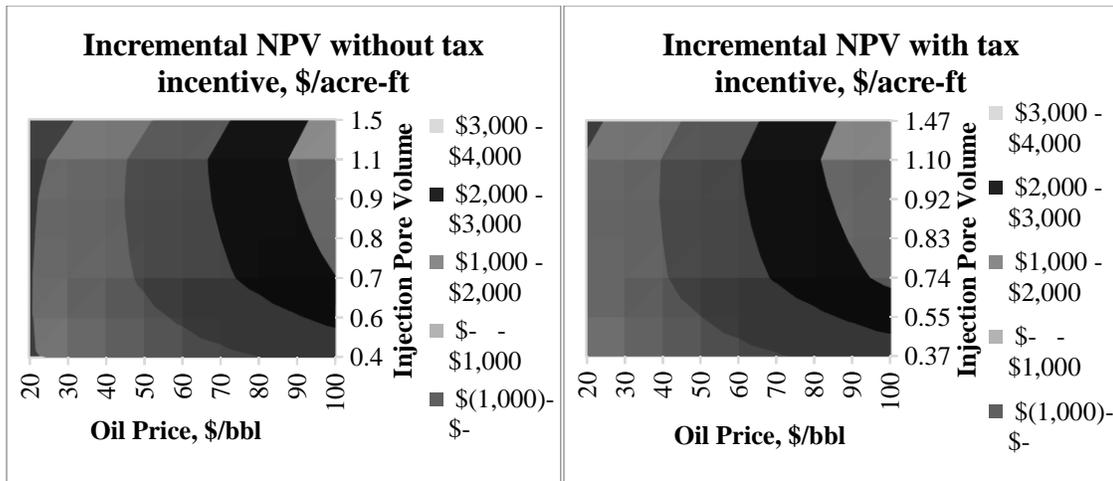


Figure 66 – Comparisons of the incremental NPV resulted from the cases with and without the Section 45Q tax incentive program in light oil reservoir.

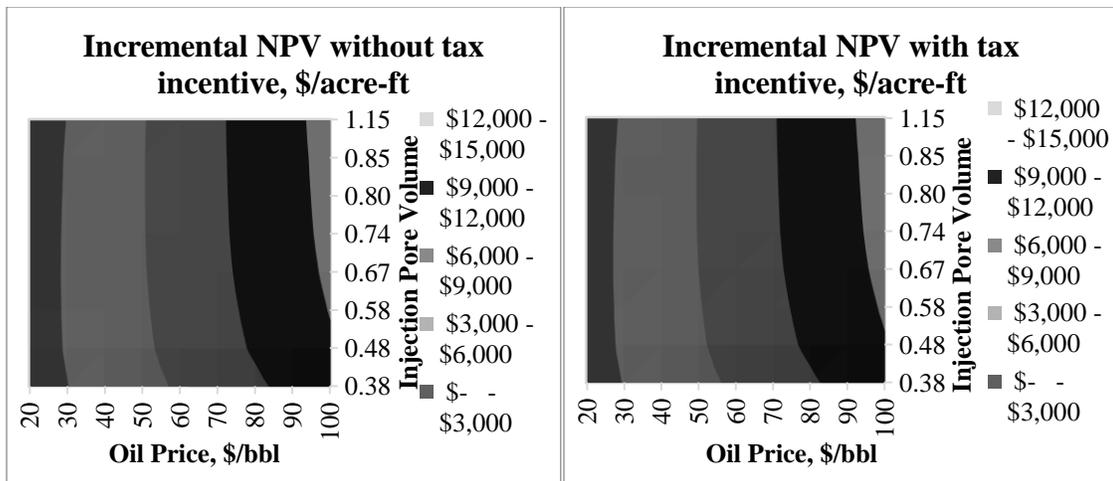


Figure 67 – Comparisons of the incremental NPV resulted from the cases with and without the Section 45Q tax incentive program in heavy oil reservoir

Section 45Q tax incentive offers significant improvement in incremental NPV as considerable amounts of CO₂ is stored in the reservoir at the end of the project. Generally, the tax incentive program will improve the incremental NPV by about \$100/acre-ft, offering extra incentive to conduct CO₂-EOR project under low oil price environment.

7.4.5 Local Grid Refinement

Numerical dispersion in coarse grid model is proven to be significant in the previous chapter, leading to results with large errors. Local grid refinement can be applied around wells (producers and injector) to reduce the numerical dispersion and improve the accuracy of the results obtained. Simulation results based upon coarse grid model without local grid refinement should be examined closely as it may lead to wrong development strategies. To evaluate the impact of local grid refinement application on the economic performance, the incremental NPV is evaluated for the cases with and without local grid refinement. The results are shown in Figure 68 and Figure 69 for both light and heavy oil reservoirs respectively.

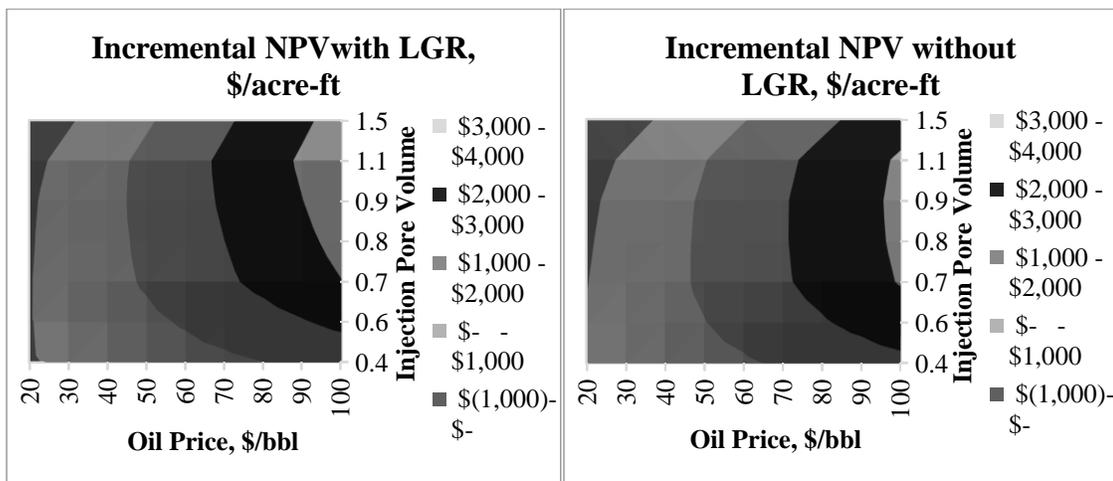


Figure 68 – Comparisons of the incremental NPV resulted from the cases with and without LGR in light oil reservoir.

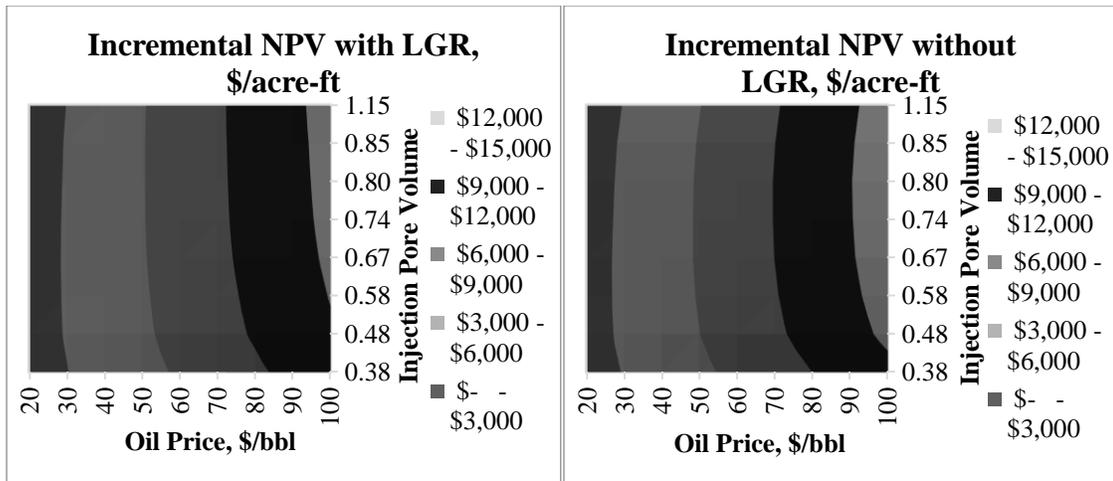


Figure 69 – Comparisons of the incremental NPV resulted from the cases with and without LGR in heavy oil reservoir.

The differences in trends due to application of LGR are significant. The incremental NPV obtained without the application of LGR can be very misleading. The results obtained without the LGR does not only alter the optimum injection pore volume trend, but also predict the economic outcome with high error which can lead to poor decision making. For example, in the light oil reservoir, the optimum injection pore volume is estimated to be around 1.1 when the oil price is at \$45/bbl. However, without the application of LGR, the optimum injection rate is around 0.7. For light oil case, when the oil price is around \$20/bbl, the incremental NPVs for all injection pore volume are negative, which will result in losses. However, without the application of LGR, the incremental NPV might be positive under low injection pore volume even if the oil price is around \$20/bbl.

CHAPTER VIII

CONCLUSIONS AND RECOMMENDATIONS

Forecasting and studying of CO₂ miscible flooding in oil reservoir requires the use of numerical models that can accurately compute the compositional phenomena. Small spatial discretization is often required due to the complex phase behaviors caused by the continuous change in fluid composition. Numerical dispersion and non-linearity in flash calculation may induce truncation errors that cause the saturation and composition dispersion. This study has shown that the application of local grid refinement (LGR) will reduce the numerical dispersion and non-linearity of flash calculations significantly. Significant error will be induced if coarse model does not apply local grid refinement. A series of sensitivity analysis towards different injection and production strategies has concluded that the error resulted from numerical dispersion and non-linearity of flash calculations can be as high as 50% in some cases. The nature of the errors induced by numerical dispersion has also been identified. The nature of the errors induced is mainly dependent on reservoir fluid and petrophysics. Thus, application of local grid refinement may result in both optimistic and pessimistic incremental recovery. Numerical dispersion occurred in the simulation does not only change the magnitude of the results, but also deviate the trends of the results which will lead to wrong decision making in most cases.

However, the application of local grid refinement has increased the computational costs greatly. Thus, a more efficient method in incorporating local grid refinement should be considered. Dynamic local grid refinement has been proposed by several authors.

Heinemann et al. (1983) practiced dynamic-LGR in reservoir simulator by using implicit-pressure and explicit saturation (IMPES) method. Even though dynamic-LGR allows the accurate illustration of pressure and saturations spatially, it forces limitation in several inactive cells and cell subdivision. Adaptive mesh refinement and coarsening (AMRC) has been introduced where the main challenge involves the identification of features that trigger the refinement process. Gonzalez (2016) has introduced a new technique for AMRC by using an implicit-pressure, explicit-saturation and explicit-composition (IMPESC) method. By using the AMRC approach proposed, the computational cost can be reduced from 30-63% over a static fine grid without compromising the accuracy of the results.

Optimum injection and production strategies has been identified for both light and heavy oil reservoirs by using performance yardsticks, namely CO₂ utilization factor and storage efficiency. The injection and production variables included in this study are injection pore volume, injection initiation timing, gas recycling, producer BHP, target oil rate and gas production rate limit. Optimal completion designs for both light and heavy oil reservoir have also been determined from this study. CO₂ utilization factor is really useful in predicting the efficiency of miscible flooding. It also can serve as a mean for predicting the economic performance of CO₂ miscible flooding. CO₂ utilization factor is extremely sensitive towards some variables. For example, injection pore volume, injection initiation timing and gas production rate limit have narrow ranges for optimum CO₂ utilization factor. Extreme values for these variables will result in poor CO₂ utilization factor, i.e. there exists an optimum value in the middle range of variables involved. Thus,

multiple simulations have to be run to determine the optimum development strategies. On other hand, some variables such as producer BHP, target oil rate and completion location does not influence the CO₂ utilization factor greatly. General trends are sufficient of these variables are sufficient to serve as guidelines in developing successful CO₂-EOR projects. Table 46 summarizes all the optimum development strategies for better CO₂ utilization factor in both light and heavy oil reservoirs.

Table 46 – Development strategies for optimizing CO₂ utilization factor in both light and heavy oil reservoirs.

CO₂ Utilization Factor		
Variables	Light Oil	Heavy Oil
Injection PV	0.74	0.38
Injection Initiation, nth year	6	4
Prod Gas Rate Limit, Mscf/day	75000	No effect
Producer BHP, psia	High	Low
Prod Target Oil Rate, Mbbl/day	Low	High
Completion (Injector-Producer)	Bottom-Top	Top-Bottom

As discussed in the previous chapters, CO₂-EOR does not only enhance the recovery in most reservoirs, but also help to alleviate environmental issues by implementing CO₂ sequestration. CO₂ storage efficiency is extremely crucial in sequestration projects. General trends of variables have been identified to achieve higher CO₂ storage efficiency in both light and heavy oil reservoir. Table 47 summarizes all the optimum development strategies for better CO₂ storage efficiency in both light and heavy oil reservoirs.

Table 47 – Development strategies for optimizing CO₂ storage efficiency in both light and heavy oil reservoirs.

CO₂ Storage Efficiency		
Variables	Light Oil	Heavy Oil
Injection PV	Low	Low
Injection Initiation, nth year	Late	Late
Prod Gas Rate Limit, Mscf/day	Low	Low
Producer BHP, psia	High	High
Prod Target Oil Rate, Mbbl/day	High	High
Completion (Injector-Producer)	Bottom-Top	Top-Bottom

In this study, the effect of each variable is determined by varying the variable of interest by fixing others constant. Thus, the results obtained are based upon varying one particular variable at a time. Thus, to determine the effects of multiple variables at one time, multivariate analysis (MVA) can be used. MVA is based on the statistical principles, used to conduct study across multiple dimensions while taking into considerations the effect of all variables on the responses of interest. The results obtained from multivariate analysis can be used to create an algorithm for optimization purpose.

REFERENCES

- Algharaib, M. and Al-Soof, N.A. 2008. Economical Modeling of Co₂ Capturing and Storage Projects. Paper presented at the SPE Saudia Arabia Section Technical Symposium, Al-Khobar, Saudi Arabia. Society of Petroleum Engineering. DOI: <https://doi.org/10.2118/120815-MS>.
- Chen, S., Li, H., Yang, D. et al. 2010. Optimal Parametric Design for Water-Alternating-Gas (Wag) Process in a Co₂-Miscible Flooding Reservoir. *Society of Petroleum Engineering* **49** (10).SPE-141650-PA. DOI: <https://dx.doi.org/10.2118/141650-PA>
- Climate Vulnerability Monitor: A Guide to the Cold Calculus of a Hot Planet*. 2012. DARA Group and Climate Vulnerable Forum.
- Dahlman, L. Climate Change: Global Temperature. National Oceanic and Atmospheric Administration.
- Dahowski, R.T., Davidson, C.L., Li, X.C. et al. 2012. A \$70/Tco₂ Greenhouse Gas Mitigation Backstop for China's Industrial and Electric Power Sectors: Insights from a Comprehensive Ccs Cost Curve. *International Journal of Greenhouse Gas Control* **11**: 73-85. DOI: <https://doi.org/10.1016/j.ijggc.2012.07.024>
- EIA. 2010. *Carbon Capture and Storage Technology Roadmap*. U.S. Energy Information Administration.
- EIA. 2016. *Trends in U.S. Oil and Natural Gas Upstream Costs*. U.S. Energy Information Administration.
- EIA. 2017. *International Energy Outlook*. U.S. Energy Information Administration.
- Fanchi, J.R. 1983. Multidimensional Numerical Dispersion. *Society of Petroleum Engineering* **23** (01).SPE-9018-PA. DOI: <https://doi.org/10.2118/9018-PA>
- First Global Maps from Orbiting Carbon Observatory. 2014.
- GCI. 2011. *Accelerating the Uptake of Ccs: Industrial Use of Captured Carbon Dioxide*. Global CCS Institute.

- Gharbi, R.B.C. 2004. Use of Reservoir Simulation for Optimizing Recovery Performance. *Journal of Petroleum Science and Engineering* **42** (2-4): 183-194. DOI: <https://doi.org/10.1016/j.petrol.2003.12.010>
- Ghomian, Y., Pope, G.A., and Sepehrnoori, K. 2008. Hysteresis and Field-Scale Optimization of Wag Injection for Coupled Co₂-Eor and Sequestration. Paper presented at the SPE Symposium on Improved Oil Recovery, Tulsa, Oklahoma. Society of Petroleum Engineering. DOI: <https://doi.org/10.2118/110639-MS>.
- Gonzalez, K.G. 2016. Adaptive Grid Refinement Improves Gas Injection Modeling. Paper presented at the SPE Annual Technical Conference and Exhibition, Dubai, UAE. Society of Petroleum Engineering. DOI: <https://doi.org/10.2118/184487-STU>.
- Healy, R.N., Holstein, E.D., and Batycky, J.P. 1994. Status of Miscible Flooding Technology. Paper presented at the 14th World Petroleum Congress, Stavanger, Norway. Society of Petroleum Engineering WPC-26169.
- Heddle, G., Herzog, H., and Klett, M. 2003. *The Economics of Co₂ Storage*. Laboratory for Energy and the Environment of the Massachusetts Institute of Technology.
- Heinemann, Z.E., Gerken, G., and Hantelmann, G.v. 1983. Using Local Grid Refinement in a Multiple-Application Reservoir Simulator. Paper presented at the SPE Reservoir Simulation Symposium, San Francisco, California. Society of Petroleum Engineering. DOI: <https://doi.org/10.2118/12255-MS>.
- Holm, L.W. and Josendal, V.A. 1974. Mechanisms of Oil Displacement by Carbon Dioxide. *Society of Petroleum Engineering* **26** (12).SPE-4736-PA. DOI: <https://dx.doi.org/10.2118/4736-PA>
- Jerauld, G.R. 1998. A Case Study in Scaleup for Multicontact Miscible Hydrocarbon Gas Injection. *Society of Petroleum Engineering* **1** (06).SPE-53006-PA. DOI: <https://doi.org/10.2118/53006-PA>
- KGS. 2002. *Co-Generation, Ethanol Production and Co₂ Enhanced Oil Recovery Model for Environmentally and Economically Sound Linked Energy Systems*. Kansas Geological Survey.

- KPMG. Inflation Adjustment Factor, Carbon Dioxide Sequestration under Section 45q. Klynveld Peat Marwick Goerdeler. Accessed 8 August.
- Luckow, P., Stanton, E.A., Fields, S. et al. 2015. *2015 Carbon Dioxide Price Forecast*. Synapse Energy Economics.
- Marshall, C. 2016. Strange Bedfellows Seek Tax Fix for Sequestration Projects. *E&E News*.
- Martin, D.F. and Taber, J.J. 1992. Carbon Dioxide Flooding. Society of Petroleum Engineers. *Society of Petroleum Engineering*.SPE-23564-PA. DOI: <http://dx.doi.org/10.2118/23564-PA>
- McCollum, D.L. and Ogden, J.M. 2006. Techno-Economic Models for Carbon Dioxide Compression, Transport, and Storage & Correlations for Estimating Carbon Dioxide Density and Viscosity, University of California, Davis.
- Rosenberg, D.U.v. 1982. Local Mesh Refinement for Finite Difference Methods. Paper presented at the SPE Annual Technical Conference and Exhibition, New Orleans, Louisiana. Society of Petroleum Engineering SPE-10974-MS. DOI: <https://doi.org/10.2118/10974-MS>.
- Sahni, A., Dehghani, K., Prieditis, J. et al. 2005. Benchmarking Heterogeneity of Simulation Models. Paper presented at the SPE Annual Technical Conference and Exhibition, Dallas, Texas. Society of Petroleum Engineering. DOI: <https://doi.org/10.2118/96838-MS>.
- Salem, S. and Moawad, T. 2013. Economic Study of Miscible Co₂ Flooding in a Mature Waterflooded Oil Reservoir. Paper presented at the SPE Saudi Arabia Section Technical Symposium and Exhibition, Al-Khobar, Saudi Arabia. Society of Petroleum Engineering. DOI: <https://dx.doi.org/10.2118/168064-MS>.
- Stalkup, F.I., Lo, L.L., and Dean, R.H. 1990. Sensitivity to Gridding of Miscible Flood Predictions Made with Upstream Differenced Simulators. Paper presented at the SPE/DOE Enhanced Oil Recovery Symposium, Tulsa, Oklahoma. Society of Petroleum Engineering SPE-20178-MS. DOI: <https://doi.org/10.2118/20178-MS>.

- Sudaryanto, B. and Yortsos, Y.C. 2001. Optimization of Displacements in Porous Media Using Rate Control. Paper presented at the SPE Annual Technical Conference and Exhibition, New Orleans, Louisiana. Society of Petroleum Engineering. DOI: <https://dx.doi.org/10.2118/71509-MS>.
- Wallace, M. and Kuuskraa, V. 2014. *Near-Term Projections of Co₂ Utilization for Enhanced Oil Recovery*. Energy Sector Planning and Analysis (ESPA).
- Yellig, W.F. and Metcalfe, R.S. 1980. Determination and Prediction of Co₂ Minimum Miscibility Pressures. *Society of Petroleum Engineering* **32** (01).SPE-7477-PA. DOI: <https://dx.doi.org/10.2118/7477-PA>
- Zekri, A.Y., Jerbi, K.K., and El-Honi, M. 2000. Economic Evaluation of Enhanced Oil Recovery. Paper presented at the International Oil and Gas Conference and Exhibition, Beijing, China. Society of Petroleum Engineering. DOI: <https://doi.org/10.2118/64727-MS>.

APPENDIX 1

ECLIPSE LIGHT_OIL.PVO FILE

```
ECHO
-- Units: F
RTEMP
--
-- Constant Reservoir Temperature
--
| | | 300
/

EOS
--
-- Equation of State (Reservoir EoS)
--
PR3
/

NCOMPS
--
-- Number of Components
--
| | | 6
/

PRCORR
--
-- Modified Peng-Robinson EoS
--

CNAMES
--
-- Component Names
--
'CO2'
'C1N2'
'C2'
'C3'
'C4'
'C5+'
/
```

```

MW
--
-- Molecular Weights (Reservoir EoS)
--
|      | 44.01
|      | 17.112
|      | 30.07
|      | 44.097
|      | 58.124002
|      | 100.13
/

OMEGAA
--
-- EoS Omega-a Coefficient (Reservoir EoS)
--
0.457235529
0.457235529
0.457235529
0.457235529
0.457235529
0.457235529
/

OMEGAB
--
-- EoS Omega-b Coefficient (Reservoir EoS)
--
0.077796074
0.077796074
0.077796074
0.077796074
0.077796074
0.077796074
/

-- Units: R
TCRIT
--
-- Critical Temperatures (Reservoir EoS)

```

```

--
777.123737186749
400.784183447155
559.945161333481
670.922551273378
733.028130918614
965.539999978075
/
-- Units: psia
PCRIT
--
-- Critical Pressures (Reservoir EoS)
--
909.490471571508
993.251163268884
829.675942774008
673.5400156789
526.095832183519
427.199999986617
/
-- Units: ft3 /lb-mole
VCRIT
--
-- Critical Volumes (Reservoir EoS)
--
2.5302796318043
1.23265573408577
2.04977431931245
2.99865589373809
4.08842354103027
5.89626708015795
/
ZCRIT
--
-- Critical Z-Factors (Reservoir EoS)
--

```

```
-- Critical Z-Factors (Reservoir EoS)
--
0.275945297729874
0.284666792514594
0.283018971651189
0.280520202811634
0.27343027512327
0.243099810638768
/

SSHIFT
--
-- EoS Volume Shift (Reservoir EoS)
--
-0.06733799443
-0.07233410705
-0.08830190084
-0.08655713407
-0.08000113644
0.1555391363
/

ACF
--
-- Acentric Factors (Reservoir EoS)
--
0.1736205847
0.1631889805
0.1298491186
0.1334920942
0.1471806512
0.3008923153
/

BIC
--
-- Binary Interaction Coefficients (Reservoir EoS)
--
```

```

0
0      0
0      0      0
0      0      0      0
0      0      0.01      0.01      0
/
PARACHOR
--
-- Component Parachors
--
153.228
77.9136
114.196
153.4716
192.7472
310.364
/
-- Units: ft3 /lb-mole
VCRITVIS
--
-- Critical Volumes for Viscosity Calc (Reservoir EoS)
--
2.5302796318043
1.23265573408577
2.04977431931245
2.99865589373809
4.08842354103027
5.89626708015795
/
ZCRITVIS
--
-- Critical Z-Factors for Viscosity Calculation (Reservoir EoS)
--
0.275945297729874
0.284666792514594
0.283018971651189
0.280520202811634

```

```

0.27343027512327
0.243099810638768
/
LBCCOEF
--
-- Lorentz-Bray-Clark Viscosity Correlation Coefficients
--
0.1023 0.023364 0.058533 -0.040758 0.0093324
/
--PVTi--Please do not alter these lines
--PVTi--as PVTi can use them to re-create the fluid model
--PVTiMODSPEC =====
--PVTiTITLE
--PVTiModified System: From Automatically created during keyword export
--PVTiVERSION
--PVTi 2014.2 /
--PVTiNCOMPS
--PVTi 6 /
--PVTiEOS
--PVTi PR3 /
--PVTiPRCORR
--PVTiLBC
--PVTiOPTIONS
--PVTi 0 0 0 0 0 0 1 0 0 0 0 0 0 0 0 0 0 0 0 0 0
--PVTi/
--PVTiOPTIONSEXT
--PVTi 0 1
--PVTi/
--PVTiNOECHO
--PVTiMODSYS =====
--PVTiUNITS
--PVTi FIELD ABSOL PERCENT /
--PVTiDEGREES
--PVTi Fahrenheit /
--PVTiSTCOND
--PVTi 60.0000 14.6959 /
--PVTiCNAMES
--PVTi CO2
--PVTi C1N2
--PVTi C2

```

```

--PVTi C3
--PVTi C4
--PVTi C5+
--PVTi /
--PVTiTCRIT
--PVTi 3.174537166E+02 -5.888582717E+01 1.002751465E+02 2.112525335E+02
--PVTi 2.733581115E+02 5.058699744E+02 /
--PVTiPCRIT
--PVTi 9.094904716E+02 9.932511633E+02 8.296759428E+02 6.735400157E+02
--PVTi 5.260958322E+02 4.272000000E+02 /
--PVTiVCRIT
--PVTi 2.530279724E+00 1.232655779E+00 2.049774394E+00 2.998656003E+00
--PVTi 4.088423690E+00 5.896267295E+00 /
--PVTiZCRIT
--PVTi 2.759452977E-01 2.846667925E-01 2.830189717E-01 2.805202028E-01
--PVTi 2.734302751E-01 2.430998106E-01 /
--PVTiVCRITVIS
--PVTi 2.530279724E+00 1.232655779E+00 2.049774394E+00 2.998656003E+00
--PVTi 4.088423690E+00 5.896267295E+00 /
--PVTiZCRITVIS
--PVTi 2.759452977E-01 2.846667925E-01 2.830189717E-01 2.805202028E-01
--PVTi 2.734302751E-01 2.430998106E-01 /
--PVTiSSHIFT
--PVTi -6.733799443E-02 -7.233410705E-02 -8.830190084E-02 -8.655713407E-02
--PVTi -8.000113644E-02 1.555391363E-01 /
--PVTiACF
--PVTi 1.736205847E-01 1.631889805E-01 1.298491186E-01 1.334920942E-01
--PVTi 1.471806512E-01 3.008923153E-01 /
--PVTimW
--PVTi 4.401000000E+01 1.711200000E+01 3.007000000E+01 4.409700000E+01
--PVTi 5.812400200E+01 1.001300000E+02 /
--PVTiZI
--PVTi 2.370000000E-01 4.540300000E+01 6.057000000E+00 5.011000000E+00
--PVTi 2.931000000E+00 4.036100000E+01 /
--PVTiTBOIL
--PVTi 1.234391086E+01 -2.190792132E+02 -1.220309485E+02 -4.637173031E+01
--PVTi 5.156637483E+00 2.521946540E+02 /
--PVTiTREF
--PVTi 5.999998631E+01 5.999998631E+01 5.999998631E+01 5.999998631E+01
--PVTi 5.999998631E+01 5.999998631E+01 /

```

```

--PVTiDREF
--PVTi 4.850653269E+01 2.864444975E+01 3.421052756E+01 3.633307854E+01
--PVTi 3.569007045E+01 5.249443141E+01 /
--PVTiPARACHOR
--PVTi 1.532280000E+02 7.791360000E+01 1.141960000E+02 1.534716000E+02 /
--PVTi 1.927472000E+02 3.103640000E+02 /
--PVTiHYDRO
--PVTi N H H H H H
--PVTi /
--PVTiBIC
--PVTi 0.000000000E+00
--PVTi 0.000000000E+00 0.000000000E+00
--PVTi 0.000000000E+00 0.000000000E+00 0.000000000E+00
--PVTi 0.000000000E+00 0.000000000E+00 0.000000000E+00 0.000000000E+00
--PVTi 0.000000000E+00 0.000000000E+00 1.000000000E-02 1.000000000E-02
--PVTi 0.000000000E+00
--PVTi /
--PVTiSPECHA
--PVTi -2.453495016E+00 -6.842562061E+00 4.035341843E-01 1.012336282E+00
--PVTi -3.044085157E+01 -5.534135903E+00 /
--PVTiSPECHB
--PVTi 3.056811641E-02 2.755967363E-02 2.382181309E-02 3.446781061E-02
--PVTi 1.063704646E-01 7.531717292E-02 /
--PVTiSPECHC
--PVTi -7.329175177E-06 -8.853604723E-07 -4.958314124E-06 -7.345666092E-06
--PVTi -1.407302629E-06 -1.601405486E-05 /
--PVTiSPECHD
--PVTi 0.000000000E+00 0.000000000E+00 0.000000000E+00 0.000000000E+00
--PVTi 0.000000000E+00 0.000000000E+00 /
--PVTiHEATVAPS
--PVTi 3.591296784E+04 1.257941463E+03 1.650621600E+04 3.603408601E+04
--PVTi 4.586099659E+04 9.119939320E+04 /
--PVTiCALVAL
--PVTi 4.745471637E+03 2.000233145E+03 3.323854000E+03 4.754344000E+03
--PVTi 6.184834000E+03 1.101571397E+04 /
--PVTi--End of PVTi generated section--
ZI
--
-- Overall Composition
--
0.00237
0.45403
0.06057
0.05011
0.02931
0.40361

```

APPENDIX 2

ECLIPSE HEAVY_OIL.PVO FILE

```
ECHO
-- Units: F
RTEMP
--
-- Constant Reservoir Temperature
--
| | | 300
/

EOS
--
-- Equation of State (Reservoir EoS)
--
PR3
/

NCOMPS
--
-- Number of Components
--
| | | 6
/

PRCORR
--
-- Modified Peng-Robinson EoS
--

CNAMES
--
-- Component Names
--
'CO2'
'C1N2'
'C2'
'C3'
'C4+'
'C6+'
/

MW
--
-- Molecular Weights (Reservoir EoS)
--
```

```

      44.01
16.8456351
      30.07
      44.097
66.31018044
224.0840217
/
OMEGAA
--
-- EoS Omega-a Coefficient (Reservoir EoS)
--
      0.457235529
      0.457235529
      0.457235529
      0.457235529
      0.457235529
      0.457235529
/
OMEGAB
--
-- EoS Omega-b Coefficient (Reservoir EoS)
--
      0.077796074
      0.077796074
      0.077796074
      0.077796074
      0.077796074
      0.077796074
/
-- Units: R
TCRIT
--
-- Critical Temperatures (Reservoir EoS)
--
      777.123737186749
      402.838830261585
      559.945161333481
      670.922551273378
```

```
784.650097586129
1342.43421566236
/
-- Units: psia
PCRIT
--
-- Critical Pressures (Reservoir EoS)
--
909.490471571508
975.571074069437
829.675942774008
673.5400156789
505.92498658415
239.476476792498
/
-- Units: ft3 /lb-mole
VCRIT
--
-- Critical Volumes (Reservoir EoS)
--
2.5302796318043
1.22291051844086
2.04977431931245
2.99865589373809
4.56328462372778
14.0735322372033
/
ZCRIT
--
-- Critical Z-Factors (Reservoir EoS)
--
0.275945297729874
0.275974381443224
0.283018971651189
0.280520202811634
0.274178977774604
0.233948065855011
/
```

```

SSHIFT
--
-- EoS Volume Shift (Reservoir EoS)
--
-0.06733799443
-0.1034563174
-0.08830190084
-0.08655713407
-0.06167990165
0.1568475241
/

ACF
--
-- Acentric Factors (Reservoir EoS)
--
0.1736205847
0.0982075429
0.1298491186
0.1334920942
0.1854343665
0.725951652
/

BIC
--
-- Binary Interaction Coefficients (Reservoir EoS)
--
0.09557214658
0.1 0.003953440551
0.1 0.003953440551 0
0.1 0.003953440551 0 0
0.1 0.05143374545 0.01 0.01 0
/

PARACHOR
--
-- Component Parachors
--
153.228
77.16777827

```

```
114.196
153.4716
215.6685052
580.1596603
/
-- Units: ft3 /lb-mole
VCRITVIS
--
-- Critical Volumes for Viscosity Calc (Reservoir EoS)
--
2.5302796318043
1.22291051844086
2.04977431931245
2.99865589373809
4.56328462372778
14.0735322372033
/
ZCRITVIS
--
-- Critical Z-Factors for Viscosity Calculation (Reservoir EoS)
--
0.275945297729874
0.275974381443224
0.283018971651189
0.280520202811634
0.274178977774604
0.233948065855011
/
LBCCOEF
--
-- Lorentz-Bray-Clark Viscosity Correlation Coefficients
--
0.1023 0.023364 0.058533 -0.040758 0.0093324
/
--PVTi--Please do not alter these lines
--PVTi--as PVTi can use them to re-create the fluid model
--PVTiMODSPEC =====
--PVTiTITLE
```

```

--PVTiVERSION
--PVTi 2014.2 /
--PVTiNCOMPS
--PVTi 6 /
--PVTiEOS
--PVTi PR3 /
--PVTiPRCORR
--PVTiLBC
--PVTiOPTIONS
--PVTi 0 0 0 0 0 0 1 0 0 0 0 0 0 0 0 0 0 0 0 0
--PVTi/
--PVTiOPTIONSEXT
--PVTi 0 1
--PVTi/
--PVTiNOECHO
--PVTiMODSYS =====
--PVTiUNITS
--PVTi FIELD ABSOL PERCENT /
--PVTiDEGREES
--PVTi Fahrenheit /
--PVTiSTCOND
--PVTi 60.0000 14.6959 /
--PVTiCNAMES
--PVTi CO2
--PVTi C1N2
--PVTi C2
--PVTi C3
--PVTi C4+
--PVTi C6+
--PVTi /
--PVTiTCRIT
--PVTi 3.174537166E+02 -5.683118041E+01 1.002751465E+02 2.112525335E+02
--PVTi 3.249800768E+02 8.827641801E+02 /
--PVTiPCRIT
--PVTi 9.094904716E+02 9.755710741E+02 8.296759428E+02 6.735400157E+02
--PVTi 5.059249866E+02 2.394764768E+02 /
--PVTiVCRIT
--PVTi 2.530279724E+00 1.222910563E+00 2.049774394E+00 2.998656003E+00
--PVTi 4.563284790E+00 1.407353275E+01 /
--PVTiZCRIT
--PVTi 2.759452977E-01 2.759743814E-01 2.830189717E-01 2.805202028E-01

```

```

--PVTi 2.741789778E-01 2.339480659E-01 /
--PVTiVCRITVIS
--PVTi 2.530279724E+00 1.222910563E+00 2.049774394E+00 2.998656003E+00
--PVTi 4.563284790E+00 1.407353275E+01 /
--PVTizCRITVIS
--PVTi 2.759452977E-01 2.759743814E-01 2.830189717E-01 2.805202028E-01
--PVTi 2.741789778E-01 2.339480659E-01 /
--PVTiSSHIFT
--PVTi -6.733799443E-02 -1.034563174E-01 -8.830190084E-02 -8.655713407E-02
--PVTi -6.167990165E-02 1.568475241E-01 /
--PVTiACF
--PVTi 1.736205847E-01 9.820754290E-02 1.298491186E-01 1.334920942E-01
--PVTi 1.854343665E-01 7.259516520E-01 /
--PVTiMW
--PVTi 4.401000000E+01 1.684563510E+01 3.007000000E+01 4.409700000E+01
--PVTi 6.631018044E+01 2.240840217E+02 /
--PVTiZI
--PVTi 3.665811900E-02 1.424990452E+00 1.641320340E+00 5.175937748E+00
--PVTi 1.162872440E+01 8.009236894E+01 /
--PVTiTBOIL
--PVTi 1.234391086E+01 -2.231252350E+02 -1.220309485E+02 -4.637173031E+01
--PVTi 4.618860618E+01 5.688432259E+02 /
--PVTiTREF
--PVTi 5.999998631E+01 5.999998631E+01 5.999998631E+01 5.999998631E+01
--PVTi 5.999998631E+01 5.999998631E+01 /
--PVTiDREF
--PVTi 4.850653269E+01 2.811839580E+01 3.421052756E+01 3.633307854E+01
--PVTi 3.769551020E+01 5.275973046E+01 /
--PVTiPARACHOR
--PVTi 1.532280000E+02 7.716777827E+01 1.141960000E+02 1.534716000E+02
--PVTi 2.156685052E+02 5.801596603E+02 /
--PVTiHYDRO
--PVTi N H H H H H
--PVTi /
--PVTiBIC
--PVTi 9.557214658E-02
--PVTi 1.000000000E-01 3.953440551E-03
--PVTi 1.000000000E-01 3.953440551E-03 0.000000000E+00
--PVTi 1.000000000E-01 3.953440551E-03 0.000000000E+00 0.000000000E+00
--PVTi 1.000000000E-01 5.143374545E-02 1.000000000E-02 1.000000000E-02
--PVTi 0.000000000E+00

```

```

--PVTi /
--PVTiSAMPLES
--PVTiINJECT
--PVTi 1.000000000E+02 0.000000000E+00 0.000000000E+00 0.000000000E+00
--PVTi 0.000000000E+00 0.000000000E+00 /
--PVTi /
--PVTiSAMTITLE
--PVTi /
--PVTiSPECHA
--PVTi -2.453495016E+00 -1.746871772E+02 4.035341843E-01 1.012336282E+00
--PVTi -1.045011710E+01 1.650714961E+00 /
--PVTiSPECHB
--PVTi 3.056811641E-02 3.264669433E-01 2.382181309E-02 3.446781061E-02
--PVTi 7.541901207E-02 1.676899106E-01 /
--PVTiSPECHC
--PVTi -7.329175177E-06 3.722268564E-05 -4.958314124E-06 -7.345666092E-06
--PVTi -7.860484437E-06 -3.727658078E-05 /
--PVTiSPECHD
--PVTi 0.000000000E+00 0.000000000E+00 0.000000000E+00 0.000000000E+00
--PVTi 0.000000000E+00 0.000000000E+00 /
--PVTiHEATVAPS
--PVTi 3.591296784E+04 2.154695257E+04 1.650621600E+04 3.603408601E+04
--PVTi 5.375194286E+04 1.888846623E+05 /
--PVTiCALVAL
--PVTi 4.745471637E+03 3.690907513E+03 3.323854000E+03 4.754344000E+03
--PVTi 7.019670334E+03 2.352652212E+04 /
--PVTi--End of PVTi generated section--
ZI
--
-- Overall Composition
--
0.00036658119
0.01424990452
0.0164132034
0.05175937748
0.116287244
0.8009236894
/

```

APPENDIX 3

ECLIPSE *.DATA FILE FOR REFERENCE CASE (NATURAL DEPLETION)

```
=====
RUNSPEC This section is mandatory and it is used to set up the
--      specification for the simulation run.
=====

DIMENS
--Grid dimensions, you need to change Nz
--Nx Ny Nz
17 17 23 /

FIELD
--Request the unit convention to be used

WELLDIMS
6 100 8* /

COMPS
--Number of components
6 /

START
1 JAN 2017 /

TABDIMS
--Determines the # of pressure and saturation tables and the maximum # of rows
1 1 40 40 /

--WATER
--Water is present (NOT FOR THIS CASE)

AIM
--AIM solution method, avoids time step restrictions

EOS
--Peng-Robinson equation of state to be used
PR /

--*commented out parallel
PARALLEL
4 /

--MISCIBLE
--/
```

```

=====
GRID      This section is mandatory and it is used to input the grid
--        or cells to be used into the simulation model.
=====
-- MODEL 17*17*23 EACH BLOCK (PERMEABILITY AND POROSITY DISTRIBUTION)

--*Depth DZ last layer split
EQUALS
--      VALUE   X     X     Y     Y     Z     Z
DX      460     1     1     1     17    1     23 /
DY      460     1    17     1     1     1     23 /
DX      690     2    16     1    17     1     23 /
DY      690     1    17     2    16     1     23 /
DX      460    17    17     1    17     1     23 /
DY      460     1    17    17    17     1     23 /
DZ      20.93    1    17     1    17     1     21 /
DZ      6.66     1    17     1    17     22     23 /
/

TOPS

--DEVON FLUID
289*9554

--HEAVY FLUID
--289*11964
/

PORO
289*0.1167 289*0.1621 289*0.1681
289*0.1603 289*0.1433 289*0.1306
289*0.1707 289*0.1644 289*0.1296
289*0.1723 289*0.1198 289*0.1271
289*0.1103 289*0.1231 289*0.1459
289*0.0841 289*0.1271 289*0.1616
289*0.1720 289*0.1271 289*0.0588
289*0.0960 289*0.1160
/

PERMX
289*45.00 289*498.0 289*685.0
289*453.0 289*184.0 289*94.00
289*786.0 289*562.0 289*89.00
289*854.0 289*53.00 289*78.00
289*32.00 289*63.00 289*211.0

```

```

289*8.000 289*78.00 289*485.0
289*841.0 289*78.00 289*2.100
289*45.00 289*325.0
/

PERMY
289*45.00 289*498.0 289*685.0
289*453.0 289*184.0 289*94.00
289*786.0 289*562.0 289*89.00
289*854.0 289*53.00 289*78.00
289*32.00 289*63.00 289*211.0
289*8.000 289*78.00 289*485.0
289*841.0 289*78.00 289*2.100
289*45.00 289*325.0
/

PERMZ
289*4.500 289*49.80 289*68.50
289*45.30 289*18.40 289*9.400
289*78.60 289*56.20 289*8.900
289*85.40 289*5.300 289*7.800
289*3.200 289*6.300 289*21.10
289*0.800 289*7.800 289*48.50
289*84.10 289*7.800 289*0.210
289*4.500 289*32.50
/

INIT

-----
PROPS This section is mandatory and it is used to incorporate the
-- fluid and reservoir properties
-----

INCLUDE

644-Light-Devon.PVO /
--644-Heavy.pvo/

SGFN
--Gas saturation functions (you may change these)

```

--	SGAS	KRG	PCOG
	0.00	0.000	0.0
	0.04	0.005	0.1
	0.08	0.013	0.2
	0.12	0.026	0.3
	0.16	0.040	0.4
	0.20	0.058	0.5
	0.24	0.078	0.6
	0.28	0.100	0.7
	0.32	0.126	0.8
	0.36	0.156	0.9
	0.40	0.187	1.0
	0.44	0.222	1.1
	0.48	0.260	1.2
	0.56	0.349	1.4
	0.60	0.400	1.5
	0.64	0.450	1.6
	0.68	0.505	1.7
	0.72	0.562	1.8
	0.76	0.620	1.9
	0.80	0.680	2.0
	0.84	0.740	2.1
/			
SOF2			
--	SOIL	KRO	
	0.00	0.000	
	0.04	0.000	
	0.08	0.000	
	0.12	0.000	
	0.16	0.000	
	0.20	0.000	
	0.24	0.000	
	0.28	0.005	
	0.32	0.012	
	0.36	0.024	
	0.40	0.040	
	0.44	0.060	
	0.48	0.082	
	0.52	0.112	
	0.56	0.150	
	0.60	0.196	
	0.68	0.315	
	0.72	0.400	
	0.76	0.513	
	0.80	0.650	
	0.84	0.800	/

```

ROCK
4128 4e-6/

=====
SOLUTION This section is mandatory
=====

EQUIL
-- FT PRES WGC pc (you may change these)
  9554 4128 18000 /

OUTSOL
--Solution output for GRAF (you may change these and add more performance indicators)
PRESSURE SOIL SWAT SGAS XMF YMF ZMF /

RPTSOL
--Output to the initial solution to the print files (you may change these)
PRESSURE SOIL SWAT SGAS /

--Eliminate
RPTRST

--Output Controls on output to the RESTART file
--BASIC=2 writes flows required for restarting the run at any given time

BASIC=2 PRESSURE SOIL SWAT SGAS XMF YMF ZMF VOIL VGAS DENO DENG /

--You may change the separator conditions and number of separators
-- Jorge: You had 3 separators is OK - copy
FIELDSEP
  1 150 70 /
  2 60 14.7 /
/

=====
SUMMARY This optional section specifies quantities to be written to
-- the summary file to be read by GRAF
=====

RUNSUM

```

```
--Field oil production rate and total, GOR and field pressure
FPR
FOIP
FOPR
FOPT
FGPR
FGPT
FGIR
FGIT
FGIP
FGOR

FOSAT
FGSAT

FOE

WGIR
/
WBHP
/
WGOR
/
WOPR
/
WGPR
/
WXMf
'P*' 1 /
/

WYMF
'P*' 1 /
/

WBHP
'I*'
/
```

```
=====
SCHEDULE Specifies the production system
=====
```

```
RPTSCHED
```

```
PRESSURE SOIL SWAT SGAS VGAS VOIL DENG DENO /
```

```
WELSPECS
```

```
-- Define injection and production wells
```

```
I INJ1 9 9 1* GAS 2* /
P1 PROD 3 3 1* OIL 2* /
P2 PROD 15 3 1* OIL 2* /
P3 PROD 3 15 1* OIL 2* /
P4 PROD 15 15 1* OIL 2* /
I2 PROD 15 15 1* GAS 2* /
/
```

```
COMPDAT
```

```
-- Defines well completion
```

```
-- WELL -- LOCAL-- LOCATION -- OPEN -- SAT -- CONN -- WELL
-- NAME -- GRID--IR JTH K1 K2 -- SHUT -- TAB -- FACT -- DIAM
I 9 9 1 23 OPEN 1 0 0.8 0 -2 /
--I 25 25 33 40 OPEN 2* /
--I 25 25 43 46 OPEN 2* /
P1 3 3 1 23 OPEN 1 0 0.8 0 -2 /
--P1 7 7 33 40 OPEN 2* /
--P1 7 7 43 46 OPEN 2* /
P2 15 3 1 23 OPEN 1 0 0.8 0 -2 /
--P2 43 7 33 40 OPEN 2* /
--P2 43 7 43 46 OPEN 2* /
P3 3 15 1 23 OPEN 1 0 0.8 0 -2 /
--P3 7 43 33 40 OPEN 2* /
--P3 7 43 43 46 OPEN 2* /
P4 15 15 1 23 OPEN 1 0 0.8 0 -2 /
--P4 43 43 33 40 OPEN 2* /
--P4 43 43 43 46 OPEN 2* /
I2 15 15 1 23 OPEN 1 0 0.8 0 -2 /
--I2 43 43 33 40 OPEN 2* /
--I2 43 43 43 46 OPEN 2* /
/
```

```
WCONPROD
--Well P set to target gas rate of xxxx, with min bhp of xxxx psi
P1 OPEN ORAT 20000 1* 1* 1* 1* 1200 /
P2 OPEN ORAT 20000 1* 1* 1* 1* 1200 /
P3 OPEN ORAT 20000 1* 1* 1* 1* 1200 /
P4 OPEN ORAT 20000 1* 1* 1* 1* 1200 /
/
```

```
WECON
P1 100 4* WELL /
P2 100 4* WELL /
P3 100 4* WELL /
P4 100 4* WELL /
/
```

```
DATES
1 JAN 2018 /
1 JAN 2019 /
1 JAN 2020 /
1 JAN 2021 /
1 JAN 2022 /
1 JAN 2023 /
1 JAN 2024 /
1 JAN 2025 /
1 JAN 2026 /
1 JAN 2027 /
1 JAN 2028 /
1 JAN 2029 /
1 JAN 2030 /
1 JAN 2031 /
1 JAN 2032 /
1 JAN 2033 /
1 JAN 2034 /
1 JAN 2035 /
1 JAN 2036 /
1 JAN 2037 /
```

APPENDIX 4

ECLIPSE *.DATA FILE FOR CO2 INJECTION CASE

```
=====
RUNSPEC This section is mandatory and it is used to set up the
--      specification for the simulation run.
=====

DIMENS
--Grid dimensions, you need to change Nz
--Nx Ny Nz
17 17 23 /

FIELD
--Request the unit convention to be used

WELLDIMS
6 100 8* /

COMPS
--Number of components
6 /

START
1 JAN 2017 /

TABDIMS
--Determines the # of pressure and saturation tables and the maximum # of rows
1 1 40 40 /

--WATER
--Water is present (NOT FOR THIS CASE)

AIM
--AIM solution method, avoids time step restrictions

EOS
--Peng-Robinson equation of state to be used
PR /

--*commented out parallel
PARALLEL
4 /

--MISCIBLE
--/
```

```

=====
GRID      This section is mandatory and it is used to input the grid
--        or cells to be used into the simulation model.
=====
-- MODEL 17*17*23 EACH BLOCK (PERMEABILITY AND POROSITY DISTRIBUTION)

--*Depth DZ last layer split
EQUALS
--      VALUE   X     X     Y     Y     Z     Z
DX      460     1     1     1     17    1     23  /
DY      460     1    17     1     1     1     23  /
DX      690     2    16     1    17     1     23  /
DY      690     1    17     2    16     1     23  /
DX      460    17    17     1    17     1     23  /
DY      460     1    17    17    17     1     23  /
DZ      20.93    1    17     1    17     1     21  /
DZ      6.66     1    17     1    17     22     23  /
/

TOPS

--DEVON FLUID
289*9554

--HEAVY FLUID
--289*11964
/

PORO
289*0.1167  289*0.1621  289*0.1681
289*0.1603  289*0.1433  289*0.1306
289*0.1707  289*0.1644  289*0.1296
289*0.1723  289*0.1198  289*0.1271
289*0.1103  289*0.1231  289*0.1459
289*0.0841  289*0.1271  289*0.1616
289*0.1720  289*0.1271  289*0.0588
289*0.0960  289*0.1160
/

PERMX
289*45.00  289*498.0  289*685.0
289*453.0  289*184.0  289*94.00
289*786.0  289*562.0  289*89.00
289*854.0  289*53.00  289*78.00
289*32.00  289*63.00  289*211.0

```

```

289*8.000 289*78.00 289*485.0
289*841.0 289*78.00 289*2.100
289*45.00 289*325.0
/

PERMY
289*45.00 289*498.0 289*685.0
289*453.0 289*184.0 289*94.00
289*786.0 289*562.0 289*89.00
289*854.0 289*53.00 289*78.00
289*32.00 289*63.00 289*211.0
289*8.000 289*78.00 289*485.0
289*841.0 289*78.00 289*2.100
289*45.00 289*325.0
/

PERMZ
289*4.500 289*49.80 289*68.50
289*45.30 289*18.40 289*9.400
289*78.60 289*56.20 289*8.900
289*85.40 289*5.300 289*7.800
289*3.200 289*6.300 289*21.10
289*0.800 289*7.800 289*48.50
289*84.10 289*7.800 289*0.210
289*4.500 289*32.50
/

INIT

-----
PROPS This section is mandatory and it is used to incorporate the
-- fluid and reservoir properties
-----

INCLUDE

644-Light-Devon.PVO /
--644-Heavy.pvo/

SGFN
--Gas saturation functions (you may change these)

```

--	SGAS	KRG	PCOG
	0.00	0.000	0.0
	0.04	0.005	0.1
	0.08	0.013	0.2
	0.12	0.026	0.3
	0.16	0.040	0.4
	0.20	0.058	0.5
	0.24	0.078	0.6
	0.28	0.100	0.7
	0.32	0.126	0.8
	0.36	0.156	0.9
	0.40	0.187	1.0
	0.44	0.222	1.1
	0.48	0.260	1.2
	0.56	0.349	1.4
	0.60	0.400	1.5
	0.64	0.450	1.6
	0.68	0.505	1.7
	0.72	0.562	1.8
	0.76	0.620	1.9
	0.80	0.680	2.0
	0.84	0.740	2.1
/			
SOF2			
--	SOIL	KRO	
	0.00	0.000	
	0.04	0.000	
	0.08	0.000	
	0.12	0.000	
	0.16	0.000	
	0.20	0.000	
	0.24	0.000	
	0.28	0.005	
	0.32	0.012	
	0.36	0.024	
	0.40	0.040	
	0.44	0.060	
	0.48	0.082	
	0.52	0.112	
	0.56	0.150	
	0.60	0.196	
	0.68	0.315	
	0.72	0.400	
	0.76	0.513	
	0.80	0.650	
	0.84	0.800	/

```

ROCK
4128 4e-6/

=====
SOLUTION This section is mandatory
=====

EQUIL
-- FT PRES WGC pc (you may change these)
  9554 4128 18000 /

OUTSOL
--Solution output for GRAF (you may change these and add more performance indicators)
PRESSURE SOIL SWAT SGAS XMF YMF ZMF /

RPTSOL
--Output to the initial solution to the print files (you may change these)
PRESSURE SOIL SWAT SGAS /

--Eliminate
RPTRST

--Output Controls on output to the RESTART file
--BASIC=2 writes flows required for restarting the run at any given time

BASIC=2 PRESSURE SOIL SWAT SGAS XMF YMF ZMF VOIL VGAS DENO DENG /

--You may change the separator conditions and number of separators
-- Jorge: You had 3 separators is OK - copy
FIELDSEP
  1 150 70 /
  2 60 14.7 /
/

=====
SUMMARY This optional section specifies quantities to be written to
-- the summary file to be read by GRAF
=====

RUNSUM

```

```
--Field oil production rate and total, GOR and field pressure
FPR
FOIP
FOPR
FOPT
FGPR
FGPT
FGIR
FGIT
FGIP
FGOR

FOSAT
FGSAT

FOE

WGIR
/
WBHP
/
WGOR
/
WOPR
/
WGPR
/
WXMF
'P*' 1 /
/

WYMF
'P*' 1 /
/

WBHP
'I*'
/
```

```

=====
SCHEDULE Specifies the production system
=====

RPTSCHED
PRESSURE SOIL SWAT SGAS VGAS VOIL DENG DENO /

WELSPECS
-- Define injection and production wells
I INJ1 9 9 1* GAS 2* /
P1 PROD 3 3 1* OIL 2* /
P2 PROD 15 3 1* OIL 2* /
P3 PROD 3 15 1* OIL 2* /
P4 PROD 15 15 1* OIL 2* /
I2 PROD 15 15 1* GAS 2* /
/

COMPDAT
-- Defines well completion
-- WELL -- LOCAL-- LOCATION -- OPEN -- SAT -- CONN -- WELL
-- NAME -- GRID--IR JTH K1 K2 -- SHUT -- TAB -- FACT -- DIAM
I 9 9 1 23 OPEN 1 0 0.8 0 -2 /
--I 25 25 33 40 OPEN 2* /
--I 25 25 43 46 OPEN 2* /
P1 3 3 1 23 OPEN 1 0 0.8 0 -2 /
--P1 7 7 33 40 OPEN 2* /
--P1 7 7 43 46 OPEN 2* /
P2 15 3 1 23 OPEN 1 0 0.8 0 -2 /
--P2 43 7 33 40 OPEN 2* /
--P2 43 7 43 46 OPEN 2* /
P3 3 15 1 23 OPEN 1 0 0.8 0 -2 /
--P3 7 43 33 40 OPEN 2* /
--P3 7 43 43 46 OPEN 2* /
P4 15 15 1 23 OPEN 1 0 0.8 0 -2 /
--P4 43 43 33 40 OPEN 2* /
--P4 43 43 43 46 OPEN 2* /
I2 15 15 1 23 OPEN 1 0 0.8 0 -2 /
--I2 43 43 33 40 OPEN 2* /
--I2 43 43 43 46 OPEN 2* /
/

```

```

WCONPROD
--Well P set to target gas rate of xxxx, with min bhp of xxxx psi
P1 OPEN ORAT 20000 1* 1* 1* 1* 1200 /
P2 OPEN ORAT 20000 1* 1* 1* 1* 1200 /
P3 OPEN ORAT 20000 1* 1* 1* 1* 1200 /
P4 OPEN ORAT 20000 1* 1* 1* 1* 1200 /
/

WECON
P1 100 4* WELL /
P2 100 4* WELL /
P3 100 4* WELL /
P4 100 4* WELL /
/

--INJECTING CO2 since begining
WELLSTRE
'CO2' 1.0 0 0 0 0 /
/

WINJGAS
I STREAM CO2 /
/

WCONINJE
      I   GAS OPEN      RATE 100000 1* 7500 /
/

DATES
1 JAN 2018 /
1 JAN 2019 /
1 JAN 2020 /
1 JAN 2021 /
1 JAN 2022 /
1 JAN 2023 /
1 JAN 2024 /
1 JAN 2025 /
1 JAN 2026 /
1 JAN 2027 /
1 JAN 2028 /
1 JAN 2029 /
1 JAN 2030 /
1 JAN 2031 /
1 JAN 2032 /
1 JAN 2033 /
1 JAN 2034 /
1 JAN 2035 /
1 JAN 2036 /
1 JAN 2037 /

```

APPENDIX 5

ECLIPSE GRID.INC FILE FOR LGR GRID CONFIGURATION

```

=====
GRID      This section is mandatory and it is used to input the grid
--        or cells to be used into the simulation model.
=====
-- MODEL 17*17*23 EACH BLOCK, 230FT by 230FT (PERMEABILITY AND POROSITY DISTRIBUTION)

--*Depth DZ last layer split
EQUALS
--  VALUE   X     X     Y     Y     Z     Z
DX     460     1     1     1     17     1     23 /
DY     460     1    17     1     1     1     23 /
DX     690     2    16     1    17     1     23 /
DY     690     1    17     2    16     1     23 /
DX     460    17    17     1    17     1     23 /
DY     460     1    17    17    17     1     23 /
DZ     20.93    1    17     1    17     1     21 /
DZ     6.66     1    17     1    17     22     23 /
/

-- Jorge you will have to change the depth for both fluids

TOPS

--DEVON FLUID
289*9554

--HEAVY FLUID
--289*11964
/

PORO
289*0.1167 289*0.1621 289*0.1681
289*0.1603 289*0.1433 289*0.1306
289*0.1707 289*0.1644 289*0.1296
289*0.1723 289*0.1198 289*0.1271
289*0.1103 289*0.1231 289*0.1459
289*0.0841 289*0.1271 289*0.1616
289*0.1720 289*0.1271 289*0.0588
289*0.0960 289*0.1160
/

```

```

PERMX
289*45.00 289*498.0 289*685.0
289*453.0 289*184.0 289*94.00
289*786.0 289*562.0 289*89.00
289*854.0 289*53.00 289*78.00
289*32.00 289*63.00 289*211.0
289*8.000 289*78.00 289*485.0
289*841.0 289*78.00 289*2.100
289*45.00 289*325.0
/

PERMY
289*45.00 289*498.0 289*685.0
289*453.0 289*184.0 289*94.00
289*786.0 289*562.0 289*89.00
289*854.0 289*53.00 289*78.00
289*32.00 289*63.00 289*211.0
289*8.000 289*78.00 289*485.0
289*841.0 289*78.00 289*2.100
289*45.00 289*325.0
/

PERMZ
289*4.500 289*49.80 289*68.50
289*45.30 289*18.40 289*9.400
289*78.60 289*56.20 289*8.900
289*85.40 289*5.300 289*7.800
289*3.200 289*6.300 289*21.10
289*0.800 289*7.800 289*48.50
289*84.10 289*7.800 289*0.210
289*4.500 289*32.50
/

--Define Cartesian Local Grid Refinement
CARFIN
--Name I1 I2 J1 J2 K1 K2 NX NY NZ
LGRI 8 10 8 10 1 23 33 33 46 /

NXFIN
9 15 9 /
NYFIN
9 15 9 /
NZFIN
2 2 2 2 2 2 2 2 2 2 2 2 2 2 2 2 2 2 2 2 /

```

```

ENDFIN

CARFIN
--Name I1 I2 J1 J2 K1 K2 NX NY NZ
LGRP2  2  4 14 16  1 23 33 33 46 /

NXFIN
  9 15 9 /
NYFIN
  9 15 9 /
NZFIN
  2 2 2 2 2 2 2 2 2 2 2 2 2 2 2 2 2 2 2 2 2 2 /

ENDFIN

CARFIN
--Name I1 I2 J1 J2 K1 K2 NX NY NZ
LGRP3 14 16 14 16  1 23 33 33 46 /

NXFIN
  9 15 9 /
NYFIN
  9 15 9 /
NZFIN
  2 2 2 2 2 2 2 2 2 2 2 2 2 2 2 2 2 2 2 2 2 2 /

ENDFIN

CARFIN
--Name I1 I2 J1 J2 K1 K2 NX NY NZ
LGRP4 14 16 2  4  1 23 33 33 46 /

NXFIN
  9 15 9 /
NYFIN
  9 15 9 /
NZFIN
  2 2 2 2 2 2 2 2 2 2 2 2 2 2 2 2 2 2 2 2 2 2 /

ENDFIN

```

APPENDIX 6

ECLIPSE SCHEDULE.INC FILE FOR LGR CASES

```

=====
SCHEDULE Specifies the production system
=====

RPTSCHED
PRESSURE SOIL SWAT SGAS VGAS VOIL DENG DENO /

WELSPECL
--Define injection and production wells -
I FIELD LGRI 17 17 1* GAS 6* 1 /
P1 FIELD LGRP1 17 17 1* OIL 6* 1 /
P2 FIELD LGRP2 17 17 1* OIL 6* 1 /
P3 FIELD LGRP3 17 17 1* OIL 6* 1 /
P4 FIELD LGRP4 17 17 1* OIL 6* 1 /
/

COMPDATL
--Defines well completion
-- WELL -- LOCAL-- LOCATION -- OPEN -- SAT -- CONN -- WELL
-- NAME -- GRID--IR JTH K1 K2 -- SHUT -- TAB -- FACT -- DIAM
I LGRI 17 17 1 46 OPEN 1 0 0.8 0 -2/
P1 LGRP1 17 17 1 46 OPEN 1 0 0.8 0 -2/
P2 LGRP2 17 17 1 46 OPEN 1 0 0.8 0 -2/
P3 LGRP3 17 17 1 46 OPEN 1 0 0.8 0 -2/
P4 LGRP4 17 17 1 46 OPEN 1 0 0.8 0 -2/
/

WCONPROD
--Well P set to target gas rate of xxxx, with min bhp of xxxx psi
P1 OPEN ORAT 20000 1* 1* 1* 1* 1200 /
P2 OPEN ORAT 20000 1* 1* 1* 1* 1200 /
P3 OPEN ORAT 20000 1* 1* 1* 1* 1200 /
P4 OPEN ORAT 20000 1* 1* 1* 1* 1200 /
/

WECON
P1 100 4* WELL /
P2 100 4* WELL /
P3 100 4* WELL /
P4 100 4* WELL /
/

```

```
--INJECTING CO2 since begining
WELLSTRE
'CO2' 1.0 0 0 0 0 /
/

WINJGAS
I STREAM CO2 /
/

WCONINJE
      I   GAS OPEN   RATE 100000 1* 7500 /
/

DATES
1 JAN 2018 /
1 JAN 2019 /
1 JAN 2020 /
1 JAN 2021 /
1 JAN 2022 /
1 JAN 2023 /
1 JAN 2024 /
1 JAN 2025 /
1 JAN 2026 /
1 JAN 2027 /
1 JAN 2028 /
1 JAN 2029 /
1 JAN 2030 /
1 JAN 2031 /
1 JAN 2032 /
1 JAN 2033 /
1 JAN 2034 /
1 JAN 2035 /
1 JAN 2036 /
1 JAN 2037 /
```

APPENDIX 7

ECLIPSE SCHEDULE.INC FILE FOR RECYCLING PRODUCED GAS

```

=====
SCHEDULE Specifies the production system
=====

RPTSCHED
PRESSURE SOIL SWAT SGAS VGAS VOIL DENG DENO /

WELSPECL
--Define injection and production wells -
I FIELD LGRI 17 17 1* GAS 6* 1 /
P1 FIELD LGRP1 17 17 1* OIL 6* 1 /
P2 FIELD LGRP2 17 17 1* OIL 6* 1 /
P3 FIELD LGRP3 17 17 1* OIL 6* 1 /
P4 FIELD LGRP4 17 17 1* OIL 6* 1 /
/

COMPDATL
--Defines well completion
-- WELL -- LOCAL-- LOCATION -- OPEN -- SAT -- CONN -- WELL
-- NAME -- GRID--IR JTH K1 K2 -- SHUT -- TAB -- FACT -- DIAM
I LGRI 17 17 1 46 OPEN 1 0 0.8 0 -2/
P1 LGRP1 17 17 1 46 OPEN 1 0 0.8 0 -2/
P2 LGRP2 17 17 1 46 OPEN 1 0 0.8 0 -2/
P3 LGRP3 17 17 1 46 OPEN 1 0 0.8 0 -2/
P4 LGRP4 17 17 1 46 OPEN 1 0 0.8 0 -2/
/

WCONPROD
--Well P set to target gas rate of xxxx, with min bhp of xxxx psi
P1 OPEN ORAT 20000 1* 1* 1* 1* 1200 /
P2 OPEN ORAT 20000 1* 1* 1* 1* 1200 /
P3 OPEN ORAT 20000 1* 1* 1* 1* 1200 /
P4 OPEN ORAT 20000 1* 1* 1* 1* 1200 /
/

WECON
P1 100 4* WELL /
P2 100 4* WELL /
P3 100 4* WELL /
P4 100 4* WELL /
/

```

```
TUNING
/
/
2* 200 /

NSTACK
100 /

MESSAGES
2* 1000000 5* 1000000 /

--INJECTING CO2 since begining
WELLSTRE
'CO2' 1.0 0 0 0 0 /
/

WINJGAS
I STREAM CO2 /
/

WCONINJE
      I   GAS OPEN      RATE 250000 1* 7500 /
/

ACTIONW
START_INJRecom 'P*' WYMF_01 > 0.10 /

WELOPEN
P4 SHUT /
/

GINJGAS
PROD GV PROD /
/

GCONINJE
'P*' GAS REIN 2* 1 /
/

WCONINJE
I2 GAS OPEN GRUP 2* 7500 /
/

ENDACTIO
```

APPENDIX 8

INCREMENTAL NPV DATA USED TO PLOT THE CONTOUR

Table A.8.1 – Incremental NPV of the light oil reservoir at different injection pore volumes with varying oil prices (with LGR).

NPV Discounting at 10%, \$/acre-ft									
Injection Pore Volume	Oil Price, \$/bbl								
	20	30	40	50	60	70	80	90	100
0.37	\$ (52)	\$ 122	\$ 295	\$ 469	\$ 642	\$ 815	\$ 989	\$ 1,162	\$ 1,335
0.55	\$ (31)	\$ 250	\$ 531	\$ 813	\$ 1,094	\$ 1,375	\$ 1,657	\$ 1,938	\$ 2,220
0.74	\$ (35)	\$ 342	\$ 720	\$ 1,097	\$ 1,475	\$ 1,852	\$ 2,229	\$ 2,607	\$ 2,984
0.83	\$ (62)	\$ 350	\$ 762	\$ 1,174	\$ 1,586	\$ 1,999	\$ 2,411	\$ 2,823	\$ 3,235
0.92	\$ (101)	\$ 341	\$ 782	\$ 1,224	\$ 1,666	\$ 2,107	\$ 2,549	\$ 2,990	\$ 3,432
1.10	\$ (224)	\$ 253	\$ 729	\$ 1,206	\$ 1,683	\$ 2,160	\$ 2,637	\$ 3,113	\$ 3,590
1.47	\$ (582)	\$ (92)	\$ 399	\$ 889	\$ 1,379	\$ 1,869	\$ 2,359	\$ 2,850	\$ 3,340

Table A.8.2 – Incremental NPV of the light oil reservoir at different injection pore volumes with varying oil prices (without LGR).

NPV Discounting at 10%, \$/acre-ft									
Injection Pore Volume	Oil Price, \$/bbl								
	20	30	40	50	60	70	80	90	100
0.37	\$ 31	\$ 247	\$ 462	\$ 678	\$ 893	\$ 1,109	\$ 1,324	\$ 1,540	\$ 1,756
0.55	\$ 33	\$ 347	\$ 661	\$ 975	\$ 1,290	\$ 1,604	\$ 1,918	\$ 2,232	\$ 2,546
0.74	\$ (21)	\$ 363	\$ 748	\$ 1,132	\$ 1,517	\$ 1,901	\$ 2,285	\$ 2,670	\$ 3,054
0.83	\$ (79)	\$ 324	\$ 728	\$ 1,132	\$ 1,536	\$ 1,940	\$ 2,344	\$ 2,748	\$ 3,151
0.92	\$ (150)	\$ 267	\$ 683	\$ 1,100	\$ 1,517	\$ 1,934	\$ 2,351	\$ 2,767	\$ 3,184
1.10	\$ (318)	\$ 111	\$ 540	\$ 969	\$ 1,398	\$ 1,827	\$ 2,256	\$ 2,685	\$ 3,114
1.47	\$ (722)	\$ (303)	\$ 116	\$ 535	\$ 955	\$ 1,374	\$ 1,793	\$ 2,212	\$ 2,631

Table A.8.3 – Incremental NPV of the heavy oil reservoir at different injection pore volumes with varying oil prices (with LGR).

NPV Discounting at 10%, \$/acre-ft									
Injection Pore Volume	Oil Price, \$/bbl								
	20	30	40	50	60	70	80	90	100
0.38	\$ 1,812	\$ 2,941	\$ 4,070	\$ 5,199	\$ 6,328	\$ 7,457	\$ 8,586	\$ 9,715	\$ 10,845
0.48	\$ 1,907	\$ 3,134	\$ 4,361	\$ 5,588	\$ 6,815	\$ 8,042	\$ 9,269	\$ 10,496	\$ 11,723
0.58	\$ 1,906	\$ 3,181	\$ 4,456	\$ 5,732	\$ 7,007	\$ 8,282	\$ 9,557	\$ 10,833	\$ 12,108
0.67	\$ 1,889	\$ 3,206	\$ 4,522	\$ 5,838	\$ 7,154	\$ 8,470	\$ 9,786	\$ 11,102	\$ 12,418
0.74	\$ 1,850	\$ 3,195	\$ 4,540	\$ 5,885	\$ 7,230	\$ 8,575	\$ 9,920	\$ 11,265	\$ 12,610
0.80	\$ 1,796	\$ 3,162	\$ 4,528	\$ 5,894	\$ 7,259	\$ 8,625	\$ 9,991	\$ 11,357	\$ 12,723
0.85	\$ 1,737	\$ 3,122	\$ 4,506	\$ 5,890	\$ 7,274	\$ 8,659	\$ 10,043	\$ 11,427	\$ 12,812
1.15	\$ 1,607	\$ 3,022	\$ 4,437	\$ 5,851	\$ 7,266	\$ 8,681	\$ 10,096	\$ 11,510	\$ 12,925

Table A.8.4 – Incremental NPV of the heavy oil reservoir at different injection pore volumes with varying oil prices (without LGR).

NPV Discounting at 10%, \$/acre-ft									
Injection Pore Volume	Oil Price, \$/bbl								
	20	30	40	50	60	70	80	90	100
0.38	\$ 1,916	\$ 3,098	\$ 4,280	\$ 5,462	\$ 6,644	\$ 7,827	\$ 9,009	\$ 10,191	\$ 11,373
0.48	\$ 2,060	\$ 3,365	\$ 4,669	\$ 5,974	\$ 7,279	\$ 8,583	\$ 9,888	\$ 11,193	\$ 12,498
0.58	\$ 2,069	\$ 3,427	\$ 4,785	\$ 6,143	\$ 7,502	\$ 8,860	\$ 10,218	\$ 11,576	\$ 12,935
0.67	\$ 2,045	\$ 3,440	\$ 4,835	\$ 6,231	\$ 7,626	\$ 9,021	\$ 10,416	\$ 11,811	\$ 13,206
0.74	\$ 1,991	\$ 3,407	\$ 4,822	\$ 6,238	\$ 7,654	\$ 9,070	\$ 10,486	\$ 11,902	\$ 13,318
0.80	\$ 1,923	\$ 3,352	\$ 4,782	\$ 6,212	\$ 7,641	\$ 9,071	\$ 10,501	\$ 11,930	\$ 13,360
0.85	\$ 1,829	\$ 3,259	\$ 4,689	\$ 6,119	\$ 7,550	\$ 8,980	\$ 10,410	\$ 11,840	\$ 13,270
1.15	\$ 1,640	\$ 3,070	\$ 4,500	\$ 5,930	\$ 7,361	\$ 8,791	\$ 10,221	\$ 11,651	\$ 13,081

Table A.8.5 – Incremental NPV of the light oil reservoir at different injection pore volumes with varying CO₂ prices (with LGR).

NPV Discounting at 10%, \$/acre-ft						
Injection Pore Volume	CO ₂ Price, \$/Mcf					
	0.5	0.8	1	1.5	2	2.5
0.37	\$ 453	\$ 382	\$ 335	\$ 217	\$ 99	\$ (19)
0.55	\$ 778	\$ 672	\$ 601	\$ 425	\$ 248	\$ 71
0.74	\$ 1,050	\$ 908	\$ 814	\$ 578	\$ 343	\$ 107
0.83	\$ 1,127	\$ 968	\$ 862	\$ 597	\$ 332	\$ 66
0.92	\$ 1,180	\$ 1,003	\$ 885	\$ 591	\$ 296	\$ 1
1.10	\$ 1,180	\$ 968	\$ 826	\$ 473	\$ 119	\$ (234)
1.47	\$ 927	\$ 644	\$ 455	\$ (16)	\$ (488)	\$ (959)

Table A.8.6 – Incremental NPV of the heavy oil reservoir at different injection pore volumes with varying CO₂ prices (with LGR).

NPV Discounting at 10%, \$/acre-ft						
Injection Pore Volume	CO ₂ Price, \$/Mcf					
	0.5	0.8	1	1.5	2	2.5
0.38	\$ 4,705	\$ 4,635	\$ 4,587	\$ 4,470	\$ 4,352	\$ 4,234
0.48	\$ 5,063	\$ 4,975	\$ 4,916	\$ 4,768	\$ 4,621	\$ 4,474
0.58	\$ 5,200	\$ 5,094	\$ 5,023	\$ 4,846	\$ 4,670	\$ 4,493
0.67	\$ 5,303	\$ 5,180	\$ 5,097	\$ 4,891	\$ 4,685	\$ 4,478
0.74	\$ 5,354	\$ 5,213	\$ 5,118	\$ 4,883	\$ 4,647	\$ 4,411
0.80	\$ 5,370	\$ 5,211	\$ 5,105	\$ 4,839	\$ 4,574	\$ 4,309
0.85	\$ 5,375	\$ 5,198	\$ 5,080	\$ 4,785	\$ 4,491	\$ 4,196
1.15	\$ 5,356	\$ 5,144	\$ 5,002	\$ 4,649	\$ 4,295	\$ 3,942

Table A.8.7 – Incremental NPV of the light oil reservoir at different injection pore volumes with section 45Q tax credits.

NPV Discounting at 10%, \$/acre-ft									
Injection Pore Volume	Oil Price, \$/bbl								
	20	30	40	50	60	70	80	90	100
0.37	\$ 73	\$ 247	\$ 420	\$ 594	\$ 767	\$ 940	\$ 1,114	\$ 1,287	\$ 1,461
0.55	\$ 146	\$ 428	\$ 709	\$ 990	\$ 1,272	\$ 1,553	\$ 1,835	\$ 2,116	\$ 2,397
0.74	\$ 186	\$ 563	\$ 941	\$ 1,318	\$ 1,695	\$ 2,073	\$ 2,450	\$ 2,827	\$ 3,205
0.83	\$ 178	\$ 590	\$ 1,002	\$ 1,415	\$ 1,827	\$ 2,239	\$ 2,651	\$ 3,063	\$ 3,476
0.92	\$ 158	\$ 599	\$ 1,041	\$ 1,482	\$ 1,924	\$ 2,366	\$ 2,807	\$ 3,249	\$ 3,691
1.10	\$ 68	\$ 545	\$ 1,022	\$ 1,498	\$ 1,975	\$ 2,452	\$ 2,929	\$ 3,405	\$ 3,882
1.47	\$ (226)	\$ 264	\$ 754	\$ 1,245	\$ 1,735	\$ 2,225	\$ 2,715	\$ 3,205	\$ 3,696

Table A.8.8 – Incremental NPV of the heavy oil reservoir at different injection pore volumes with section 45Q tax credits.

NPV Discounting at 10%, \$/acre-ft									
Injection Pore Volume	Oil Price, \$/bbl								
	20	30	40	50	60	70	80	90	100
0.38	\$ 1,923	\$ 3,052	\$ 4,181	\$ 5,310	\$ 6,439	\$ 7,568	\$ 8,697	\$ 9,826	\$ 10,955
0.48	\$ 2,037	\$ 3,264	\$ 4,491	\$ 5,718	\$ 6,945	\$ 8,172	\$ 9,399	\$ 10,626	\$ 11,853
0.58	\$ 2,052	\$ 3,327	\$ 4,602	\$ 5,878	\$ 7,153	\$ 8,428	\$ 9,704	\$ 10,979	\$ 12,254
0.67	\$ 2,052	\$ 3,368	\$ 4,684	\$ 6,000	\$ 7,316	\$ 8,632	\$ 9,948	\$ 11,264	\$ 12,581
0.74	\$ 2,023	\$ 3,368	\$ 4,713	\$ 6,058	\$ 7,403	\$ 8,748	\$ 10,093	\$ 11,438	\$ 12,783
0.80	\$ 1,974	\$ 3,340	\$ 4,706	\$ 6,072	\$ 7,438	\$ 8,804	\$ 10,169	\$ 11,535	\$ 12,901
0.85	\$ 1,920	\$ 3,304	\$ 4,688	\$ 6,073	\$ 7,457	\$ 8,841	\$ 10,225	\$ 11,610	\$ 12,994
1.15	\$ 1,797	\$ 3,212	\$ 4,626	\$ 6,041	\$ 7,456	\$ 8,871	\$ 10,285	\$ 11,700	\$ 13,115

Table A.8.9 – Incremental NPV of the light oil reservoir at different injection rates with recycling of produced gas.

NPV Discounting at 10%, \$/acre-ft									
Injection Rate, MMscf/day	Oil Price, \$/bbl								
	20	30	40	50	60	70	80	90	100
250	\$ (453)	\$ 30	\$ 512	\$ 995	\$ 1,478	\$ 1,960	\$ 2,443	\$ 2,925	\$ 3,408
300	\$ (768)	\$ (315)	\$ 137	\$ 590	\$ 1,042	\$ 1,495	\$ 1,947	\$ 2,400	\$ 2,852
350	\$ (1,042)	\$ (617)	\$ (192)	\$ 233	\$ 658	\$ 1,083	\$ 1,508	\$ 1,933	\$ 2,358

Table A.8.10 – Incremental NPV of the heavy oil reservoir at different injection rates with recycling of produced gas.

NPV Discounting at 10%, \$/acre-ft									
Injection Rate, MMscf/day	Oil Price, \$/bbl								
	20	30	40	50	60	70	80	90	100
100	\$ 1,929	\$ 3,135	\$ 4,342	\$ 5,549	\$ 6,755	\$ 7,962	\$ 9,169	\$ 10,375	\$ 11,582
125	\$ 1,793	\$ 2,984	\$ 4,175	\$ 5,365	\$ 6,556	\$ 7,747	\$ 8,938	\$ 10,129	\$ 11,319
150	\$ 1,671	\$ 2,848	\$ 4,026	\$ 5,203	\$ 6,380	\$ 7,558	\$ 8,735	\$ 9,912	\$ 11,090